Distributed optical fiber sensors: physical aspects, development and applications

Aghiad Khadour

UNIVERSITÉ PARIS-EST

Synthèse des travaux de recherche en vue d'obtenir
L'Habilitation à Diriger des Recherches de l'Ecole Doctorale Sciences, Ingénierie, Environnement de l'Université Paris-Est

Spécialité : Sciences de l'ingénieur

Capteurs distribués à fibres optiques : aspects physiques, développement et applications

Aghiad KHADOUR
Chargé de recherche à l'IFSTTAR

Membres du jury :

Référent HdR	Cathrine ALGANI, Professeur des universités, Le Cnam, France
Rapporteurs	Farhad ANSARI, Professor, University of Illinois at Chicago, USA
	Olivier BOUR, Professeur des universités, Université de Rennes 1, France
	Anne TROPPER, Professor at Quantum technology Center, University of Southampton, UK
Examinateurs	Farid BENBOUDJEMA, Professeur des universités, ENS Paris-Saclay, France
	Ammar HIDEUR, Professeur des universités, Université de Rouen, France
	Razvigor OSSIKOVSKI, Professeur à l'Ecole Polytechnique, France
	Jean-Louis OUDAR, Directeur de Recherche, C2N, France

Travaux de Recherche Effectués à l'IFSTTAR
Laboratoire Instrumentation, Simulation et Informatique Scientifique (LISIS)

Viva held on 26th July 2018

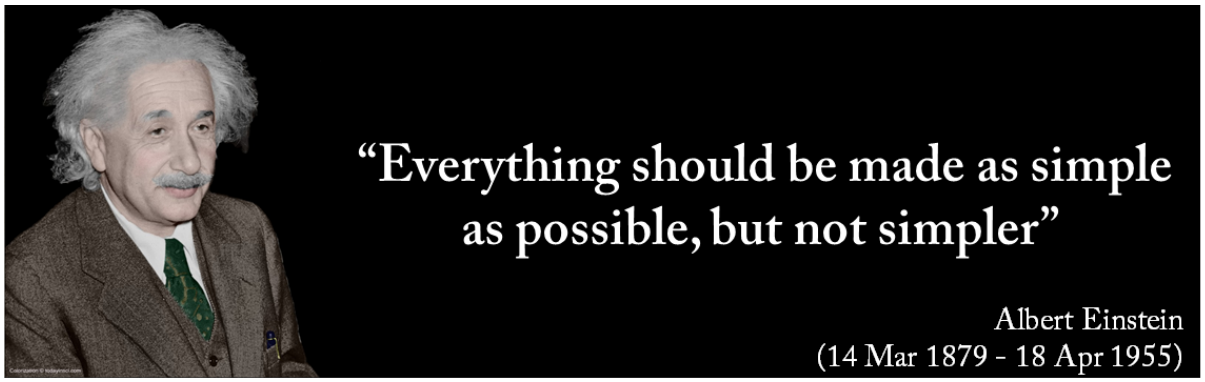
“Everything should be made as simple as possible, but not simpler”
Albert Einstein
(14 Mar 1879 - 18 Apr 1955)

Résumé

Cette synthèse présente mes travaux pour l'obtention de l'Habilitation à Diriger des Recherches qui est composé de deux parties distinctes : un résumé de ma carrière professionnelle avec les activités de recherche dans les différents postes que j'ai pu occuper depuis l'obtention de mon diplôme d'ingénieur, et les principales thématiques de recherche auxquelles je m'intéresse ; et une partie scientifique qui décrit plus précisément le contenu de mes recherches dans des domaines liés au développement des capteurs distribués à fibre optique, l'utilisation des capteurs distribués à fibres optiques dans des structures de génie civil, et les paramètres impactant les performances des capteurs à fibres optiques lors de leur intégration dans des structures spécifiques.

Le résumé de ma carrière professionnelle permet de mettre en relief un des aspects particuliers de mon profil puisque j'ai eu la chance de travailler dans le domaine de la recherche appliquée avant ma thèse, comme ingénieur de recherche en optoélectronique. Cette expérience, au sein de laboratoire réalisant des activités de conception, de réalisation et de caractérisation de sources lasers solides, permet d'étendre les longueurs d'ondes de l'émission laser avec l'utilisation de cristaux optiques non-linéaires par la génération de la seconde harmonique ou l'oscillation paramétrique optique. Ceci m'a permis de mener des travaux de recherche appliquée et de réaliser l'importance de travailler en équipe. L'expérience de la thèse dans les lasers semiconducteurs en cavité vertical externe pour la génération des impulsions brèves m'a permis d'acquérir des nouvelles connaissances et de nouveaux savoir-faire dans l'optique non-linéaire rapide, et la dynamique des lasers. Cette étape est suivie par mon expérience en post-doctorat, dans laquelle j'ai acquis les techniques de tris de nanotubes de carbones, leurs caractéristiques photoniques, et leurs utilisations comme absorbants saturables dans les lasers.

Suite à mon recrutement à l'IFSTTAR (ex : LCPC) en Octobre 2010, en tant que Chargé de recherche sur la thématique des capteurs à fibres optiques, je me suis investi pour faire émerger l'utilisation de capteurs a fibres optiques comme une solution évidente dans les structures de génie civil, pour la surveillance de la santé de ces infrastructures sur les volets SHM et CND, mais aussi de confronter l'utilisation de la fibre dans des nouvelles applications de contrôle non destructif et de monitoring dans des cas spécifiques. J'ai développé en parallèle une activité de recherche sur le « développement des capteurs à fibres optiques distribués ». J'ai cherché à caractériser l'impact de chaque composant du système et à me concentrer en premier lieu au cœur d'un système de capteur à fibre distribué qui est le laser.

Dans ce mémoire, j'introduis les problématiques et les enjeux de mes travaux, je décris les principales investigations menées et leurs résultats, et je préfigure les travaux de recherche à moyen et long terme.

Abstract

This report dedicated to obtaining the HDR (Habilitation à Diriger des Recherches), is composed of two distinct parts: the first one summarizes my professional career highlighting my research activities in the different positions that I have held since obtaining my engineering degree, and the main research topics I am interested in. The scientific part describes precisely the content of my research related to the development of fiber-optic distributed sensors, the applications of distributed optical fiber sensors in civil engineering structures and other specific structures, and secondly, the impact of environmental parameters on the performances of optical fiber sensors.

The summary of my professional career highlights a particular aspect of my profile since I had the chance to work in the field of applied research before my thesis, as a research engineer in optoelectronics. This experiment, in a laboratory carrying out activities of design, realization and characterization of solid laser sources, makes it possible to extend the wavelengths of the laser emission by using nonlinear optical crystals through the generation of the second harmonic or the optical parametric oscillation. This allowed me to conduct applied research and realize the importance of working in a team. The experience of the thesis in vertical external cavity semiconductor lasers for the generation of short pulses has allowed me to acquire new knowledge in fast non-linear optics, and the dynamics of semiconductor lasers. This step is followed by my postdoctoral experience, in which I worked on sorting techniques of carbon nanotubes, their photonic characteristics, and their uses as saturable absorbers in lasers.

Following my recruitment at IFSTTAR (ex: LCPC) in October 2010, as a researcher on the theme of fiber optic sensors, I have invested in different projects, to make the use of distributed optical fiber sensors an evident solution in the civil engineering structures monitoring, integration of optical fiber sensors in new specific applications. In parallel, I developed a research activity related to the "development of distributed optical fiber sensors". I worked on the study of impact of each component of the system and to focus first and foremost on the heart of a distributed fiber sensor system: the laser.

In this thesis, I introduce the issues and challenges of my work, describe the main investigations conducted and their results, and prefigure medium and long-term research.

Table des matières :

1 Parcours professionnel 1

1.1 Formation initiale et évolution professionnelle 1

1.1.1 Avant la formation doctorale 1

1.1.2 La formation doctorale 2

1.1.3 La formation postdoctorale 4

1.1.4 Chargé de recherche à l'IFSTTAR 5

1.2 Enseignement 6

1.3 Structuration des activités de recherche 7

1.4 Encadrements et production scientifique 8

1.4.1 Encadrement 8

1.4.2 Production scientifique 17

1.5 Collaboration, participation aux projets de recherche et réalisation des expertises 18

1.6 Développement, acquisition de matériels 20

1.7 Conclusion, et introduction de la synthèse scientifique 21

2 Scientific activities 22

2.1 Background and motivations 22

2.2 Optical Fiber 27

2.2.1 Optical Fibers classifications: 29

2.2.2 Light interaction with glass 32

2.2.3 Optical Fibers by ITU Standards: 45

2.3 Intrinsic distributed optical fiber sensors 47

2.4 Optical reflectometry techniques 49

2.4.1 Optical Time-Domain Reflectometer based techniques 50

2.4.2 Optical Frequency-Domain Reflectometer based techniques 53

2.5 Distributed sensing configurations: 57

2.5.1 Rayleigh based sensing configurations 57

2.5.2 Brillouin based sensing configurations: 59

2.5.3 Raman based sensing configurations: 63
2.6 New solutions for distributed sensing 64
2.6.1 The laser 65
2.6.2 The sensing schema 67
2.7 Optical fiber sensing cables 69
2.8 Distributed optical fiber sensors applications 71
2.8.1 Distributed optical fiber sensors concrete structures 71
2.8.2 Distributed optical fiber sensors in composite structures 88
2.8.3 Distributed optical fiber sensors for geo-science and geotechnical applications. 95
2.8.4 Photonic components characterization 99
2.9 Summery and Roadmap Future Trends 102
2.9.1 Distributed Optical Fiber Sensors Applications (medium-term) 102
2.9.2 Reliability of Optical Fiber Optic Sensors and interrogation systems (medium-term) 103
2.9.3 Distributed optical fiber sensors as perception neural networks for large scale infrastructures (medium-term) 104
2.9.4 New design of optical fiber sensors (medium/long-term plan) 104
2.9.5 Distributed chemical sensors (long-term plan) 104
2.10 Master and PhD Students projects involved in my scientific activities 105
2.10.1 Master (M1 and M2) 105
2.10.2 PhD students 105
2.11 Finished and actual projects 107
2.12 Scientific and technical expertise activity 108
3 Appendix 110
3.1 Curriculum vitæ 110
3.2 Publications 112
3.2.1 Articles 112
3.2.2 International conferences 114
3.2.3 National conferences 118

3.2.4 National seminars 119
3.2.5 Invited talks 119
3.2.6 Research reports 120
3.2.7 PhD dissertation 121
4 Bibliography 122

1 Parcours professionnel

Ce chapitre a pour objectif de présenter mon parcours professionnel, en mettant en avant mes activités de recherche dans le domaine des capteurs distribués à fibres optiques, d'encadrement de la recherche, et de ma formation initiale à aujourd'hui.

Dans un premier temps, je présenterai ma formation initiale et mon parcours professionnel. Il y sera fait état de la teneur de mes formations, de la description des travaux que j'ai menés dans les trois phases de mon parcours : avant la thèse, pendant la thèse et après, en m'appuyant notamment mes activités de recherche et d'encadrement. Je détaillerai ensuite mes implications dans le domaine de l'enseignement avant d'aborder la structuration de mes activités de recherche, pour pouvoir présenter mon implication et la maturation de mes projets. Celle-ci sera détaillée autour de deux axes principaux de mon projet de recherche

-Le développement des capteurs distribués à fibres optiques,

-Les applications des capteurs à fibres optiques distribués dans des milieux cimentiers et composites.

Dans le chapitre suivant je présenterai un résumé de mes encadrements et de mes publications en lien avec ces deux axes. J'aborderai également ma participation à des projets de recherche collaboratifs. Ceci me permettra de détailler les collaborations académiques et industrielles réalisées dans le cadre de mes activités. Enfin, je développerai un paragraphe dédié à mes activités dans le cadre de développement et d'acquisition de matériels d'essais et d'outils d'instrumentation.

Mon Curriculum Vitae, en annexe de ce manuscrit, donne un résumé de l'ensemble de ces sujets et de mon parcours.

1.1 Formation initiale et évolution professionnelle

Mon expérience professionnelle antérieure à ma fonction comme chargé de recherche à l'IFSTTAR en 2010, se décompose en trois étapes, pendant lesquelles j'ai travaillé sur des thématiques complémentaires. Cette évolution a enrichi mon expérience scientifique au fil des années. Je présente dans ce paragraphe, les thématiques développées durant chaque étape.

1.1.1 Avant la formation doctorale

Mes premiers contacts avec le monde de la recherche ont eu lieu dès le stage de fin d'études en école d'ingénieur en optoélectronique au sein de l'ISSAT[1] à Damas. Ce stage a porté sur la génération des impulsions brèves d'un laser solide en utilisant deux éléments

[1] Institut Supérieur des Sciences Appliquées et de Technologie.

commutateurs-Q (Q-switch). Ce stage s'est extrêmement bien déroulé et j'ai été sollicité pour travailler dans le laboratoire comme ingénieur de recherche.

Mon travail comme ingénieur de recherche a été orienté vers la caractérisation des lasers et la conception des systèmes optiques pour les lasers solides :

-Réalisation d'un banc de test pour caractériser des faisceaux laser (impulsionnels et continus). L'objectif était de faire un système performant et à bas cout.

-Étude des lasers solides avec milieu à gain Nd:YAG[2] pour la génération des impulsions dites géantes, et l'optimisation d'un système de Q-switch pour en faire un système à bas cout utilisant des matériaux piézoélectriques. Ce développement a été réalisé dans l'atelier optique du département.

- Analyse des cristaux solides de type Nd:GGG[3] afin d'obtenir une bonne stabilité thermique des lasers solides. Cette stabilité est nécessaire pour permettre une résistance élevée à l'endommagement. Cette analyse était couplée à des campagnes de tests de seuil d'endommagement des cristaux Nd:GGG.

- Génération de la seconde harmonique à l'aide de dispositifs d'optique non-linéaire afin d'obtenir une émission laser verte à 0,531µm à partir d'un laser Nd:GGG à 1,062µm. Le cristal utilisé était de type KTP[4]. Dans le cadre d'un projet industriel, j'ai utilisé ce cristal pour réaliser un oscillateur paramétrique (obtenir une source de laser accordable dans certaines longueurs d'onde avec le changement de l'orientation du cristal).

- Etude des diodes laser haute luminescence afin d'obtenir une bonne source laser à partir de plusieurs sources laser diodes non performantes.

1.1.2 La formation doctorale

J'ai obtenu mon diplôme de docteur de l'école polytechnique à Palaiseau avec une thèse intitulée « Source d'impulsions brèves à 1,55µm en laser à cavité verticale externe pour application à l'échantillonnage optique linéaire » encadrée par Jean-Louis OUDAR. Cette thèse s'est déroulée dans le cadre d'un projet ANR-TONICS[5] au LPN-CNRS[6]. Pendant la thèse j'ai travaillé sur une procédure complète qui allait de la fabrication d'une structure semiconductrice

[2] Neodymium-doped Attrium Aluminium Garnet (Nd: $Y_3Al_5O_{12}$).

[3] Neodymium-doped Gadolinium Gallium Garnet (Nd: $Gd_3Ga_5O_{12}$).

[4] Potassium Titanyle Phosphate (KTP)– $KTiOPO_4$

[5] Technologies d'échantillONnage linéaire et non-linéaire pour applications en Conversion analogique/numérique et en transmission à très haut-débit.

[6] Laboratoire de Photonique et de Nanostructures.

utilisée dans les lasers VECSEL[7], en passant par les caractérisations optiques et thermiques jusqu'à l'utilisation dans une cavité laser. J'ai réalisé la conception de la cavité avec les deux éléments nécessaires pour le fonctionnement en régime de verrouillage des modes passifs (VECSEL et SESAM[8]).

J'ai décidé de réaliser le fonctionnement du VECSEL à la température ambiante (25°C) et non pas à basse température. Ceci a constitué une réelle difficulté car le fonctionnement des structures VECSEL à 1,55µm se dégrade avec la température, à cause de la mauvaise conductivité thermique des substrats lnP utilisés pour la réalisation de ce type de structures. Ce problème a été résolu grâce à une solution originale qui consiste à remplacer une épaisseur importante du substrat par du diamant, et à utiliser un traitement de la surface avec un antireflet pour garantir une meilleure absorption du pompage optique. Au cours de ma thèse, j'ai également réalisé des caractérisations et l'optimisation des structures passives SESAM. À la fin de la thèse, j'ai obtenu une source VECSEL continue avec une puissance de sortie de ~120mW limité par le pompage optique de ~1,7W. Le fonctionnement monomode longitudinal a été démontré aussi. Une source impulsionnelle a été réalisée avec une fréquence de répétitions de 2GHz et une largeur d'impulsion de 1,4ps à la température ambiante (pouvant descendre jusqu'à 1ps à 0°C), avec une largeur de raie de la première harmonique de ~800Hz. En parallèle, un système d'échantillonnage optique linéaire dans l'espace libre a été réalisé. La résolution temporelle du montage a été validée par la visualisation d'une séquence NRZ à 40 Gbit/s. Ce system a été utilisé dans les thèses suivantes mon départ du LPN.

Pendant ma thèse j'ai effectué deux échanges juniors dans le cadre du programme européen JRA 'Short pulses' du réseau d'excellence NoE ePIXnet. Mon premier séjour s'est déroulé à ETH Zürich, dans le groupe du Dr. Ursula KELLER pour réaliser des caractérisations des structures SESAM, et bénéficier des équipements modernes au sein du laboratoire de l'optique rapide. Le second séjour s'est déroulé à l'université de Southampton en Angleterre au laboratoire de photonique chez le Dr. Anne TROPPER, l'objectif était de bénéficier du banc de stabilisation actif développé pour garantir un bruit de phase très faible aux lasers VECSEL.

La soutenance de la thèse s'est déroulée le 2 Décembre 2009, les membres du jury (par ordre alphabétique) étaient :
Sophie BOUCHOULE, LPN -CNRS UPR 20, Chargé de recherche ; Examinatrice.

[7] Vertical-External-Cavity Surface-Emitting-Laser.

[8] SEmiconductor Saturable Absorber Mirror.

Antonello DE-MARTINO, LPICM, École Polytechnique, directeur de recherche ; Président du jury.

Daniel DOLFI, Thales Research and Technology (TRT) Ingénieur de recherche ; Examinateur.

Guanghua DUAN, Alcatel Thales III-V Lab Ingénieur de recherche ; Rapporteur.

Alain LE-CORRE, INSA de Rennes Professeur des universités ; Rapporteur.

Gilles MARTEL, CNRS UMR 6614 –CORIA Maître de conférences ; Examinateur.

Jean-Louis OUDAR, LPN-CNRS UPR 20 Directeur de recherche ; Directeur de thèse.

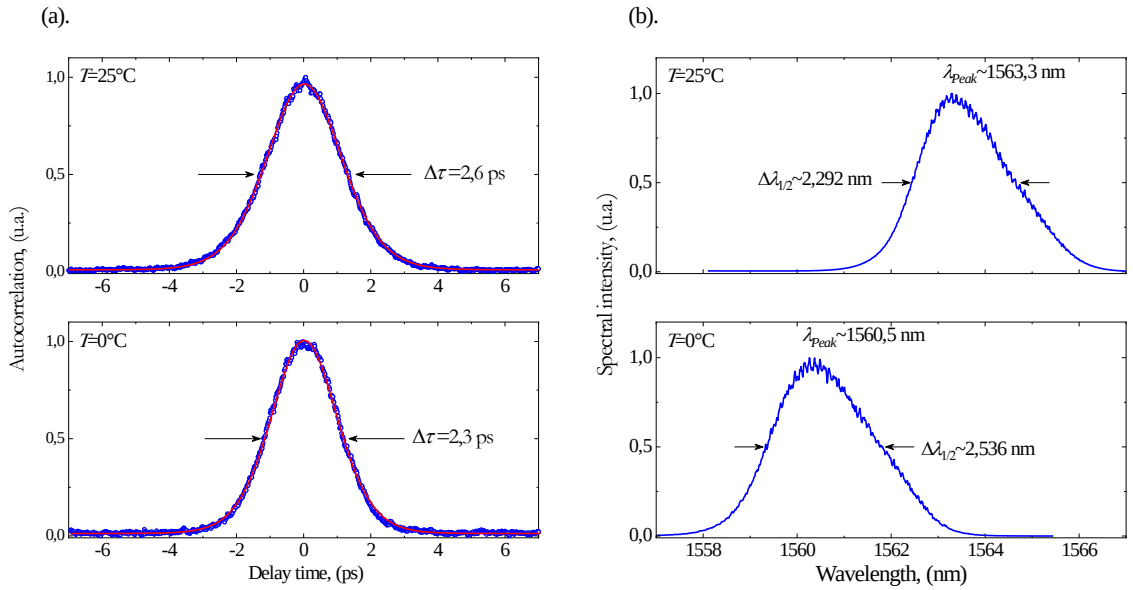

Figure 1-1 : Exemple des impulsions brèves obtenues par un laser VECSEL à 1,55µm ; (a) les largeurs temporelles à 0°C et 25°C, (b) les spectres optiques correspondants.

1.1.3 La formation postdoctorale

Suite à ma thèse, j'ai effectué un stage postdoctoral au laboratoire CORIA[9] (Rouen), dans le cadre du projet européen SFIVE[10] pour réaliser un système de tri des nanotubes de carbones semi-conducteurs, suivant leur spectre de photoluminescence. J'ai réalisé le montage d'un microscope inversé avec un laser de pompage pour la photoluminescence et un laser de contrôle par un SLM[11] La solution qui contient les nanotubes est injectée par un système de micro-pompes dans une cellule micro fluidique avec un débit de 1mL/h. Le système présenté dans la Figure 1-2 a fonctionné pour certaines dimensions des nanotubes. Une étape de caractérisation

[9] COmplexe de Recherche Interprofessionnel en Aérothermochimie.

[10] Sort Single Single-walled nanotubes of Specific Sizes.

[11] Spatial Light Modulator.

des nanotubes déposés sur des miroirs diélectriques a été réalisée à l'issue de cette séparation. Elle a permis d'établir un régime de verrouillage de mode passif avec une faible énergie par impulsion, à cause de la conductivité électrique des nanotubes (quenching effect).

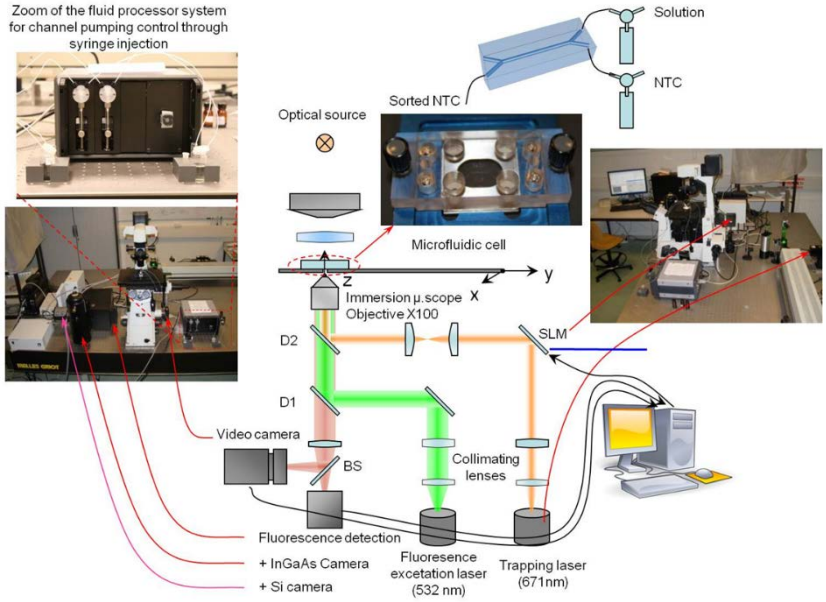

Figure 1-2 : Le montage expérimental réalisé pour la détection des spectres de photoluminescence et le tri des nanotubes de carbones dans une cellule micro-fluidique.

1.1.4 Chargé de recherche à l'IFSTTAR

Depuis mon recrutement en tant que chargé de recherche à l'IFSTTAR, au sein du laboratoire LISIS[12], mon activité principale en tant que chercheur s'articule autour des capteurs distribués à fibres optiques, c'est-à-dire l'utilisation de toute la longueur de la fibre pour mesurer les paramètres physiques autour. Dans le cadre de ce nouveau poste, il m'a été nécessaire de me former sur le sujet des capteurs à fibres optiques distribués, leur technologie, et les champs d'applications, pour pouvoir proposer des sujets de recherche pertinents avec les activités scientifiques du laboratoire LISIS. J'ai essayé sur certains aspects de continuer des collaborations antérieures dans le domaine académique, et en amorcer de nouvelles dans les domaines académique et industriel. Certains résultats des différentes collaborations seront présentés dans la partie consacrée à la synthèse scientifique.

Dans la Figure 1-3 je présente l'Organigramme fonctionnel du laboratoire LISIS. Le laboratoire LISIS fait partie du département Cosys (Composants et systèmes). Le nombre des chercheurs permanents de 10, qui répondent aux questions de la recherche liés à l'instrumentation jusqu'au modélisation.

[12] Laboratoire Instrumentation, Simulation et Informatique Scientifique.

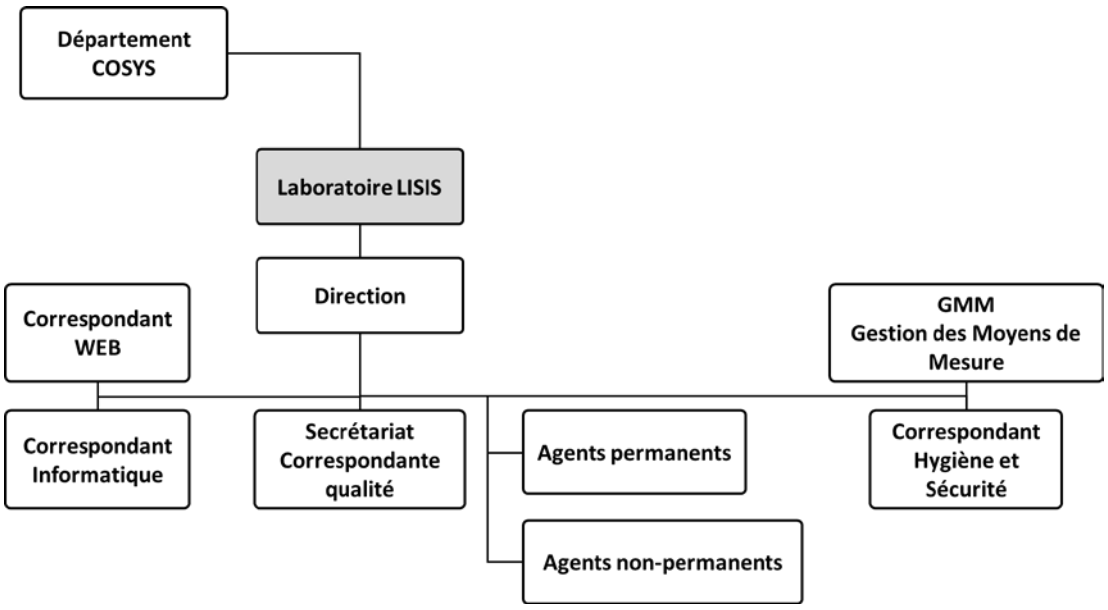

Figure 1-3 : Organigramme fonctionnel du laboratoire LISIS à l'IFSTTAR au 1er Décembre 2017.

1.2 Enseignement

Bien que mon statut comme chargé de recherche ne soit pas en lien direct avec ce type d'activité, l'implication dans l'enseignement des sujets dans le domaine de mes recherches est un élément important pour garder le lien avec les étudiants et chercher des candidats potentiels pour des stages (ou des thèses).

J'ai pu depuis mon arrivée à l'IFSTTAR participer aux actions d'enseignement à différents niveaux au sein de différents établissements. J'ai pu nouer des contacts locaux avec l'ESIEE-Paris[13]et le département réseaux et télécom à l'IUT de Vitry-Créteil. Le volume total des heures de mes interventions dans les deux établissements sont limitées à ~70h00 par année scolaire.

Je participe depuis 2011 dans l'enseignement des guides d'ondes et fibres optiques dans le cadre du master international de recherche, spécialité : électronique, option : Micro et nano-systèmes de l'ESIEE-Paris, je suis impliqué dans les cours, les TD et les TP. Dans le même établissement, je suis en charge des cours et TD du module propagation sur supports physiques au niveau de l'école d'ingénieur. Je suis impliqué dans un module de l'école d'ingénieur concernant la physique au niveau des cours et TD.

[13] École Supérieure d'Ingénieurs en Electrotechnique et Electronique.

Dans le second établissement, qui est le département réseaux et télécom à l'IUT de Vitry, depuis 2011, je suis impliqué dans des cours, des TD et TP du module ondes électromagnétiques et fibres optiques, transmissions numériques, et transmission large bande.

1.3 Structuration des activités de recherche

L'exercice de rédaction d'une Habilitation à Diriger des Recherches permet de prendre du recul sur les activités scientifiques. Pour ce faire, j'ai décidé d'identifier les sujets principaux à partir des deux grands axes auxquels j'ai pu contribuer et qui ont fait l'objet d'articles et/ou de communications. Ces deux grands axes sont le capteur à fibre et son système d'interrogation :

Le capteur : c'est la partie du système sur laquelle porte la mesure, c'est-à-dire celle qui est modifiée par les conditions extérieures que l'on cherche à mesurer. Ici, il s'agit de la fibre optique et de son enrobage. Mes travaux sur cet axe de recherche s'inscrivent dans la continuité de travaux de recherche antérieurs à mon arrivée au LISIS, pour le renforcement de savoir-faire au sein du LISIS à travers des solutions d'instrumentation par fibres optiques originales et uniques. La réalisation de mesures distribuées de déformation à haute résolution spatiale est limitée par l'effet d'enrobage de la fibre optique. Cette question a été abordée et plusieurs modèles ont été proposés pour donner les valeurs précises des déformations mécaniques à partir des déformations mesurées par la fibre optique. Les limites constatées de tous ces modèles sont liées aux directions des efforts mécaniques extérieurs appliqués par rapport à l'axe de la fibre optique et les variations des caractéristiques mécaniques de l'enrobage de la fibre optique lors des essais mécaniques : les limites élastiques, la plastification, etc…

La plupart de mes travaux dans le domaine des capteurs, sont des travaux de recherche appliquée qui s'appuient très souvent sur des investigations expérimentales importantes et sur des travaux de modélisation numérique. La nature appliquée de ces travaux résulte des besoins d'applications des capteurs à fibres optiques à l'IFSTTAR. Ce positionnement peu classique dans le monde de la recherche m'a permis de pouvoir côtoyer différents acteurs du génie civil Français, qu'ils soient gestionnaires d'ouvrage, entreprises du BTP, experts du domaine et universitaires. C'est une des raisons pour lesquelles j'ai pu participer à de nombreux projets ayant des niveaux de TRL (Technology Readiness Level) plus ou moins élevés.

L'interrogateur pour réaliser des mesures distribuées : c'est le système d'émission-réception qui permet de provoquer des effets élastiques (Rayleigh) et non-élastiques (Brillouin, Raman) dans une fibre optique, puis de les quantifier et d'en déduire une mesure du phénomène physique : température ou contrainte mécanique. Après avoir étudié l'engouement qu'avait suscité l'amélioration des interrogateurs à effet Brillouin distribué tant spontané (B-OTDR) que stimulé (B-OTDA) durant la dernière décennie, j'ai réalisé tout l'intérêt de concevoir un interrogateur à bas coût et de hautes performances reposant sur une analyse du signal tout

optique. Mes travaux réalisés en thèse concernant le développement des sources laser à émission par la surface à cavité verticale externe (VECSEL), m'ont permis d'élaborer un projet de recherche en coopération avec le laboratoire LPN formalisé par une thèse de 2013-2016. Une étude orientée pour comprendre l'influence des paramètres liés à : l'utilisation d'une source laser bifréquence, la structure de la fibre et l'impact de l'environnement dans lequel la fibre est installée, sur les capteurs basés sur la rétrodiffusion Brillouin fait l'objet d'une thèse démarrée en octobre 2016.

Mon travail de recherche dans les deux thèmes complémentaires : capteurs et interrogateurs, a évolué à travers les différents projets et les activités d'encadrement. Un bilan sera présenté dans le paragraphe suivant, qui présente mes activités d'encadrement depuis mon arrivé à l'IFSTTAR.

1.4 Encadrements et production scientifique

Je suis impliqué dans l'encadrement des thèses et des stages, sur des sujets liés directement à la structuration de mon activité de recherche. Ces sujets sont basés sur les deux grands axes que j'ai fixés : le développement des interrogateurs à fibres optiques, et l'instrumentation par fibres optiques. La production scientifique est liée à l'évolution de l'activité d'encadrement dans sa majorité, je présenterai un bilan de la production scientifique suite à la présentation de l'activité d'encadrement.

1.4.1 Encadrement

Dans l'activité d'encadrement, il conviendra de noter qu'il s'agit de co-encadrement dans les thèses. Les doctorants que j'ai encadrés ont fini leur thèse dans les délais de 3 ans, ils ont participé à des congères internationaux, publiés des articles dans des revues avec commuté de lecture, et les soutenances des thèses se sont bien déroulées.

Il faut signaler que je suis aussi impliqué dans certaines thèses sans encadrement officiel, sur certains sujets pour lesquels j'ai estimé que mon apport n'est fondamental dans le sujet de la thèse.

Une synthèse des encadrements que j'ai effectué jusqu'à Mai 2018 est présentée dans le tableau suivant.

Le doctorant	CHACCOUR Léa (2013-2016),
Sujet de la thèse :	Développement d'une source VECSEL bifréquence, pour la mesure de l'effet Brillouin dans les fibres optiques.
Soutenance	23.09.2016

Directeur de thèse	Patrice CHATELLIER
École Doctorale	Université Paris Est-L'école doctorale Sciences, Ingénierie et Environnement (SIE)
Financement	IFSTTAR
Production scientifique	1 article, 3 conférences internationales.
Situation professionnelle	Poste ATER.

Résumé de la thèse :

Cette thèse a porté sur la réalisation d'une source VECSEL bi-fréquence émettant à 1550 nm pour les capteurs à fibres optiques distribués à base de l'effet Brillouin. La rétrodiffusion Brillouin générée dans une fibre optique monomodes SMF28, est décalée de ~11GHz par rapport à la source laser qui monomode à ~1550nm.

Une conception et réalisation de la source VECSEL bi-fréquence est présentée. L'architecteur de la cavité choisi pour réaliser le laser bifréquence est une cavité plan-concave, formé entre le coupleur de sortie et la structure active 'semiconductrice). Cette géométrie de la cavité, permet d'installer des éléments dits intra-cavités. Le bon choix et le control de ces éléments permet d'obtenir une émission bipolarisée et bi-fréquence.

Nous avons identifié les structures VECSELs au laboratoire LPN-CNRS, pour utiliser la structure la plus performante, et cette structure a été utilisée dans notre cavité finale. La structure sélectionnée fournit une puissance de sortie ~200 mW avec un schéma d'évacuation de chaleur à travers le miroir de Bragg.

Pour réaliser un laser VECSEL bifréquence avec 11GHz de séparation spectrale, une lame biréfringente YVO_4 Est installée dans la cavité optique, pour avoir deux longueurs de la cavité optique suivant l'axe de polarisation, et un étalon Fabry-Perot garantie le fonctionnement monomode suivant l'axe de polarisation.

Nous avons trouvé qu'une accordabilité (de l'ordre du GHz) peut être assurée avec la rotation de la lame biréfringente, alors qu'une accordabilité plus fine (de l'ordre du MHz) peut être assurée avec la variation de la température du cristal, ainsi que la variation de la longueur de cavité.

Après l'optimisation des éléments optiques, l'émission obtenue observée sur un analyseur de spectre optique (avec une résolution de 1 GHz) était stable. Un meilleur contrôle de la stabilité de l'émission bi-fréquence est assuré avec la focalisation du diamètre du faisceau de pompage. Pour obtenir de faibles diamètres du spot de pompage, nous avons utilisé une diode laser de pompage monomode qui permet de pomper le mode fondamental de cavité. Les puissances de sorties ont été examinées. Nous avons obtenu une puissance de sortie de

50 mW en optimisant la réflectivité du miroir de sortie ainsi que les éléments intracavité. Une émission bi-fréquence stable était observée avec un coefficient de recouvrement spatial allant jusqu'à 70%. Une largeur de raie de 200 kHz est mesurée. Pour estimer la dérive du battement fréquentiel sur des temps longs, nous avons examiné l'évolution de l'enveloppe fréquentielle sur des intervalles temporels d'une minute, avec une dérive observée de 0.8 MHz/minute.

Le doctorant :	RAMAN Venkadesh (2014-2017)
Sujet de la thèse :	Comportement en fatigue sous flexion de matériaux composites nano-renforcées et intelligent.
Soutenance :	16 juin 2017
Directeur de thèse	Monssef DRISSI-HABTI
École Doctorale :	Centrale Nantes ED SPIGA
Financement :	Contrat EVEREST - l'IRT Jules Verne
Production scientifique :	3 articles, 3 conférences internationales.
Situation professionnelle :	Post-doctorat

Résumé de la thèse :

Les structures intelligentes fondées sur des matériaux composites ont été développées pour surveiller les structures qui doivent fonctionner dans des applications industrielles exigeantes, dans des environnements difficiles comme c'est le cas de l'aéronautique, de l'aérospatiale, du génie civil, des centrales nucléaires et chimiques...

L'étude actuelle est axée sur la suggestion d'un nouveau matériau composite intelligent qui peut être utilisé avec succès dans les pâles d'éoliennes offshore de nouvelle génération. En effet, pour accentuer leur rendement, les pales de nouvelle génération doivent dépasser une longueur de 100m, ce qui représente actuellement une cible hors d'atteinte étant donné que les matériaux composites constitutifs sont fondés sur des fibres de verre, notamment connues pour être lourdes et dépourvues de rigidité significative. Par conséquent, le passage aux fibres de carbone (plus léger et 3 fois plus rigide) devient obligatoire. Dans cette thèse, nous proposons la mise en place d'un matériau composite intelligent à base de fibres de carbone et de matrice époxy (ici appelé matériau parent). Les capteurs à fibre optique (FOS) et les capteurs à résistance quantique (QRS) seront utilisés pour la détection de déformation dans toute la structure. Ce choix devrait permettre une documentation précise et un envoi instantané d'informations critiques aux ingénieurs. Pour atteindre cet objectif de développement d'un nouveau matériau intelligent pour une application critique dans la production d'énergie éolienne offshore, nous avons choisi de

proposer un document de recherche regroupant plusieurs aspects du sujet, résumés en 5 chapitres. La thèse est fondée sur des modélisations numériques et analytiques. Le document n'a pas l'ambition d'être exhaustif. Il est destiné à présenter une recherche pragmatique qui met l'accent sur la façon dont les domaines de faiblesse mécanique peuvent être diagnostiqués, quelles sont les solutions qui peuvent être suggérées et comment nous pouvons les soutenir, quelles sont les questions relatives à l'utilisation de capteurs intégrés et les résultats expérimentaux qui permettent l'évaluation du statut actuel de la performance du matériau et les moyens d'en améliorer les performances.

Le doctorant :	Miyassa SALHI (2016-2019)
Sujet de la thèse :	Étude d'un système de surveillance de structures bas coût par fibres optiques reposant sur l'effet Brillouin et analyse des paramètres influents par méthode statistique
Soutenance :	Thèse en cours.
Directeur de thèse	Anne-Laure BILLABERT
École Doctorale :	L'école doctorale Sciences, Ingénierie et Environnement (SIE)
Financement :	École doctorale.
Production scientifique :	2 conférence Nationales
Situation professionnelle :	-

Sujet de la thèse :

Le phénomène de diffusion Brillouin spontanée (ou stimulée), dans le domaine des capteurs à fibres optiques, fait l'objet d'une forte investigation scientifique depuis les années 1990.

Les solutions proposées reposent sur l'analyse spectrale de l'onde de Stokes rétrodiffusée tout le long de la fibre. Ainsi, un dispositif B-OTDR (Brillouin Optical Time-Domain Reflectometer) peut réaliser une mesure du décalage de la fréquence Brillouin (de l'ordre de 11GHz autour de 1.55µm) avec une résolution spatiale métrique et une sensibilité des mesures de déformation et de température respectivement de l'ordre de 10µm/m et 0.5°C, mais pour un coût élevé (de l'ordre de 100k€) ce qui limite leur utilisation.

Les différents travaux antérieurs et actuels réalisés par l'Ifsttar et les compétences en modélisation électrique des composants optiques et optoélectroniques au sein de l'Esycom permettront d'étudier un système bas coût à hautes performances. Ce système repose sur l'utilisation d'un laser bi-mode à la longueur d'onde de 1,55 µm. Des études d'optimisation sur les paramètres de ce laser seront menées afin d'analyser les performances du système.

D'autre part, une méthode de post-traitement sur les spectres rétrodiffusés sera développée afin d'améliorer la résolution spatiale, le long de la fibre optique, liée aux effets de bruit du système.

Les objectifs de cette thèse sont de concevoir et caractériser un système bas coût innovant pour la détection des variations de température ou de déformation dans un bâtiment, de résolution à l'état de l'art, reposant sur la mesure du décalage du spectre Brillouin vers les basses fréquences (<1GHz).

L'intérêt de l'approche de modélisation des transducteurs électro-optiques et fibre optique est de pouvoir simuler le système d'optique hétérodyne et de mener à bien son optimisation en fonction de différents paramètres. Cet axe sera mené conjointement au sein d'ESYCOM-Le Cnam (modélisation) et de l'Ifsttar (caractérisation). Le modèle électrique du laser bi-mode sera développé en s'appuyant sur les études précédentes réalisées à ESYCOM pour des lasers monomodes DFB. Pour ceci, des caractérisations optique et électrique de la source seront menées à l'Ifsttar. Le modèle de la fibre optique existant (dispersion chromatique, effet non-linéaire) sera complété pour prendre en compte les phénomènes inélastiques de l'effet Brillouin et doit être de type distribué afin d'avoir la position spatiale de la variation de température ou de déformation. Cet aspect sera mené par l'équipe d'Esycom.

A l'issue de la modélisation, le système sera simulé et validé par l'expérimentation avec une solution d'hétérodynage optique à base d'un laser DFB. Cela consiste à mélanger le signal de rétrodiffusion Brillouin avec un oscillateur local optique (OLO) pour détecter le signal Brillouin à une fréquence d'environ 11 GHz. Le système avec le laser bi-mode sera ensuite étudié par simulation. Un levier supplémentaire sera mené pour une optimisation du système reposant sur l'étude des différents paramètres influents et leurs impacts sur les performances du système par le développement d'une approche statistique, au sein d'ESYCOM UPE-MLV.

La fin de thèse portera sur la validation expérimentale du système avec le laser bi-mode dont la fréquence de battement pourra être accordée de sorte d'être proche de la fréquence Brillouin. Une étude sur le système final de certains paramètres déterminés, comme l'état de la polarisation du signal optique injecté dans la fibre optique, sera comparée avec des résultats de mesures pour réaliser une détection distribuée dynamique du spectre Brillouin innovante et à l'état de l'art. De même, des méthodes de post-traitement sur les spectres de Brillouin seront développées afin d'améliorer le rapport signal à bruit après détection et ainsi augmenter la résolution spatiale du système.

Le doctorant :	Ismail ALJ (2017-2020)
Sujet de la thèse :	Durabilité des systèmes de mesures réparties par fibres optiques fixés en parement des structures
Soutenance :	-
Directeur de thèse	Karim BENZARTI
École Doctorale :	L'école doctorale Sciences, Ingénierie et Environnement (SIE)
Financement :	IFSTTAR (50%), IRSN (50%)
Production scientifique :	-
Situation professionnelle :	-

Résumé de la thèse :

La surveillance des structures de génie civil est une étape nécessaire pour évaluer au mieux leur état, assurer la sureté des installations et augmenter leur durée de fonctionnement. Lors de la construction d'une structure en béton armé, il est possible de noyer certains capteurs dans le béton frais, lors du coulage du béton, ou d'instrumenter directement les barres d'armature en acier. Ces capteurs internes, par la diversité de leur positionnement, permettent d'évaluer précisément l'état de la structure en service et de surveiller l'évolution d'éventuelles pathologies. Dans le cas de structures existantes, il est difficile de noyer l'instrumentation et cette dernière doit être installée en parement, au moyen de fixations mécaniques ou par collage. Les ouvrages concernés sont aussi bien les bâtiments, les ponts, les barrages, les tours d'aéroréfrigérants ou les enceintes de confinement de centrales nucléaires. Les paramètres mesurés habituellement recherchés sont principalement la température et la déformation. Les capteurs à fibre optique présentent des avantages notables par rapport aux capteurs traditionnels comme le déport de l'électronique, l'immunité électromagnétique ainsi qu'un important multiplexage. Plusieurs technologies existent. Les systèmes de mesures réparties par fibre optique permettent d'obtenir en une seule acquisition, un profil de déformation ou de température tout le long de la fibre optique avec un pas de mesure centimétrique et une portée kilométrique, soit plusieurs milliers de points de mesures. On comprend que cette technique présente un avantage certain pour l'auscultation de structures présentant de grands linéaires ou de grandes surfaces. Cependant, la mise en pratique d'une instrumentation durable de structures en béton armé nécessite de résoudre certaines problématiques telles que : - la durabilité du système de mesures. En effet, le câble étant exposé aux conditions environnementales

(fibres en parement) ou au milieu cimentaire (fibre noyée), ses fonctionnalités sont susceptibles d'évoluer dans le temps en fonction des dégradations éventuelles causées aux matériaux constitutifs où aux éléments de fixation (joint de colle, attaches mécaniques). La protection par enveloppe gainant doit notamment être utilisée avec précaution, car elle modifie les conditions de transfert des efforts du milieu au capteur. La pérennité du mode de fixation externe du câble à fibre optique à la structure (attache continue ou discrète, mécanique ou par collage) sera investiguée. La thèse proposée vise à étudier ces différents aspects. Le travail du doctorant est principalement localisé à l'Ifsttar-Marne-Ma-Vallée, mais sa recherche est menée en étroite collaboration avec l'IRSN dans le cadre du projet ODOBA (Observatoire de la durabilité des ouvrages en béton armé), sur le site de Cadarache.

Une sélection de quelques câbles disponibles dans le commerce et adaptés aux applications visées, le travail de thèse est : - de caractériser avec rigueur le transfert d'effort entre la structure et les câbles considérés (détermination de la fonction de transfert mécanique des câbles), en s'appuyant à la fois sur des essais mécaniques et des modélisations appropriées. Concernant la mesure de déformation, un traitement approprié des données pourra permettre de découpler les effets de la température et de la sollicitation mécanique. - mener une étude de durabilité afin d'évaluer l'impact des facteurs environnementaux sur les fonctionnalités du câble fixé à la structure, en reliant ces évolutions à des paramètres matériaux. Des conditions de vieillissement accélérées représentatives des applications visées seront choisies (sensibilité à l'humidité, aux alcalins du béton et aux cycles thermiques).

Le doctorant :	Martin CAHN (2017-2021)
Sujet de la thèse :	Dimensionnement d'intersections d'ouvrages souterrains
Soutenance :	Thèse en cours.
Directeur de thèse	Denis BRANQUE
École Doctorale :	ENTPE
Financement :	Enterprise GEOS, INGEROP et SGP
Production scientifique :	-
Situation professionnelle :	

Objet de la thèse :

Les objets étudiés dans le cadre de cette thèse sont deux types d'intersection que l'on retrouve en travaux souterrains. Ils concernent la jonction entre :

- Un tunnel principal et un rameau secondaire ;

- Un puits circulaire principal et un tunnel secondaire.

Problématique :

Ces intersections constituent une situation hautement tridimensionnelle et sont le lieu d'une concentration de contraintes de part et d'autre du percement. Il n'existe cependant pas aujourd'hui de méthodologie éprouvée permettant leur dimensionnement. Le recours à des modélisations éléments finis 3D en phase d'études comme en phase d'exécution est limité, car le temps nécessaire à la réalisation de tels modèles et les problèmes numériques associés restent importants.

Les projets récents montrent que les travaux nécessaires à la réalisation des carrefours nécessitent généralement des dispositifs constructifs ouvrageux mais dont les justifications sont critiquables ou absentes. Les intersections nécessitent donc la réalisation de travaux complexes peu justifiés au regard des phénomènes en jeu qui sont souvent mal compris.

Une analyse fine du comportement de l'intersection nécessite une connaissance préalable précise de l'état de contraintes dans le terrain autour de l'excavation et dans le revêtement de l'ouvrage principal après son creusement. Ceci suppose la compréhension et in fine la modélisation :

- Du comportement géo-mécanique du terrain dans lequel le tunnel ou le puits est creusé ;
- Des améliorations apportées par les traitements de terrains éventuels ;
- Du processus de creusement de l'ouvrage principal et de l'état de contrainte dans le revêtement qui en résultent.

Le dimensionnement de l'intersection nécessite quant à lui :

- De pouvoir prédire les redistributions de contraintes autour de l'ouverture au moment du percement dans les structures provisoires, le revêtement définitif et le terrain ;
- De prendre en compte et de comprendre l'influence du phasage et des dispositifs de soutènement provisoires ;
- D'estimer le report de charge s'appliquant, le cas échant, sur le revêtement de l'ouvrage principal et secondaire à long terme.

a) <u>Démarche proposée :</u>

La base expérimentale de cette thèse est le chantier du T3A de la ligne 15 sud du Grand Paris. Sur ce projet, les intersections en tunnel se font entre :

- Un tunnel de 8,7 m de diamètre intérieur creusé au tunnelier et des rameaux de 5,8 m de haut et de 7,15 m de large intrados creusés en méthode traditionnelle.

Les intersections en puits se font entre :

- Le puits de départ du tunnelier de forme trilobique en parois moulées, de 24 mètres de diamètre intérieur et le tunnel au tunnelier ;
- Des puits de parois moulées de 8,9 m de diamètre intérieur et des rameaux de jonction dont les dimensions ont été déjà citées.

L'analyse du comportement de ces intersections passe par une auscultation reposant principalement sur des capteurs distribués à fibres optiques. Celle-ci est mise en œuvre à la fois dans le terrain, le revêtement et le soutènement des ouvrages principaux et secondaires. Les résultats de cette auscultation servent de point de comparaison et de référence à des modélisations éléments finis 3D complètes.

La combinaison de l'auscultation et de la modélisation 3D permet une compréhension plus fine des phénomènes en jeu et de leur importance respective.

A terme, l'objectif de la thèse est d'aboutir à des méthodes de dimensionnement simplifiées et robustes ainsi qu'à l'optimisation des méthodes constructives.

Tableau 1-1 : Une synthèse des thèses co-encadrées jusqu'à Décembre 2017.

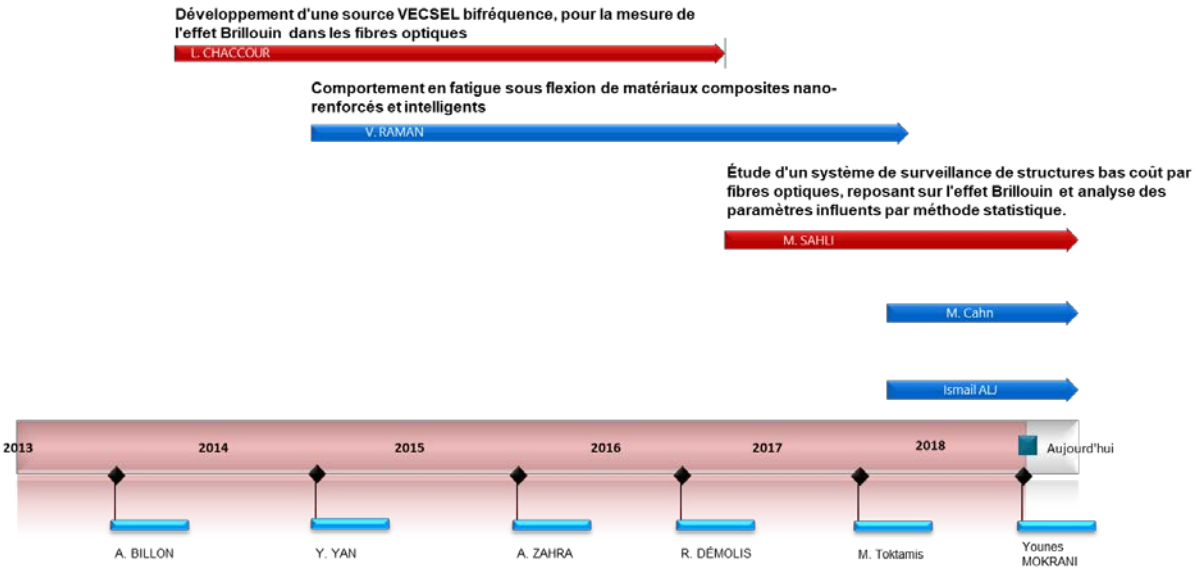

Figure 1-4 : Schéma chronologique récapitulatif de l'activité d'encadrement, liée à l'évolution de l'activité de recherche, depuis 2013.

Deux sujets de thèses avec financement CIFRE sont en cours d'élaboration. Les deux sociétés sont SIXSENSE du groupe VINCI, et un TPE français DIMIONE systems.

1.4.2 Production scientifique

Ma stratégie de publication privilégie naturellement la publication en revue internationale à comité de lecture, également les bonnes conférences internationales avec comité de lecture. La publication dans les revues internationales intervient avec des résultats très marquants.

Mon expérience depuis mon arrivée à l'IFSTTAR présente une différence importante par rapport à mon évolution dans la phase doctorale et postdoctorale. Mes efforts m'ont permis de bénéficier du changement des thématiques principales de mes recherches pendant ma carrière, et surmonter les difficultés liées au déménagement des locaux de l'IFSTTAR de Paris à Marne-la-vallée en 2013.

J'ai gardé un bon dynamique de publication, avec évolution de taux de publication, en qualité et quantité comme présenté la suite de ce paragraphe.

1.4.2.1 Synthèse des publications

Catégorie	Publiés (totale)	A l'ifsttar, (depuis 2011)	Soumis
Revue internationale	16	12	2
Chapitre d'ouvrage international	1	1	
Conférence internationale	34	19	2
Conférence francophone	19	15	
Séminaires et congrès invités	10	10	
Brevet	1	1	

Tableau 1-2 : Synthèse des publications (2008-2018)

Éléments bibliométriques (source : Publish or Perish au 10 décembre 2017) :

- Années de publications 2008-2017
- L'article le plus cité : 38 fois,
- h-index : 6,
- g-index : 11,

Je présente dans l'annexe **Error! Reference source not found.** la liste complète des publications.

1.5 Collaboration, participation aux projets de recherche et réalisation des expertises

Cette partie me permet de présenter brièvement les collaborations que j'ai pu réaliser au cours de ces dernières années aux trois niveaux : local, national et international. La stratégie que j'ai adoptée était de nouer des liens avec différents laboratoires au sien de l'IFSTTAR pour renforcer le côté applicatif à l'utilisation des capteurs à fibres optiques distribuées, et élargir ce réseau avec des partenaires extérieures. Mes objectifs dans la première phase sont de cibler des partenaires industriels pour les applications des capteurs distribués à fibre optique et des partenaires académiques pour les recherches dans le développement des capteurs.

Il est très utile de mentionner que j'ai participé activement à la préparation de réponses à des appels à projets (ANR, Européens, contrats industriels,).

Voici la liste des projets que j'ai contribué à monter. Parmi les projets Européens que j'ai montés, toutes les propositions ont franchi la barre scientifique mais insuffisamment pour être financées. Cela m'a amené à réfléchir sur le rôle essentiel du lobbying dans le montage de projets Européens. Cette activité de montage de projets prend une place non négligeable dans la vie du chercheur pour une faible probabilité de succès.

Je donne dans la liste suivante, les collaborations principales et projets réalisés et en cours :

-Projet BADIFOPS (2011-2015), un projet soutenu par *Réseau Génie Civil et Urbain* (RGC&U) : Participant, responsable de WP : capteur à fibre optique. Montant : 300keurs. Les partenaires : Eiffage, CSTB, CEREMA.

-Le projet CSASurcharge (2014-2017), un projet soutenu par *Réseau Génie Civil et Urbain* (RGC&U) : Participant, responsable de WP : capteur à fibre optique. Montant : 200keurs, Les partenaires : CEREMA.

-Le projet ANR-SSHEAR (2014-2018), Participant : Montant : 800keurs, Les partenaires : CEREMA, SNCF, Railenum, Université Paris XI.

-Projet EDF-IFSTTAR CIBEFHY (2013-2017), Participant, Montant : 500keurs, Les partenaires : CEREMA, EDF, IFSTTAR-Nantes/Bron.

-L'instrumentation poutre VIPP de Clerval (2014-2016), Participant, Montant : 300keurs, Les partenaires : ASFA, CEREMA, IFSTTAR-Nantes. *L'équipe du projet Clerval, dont je faisais partie, est le lauréat du prix de l'innovation du Cerema de 2016, pour l'ensemble des travaux réalisés, notamment l'instrumentation par fibres optiques.*

-Projet Everest soutenu par l'IRT Jules Verne (2014-2017), Participant, Montant : 1.4Meurs, Les partenaires : université de renne 1, université de Bretagne sud, ENSAM-ParisTech, Alstom, Europe technologies.
-Projet ANR-EMODI (2014-2018), Participant, Montant : 900keurs, Les partenaires : CEA, SEM-REV, IREENA, LHEEA, NEXAN, RTE.
-Projet européen FASSTbridge (2014-2018), Participant, Les partenaires : Alta Vista Solutions, COLLANTI CONCORDE S R L, Comunidad de Madrid VIA M Dirección General de Carreteras, DRAGADOS S.A, Leonhardt, Andrä und Partner, Tecnalia, USTUTT.
-Projet ELiSA (2015-2016), contrat industriel avec VALEO, Participant : Valeo, Montant 50keurs.

Enfin la liste des projets soumis et non financés :
-Empreinte carbone réduite avec le nouveau détecteur de corrosion en fibre optique. Projet Fonds France Canada pour la Recherche (FFCR) 2018, Participant, Les partenaires : Université de LAVAL au Canada.
-AGORA of the 21st century for a resilient Paris Projet tremplin AAP I-SITE.
-RETRIEVE, réponse à un appel à projets européens H2020. Participant, Les partenaires: CHALMERS-Sweden, CETMA-Italy, SMHI-Sweden, QUB-Ireland, UNICAN-Spain, IMG-Italy, BZN-Hungary, XLAB-Slovenia, ORBITON AS-Norway, ACCIONA-Spain, NPRA-Norway.
-MSCA DisdRab dans le cadre des appels ITN-ETN Marie-Curie Urban-STEP 2016.
Mon implication était pour le développer un system de mesure de la densité des gouttes de pluie par fibres optiques dans une surface >20m².
-MSCA DisdRab dans le cadre des appels ITN-ETN Marie-Curie Urban-STEP 2015.
-Projet européen PROHSITES, réponse à un appel H2020, 2015. Parteners : Federal Institute for Materials Research and Testing (BAM), Universität der Bundeswehr München (UBM), CreaLab GmbH, HBI Haerter Consulting Engineers, SP Sveriges Tekniska Forskningsinstitut AB,
Themes de Recherche: Reinforcement of materials and structures, resilience of structures and networks, smart composites and structures, nanomaterials and nanotechnologies, sensors, structural health monitoring, durability and multi-scale modelling, critical infrastructures, structural management
-Projet européen CIRIAM, réponse à un appel H2020, 2015.

Parteners : Federal Institute for Materials Research and Testing (BAM), Universität der Bundeswehr München (UBM), CreaLab GmbH, SP Sveriges Tekniska Forskningsinstitut AB
Themes de Recherche: resilience of structures and networks, smart composites and structures, transport infrastructure, structural health monitoring, durability and multi-scale modelling, structural management.
-Projet européen ENHANCE, réponse à un appel H2020, 2015.
- « INBRICOSS » à l'appel à projets générique de l'ANR, 2014. Parteners : LPN-CNRS (C2N), Thales TRT, Andra.
La thématique est pour développer un interrogateur à fibre optique avec des mesures des spectres Brillouin, basé sur une source laser bifrequence.
- « INBRICOSS » à l'appel à projets VBD de l'ANR, 2013.

1.6 Développement, acquisition de matériels

Le développement de mes compétences, l'acquisition de matériels, la thématique des systèmes d'instrumentation par fibres optiques, et la mise au point de protocoles expérimentaux ont été pour moi des sujets conséquents avec un investissement de temps non négligeable.

Depuis mon arrivée à l'IFSTTAR, j'ai constaté l'absence d'équipements nécessaires pour l'implication dans des projets d'instrumentation par fibres optiques, et mon premier défi a été l'acquisition des systèmes performants répondant aux besoins du laboratoire et à l'évolution des activités sur une période de 5 années au moins. L'option idéale était un interrogateur des fibres optiques avec une haute résolution spatiale, une portée limitée, et fonctionnel avec les fibres monomodes et multimodes. Le premier investissement est venu à travers le projet BADIFOPS, ce qui a permis l'acquisition d'un interrogateur basé sur la rétrodiffusion Rayleigh, de Luna-technologies. Dans différents projets qui ont suivi j'ai pu compléter pour obtenir toutes les options de ce système, avec des périphériques comme le commutateur optique à 8 chaines.

Un deuxième investissement important a été l'acquisition d'un interrogateur pour réaliser les mesures thermiques dans les fibres optiques, et basé sur la rétrodiffusion Raman de la société LIOS[14]. J'ai fait le choix d'un système utilisable avec les fibres monomodes.

[14] http://www.nktphotonics.com/lios/en/

Figure 1-5 : Les deux investissements majeurs depuis mon arrivée à l'IFSTTAR : à droite : OBR4600 de la société LUNA, (à droite) : Un interrogateur LIOS WELL.DONE de la société LIOS.

1.7 Conclusion, et introduction de la synthèse scientifique

La partie consacrée à mon parcours professionnel avait pour objectif de montrer les principales composantes de mon parcours, l'évolution de mes compétences et ma carrière, les variétés et les complémentarités de mes compétences. Au vu de cette analyse, j'ai décidé ci-après de ne développer que les thématiques qui ont fait l'objet de davantage de valorisation et qui sont suffisamment matures dans la suite de mon mémoire.

Je commencerai donc par une présentation des phénomènes de rétrodiffusion dans les fibres optiques, suivi par les techniques de réflectométrie optique qui donneront accès aux différents paramètres liées aux caractéristiques des fibres optiques. Les différents paramètres qui influencent les caractéristiques des fibres optiques seront présentés ensuite. Je présenterai ensuite les résultats marquants, communiqués dans des congrès et dans des revues internationales. Enfin, je terminerai par les perspectives liées au domaine des capteurs à fibres optiques, à moyen et long terme.

J'ai donc choisi d'aborder le sujet de capteurs à fibre optique selon les deux axes : les interrogateurs, et applications dans le génie civil. Je n'aborderai pas les autres activités de recherche, dans lesquelles les différents travaux réalisés sont avec des partenaires industriels.

2 Scientific activities

This part summarizes my main research activities since 2011, in LISIS laboratory at IFSTTAR. The evolution of monitoring and instrumentation solutions based on distributed fiber optic sensors is a particularly stimulating guideline for research activities related to infrastructures health monitoring and control at LISIS. In addition to the topics directly related to infrastructure health monitoring, and the impact of the environmental parameters on the performance of distributed optical fiber sensors, my research activities also concern working on the development of new configuration of Brillouin based distributed sensor, characterization and analysis of photonic components/devices. The different items will be described and the main results will be presented briefly.

2.1 Background and motivations

The concept of smart and sustainable cities is relatively new, and definitions contained within academic literature are currently evolving to reflect the ongoing development of ideas and practice. A standard definition of a smart and sustainable city is: "settlements where investments in human and social capital and traditional (transport) and modern Information and Communication Technology (ICT), communication infrastructure fuel sustainable economic growth and a high quality of life, with a wise management of natural resources, through participatory governance" [1]. That means, Smart and sustainable cities aim to integrate the recent efforts to introduce smart Information and Communication Technology-enabled, communicative and networked features of a city's infrastructure, services and citizens, and use this to manage the urban environment better to achieve growth and sustainable development. For that, governments and local authorities are seeking new ways to better manage the services they provide to their citizens, working on high-quality national infrastructure which is essential for supporting economic growth and productivity.

As cities increasingly complex challenges, which require beside the growth in the supply and safety of the different services, an interactive governance to insure an intelligent urban planning that responds to the future needs (Figure 2-1). Also, disaster prevention requires that engineers design and maintain civil engineering structures based on stress integrity assessments. These requirements turn infrastructural health monitoring into a key element of industrial businesses.

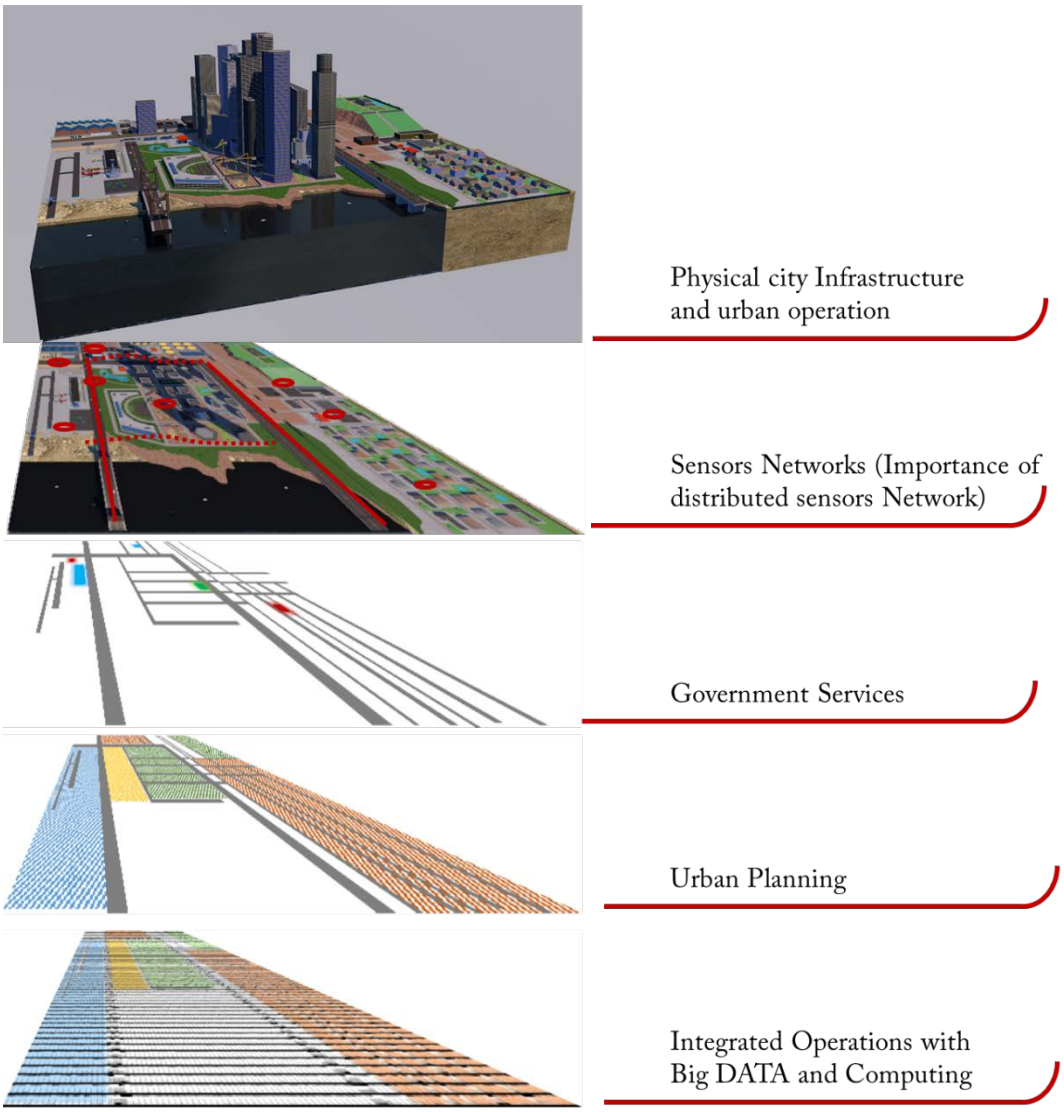

Figure 2-1 : Illustration of how solutions and infrastructures can be integrated for a complete and efficient management of urban environments [2, 3]. Infrastructure heath monitoring using distributed optical fibers sensors, is situated in the physical layer. The fiber installation can be realized during the construction phase or can be added to buildings under construction.

Different sensor networks could be used, based on IoT solutions. These point sensors offer a huge amount of physical and chemical information, and they can be widely deployed. In spite of their capacity they have some limitations related to the electrical supply, life cycle and life time, besides the difficulties related to embedding them in the structures.

Clearly there is a need for a technique that allows distributed measurements (mainly strain and temperature) to be captured in real-time over lengths of a few meters to tens of kilometers, even hundreds of kilometers inside a huge structure or close to its surface. The distributed sensing technique based on optical fibers has the advantage of satisfying all these requirements.

Following the immense impact, they had on telecommunications applications, optical fibers have established their advantageous value also in the field of sensing, fiber optic instrumentation has progressively evolved since the early 1980s. To a large degree, optical fiber sensor instrumentation has taken advantage of the maturing component market for telecommunications use, and its progress has been dictated by it.

More recently, security applications from border fences, oil and gas pipes to water leak detection, as well as the need to monitor the health of different structures such as: bridges, tall buildings, wind turbines, airplanes, train tracks, etc., have called upon the unique properties of optical fiber sensors. In addition, due to their resistance to radiation, the optical fiber sensors are potential candidates for monitoring works of radioactive waste disposal.

They can be integrated in the structure or put siding and allow remote monitoring at kilometric range. Through interactions between the light and the fiber on its entire length, a distributed sensor continuously referred to as distributed sensor. The measurement technique has the advantage of allowing continuous measurements over distances of the order of tens or even hundreds of kilometers.

Different applications of distributed optical fiber sensor in infrastructure health monitoring could be mentioned:

-Optical fibers installed at home can be used to monitor the temperature inside and outside, then evaluate the building energy efficiency all the seasons of the year. This process allows taking the suitable decision to reduce energy use at home level and neighborhood level.

-Pressures on water supplies in cities means that water efficiency is a key component for the smart city, with innovation required at city infrastructure level, so as to prevent the need for expensive and energy hungry desalination plants, optical fibers installed in water pipes give a solution for the measurement of pressure along the water pipes.

-Optical fibers installed on bridges, can give detailed information about the health of the structure (damage zones, cracks, etc...). Monitoring Bridges with optical fibers can help in localized interventions when cracks appear.

-In tall buildings, optical fibers sensors can be used to monitor retaining walls, piles, and temperature, even rebars.

-On Highways, it can be used to monitor surface movements, deep seated ground movements, and soil nails.

All the real time gathered information related to the infrastructures could be treated and used to make a "Smart Grid", which can facilitate the decision making for politics power, like making new investments and creating new infrastructures. Or maintain or improve the infrastructure. The decisions to maintain or improve the reliability and functionality of any civil engineering structures and transportation infrastructure systems, represent important challenges for a 21st-century society, and can be realized through proper integrated management planning in a life-cycle comprehensive framework. Structural Health Monitoring is the approach which can successfully assist in meeting these challenges by providing actionable, quasi-real-time information regarding structural performance and health condition.

Cost-competent maintenance and management of civil infrastructure requires balanced consideration of both the structure performance and the total cost accrued over the entire life-cycle. Most existing maintenance and management systems are developed on the basis of life-cycle cost minimization only. So, to extend an optimize these costs and have the maximum security we should be able to do some correction and preventive actions to insure the life time functionality of the civil infrastructure.

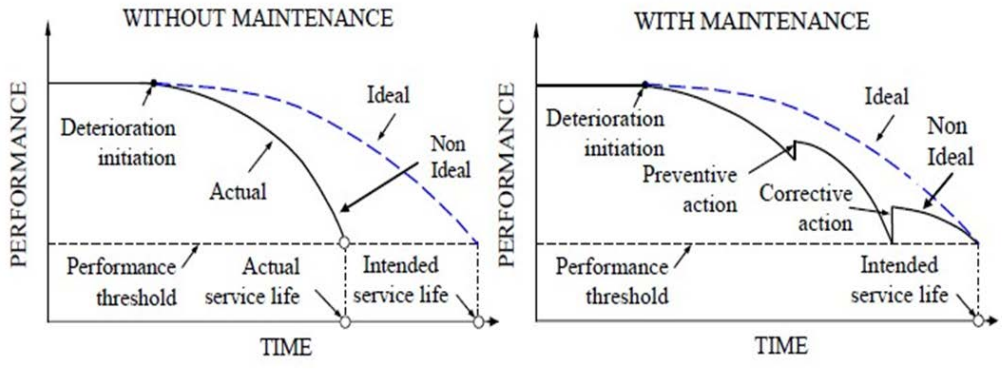

Figure 2-2 : Variation of infrastructure performance with and without maintenance [4].

Distributed fiber optic sensors provide the unique opportunity to measure strain or temperature continuously along a standard optical single mode silica fiber. The huge amount of information about strain or temperature that can be acquired within a relatively short time makes distributed fiber optic sensing technologies particularly interesting for laboratory tests and field applications.

Truly distributed sensing techniques are commonly based on some kind of light scattering mechanism occurring inside the fiber. The different scattering mechanisms could be investigated using the optical time domain reflectometry (OTDR)[5]. Where an optical pulse is launched into an optical fiber and the variations in backscattering intensity caused by physical parameter is detected as a function of time. Alternative detection techniques such as frequency-domain approaches have been also demonstrated[6].

The evolution of the distributed fiber optic sensors and their applications is in increased developed. Nowadays there are different key players in the distributed fiber optic sensor market like: Yokogawa Electric Corporation, Luna Innovations Incorporated, Silixa Ltd, Schlumberger Limited, Halliburton Company, Weatherford International plc, QinetiQ Group plc, OFS Fitel LLC, Bandweaver, OmniSens S.A., Brugg Kabel AG, AP Sensing GmbH, AFL, Neubrex Corporation, Ziebel AS.

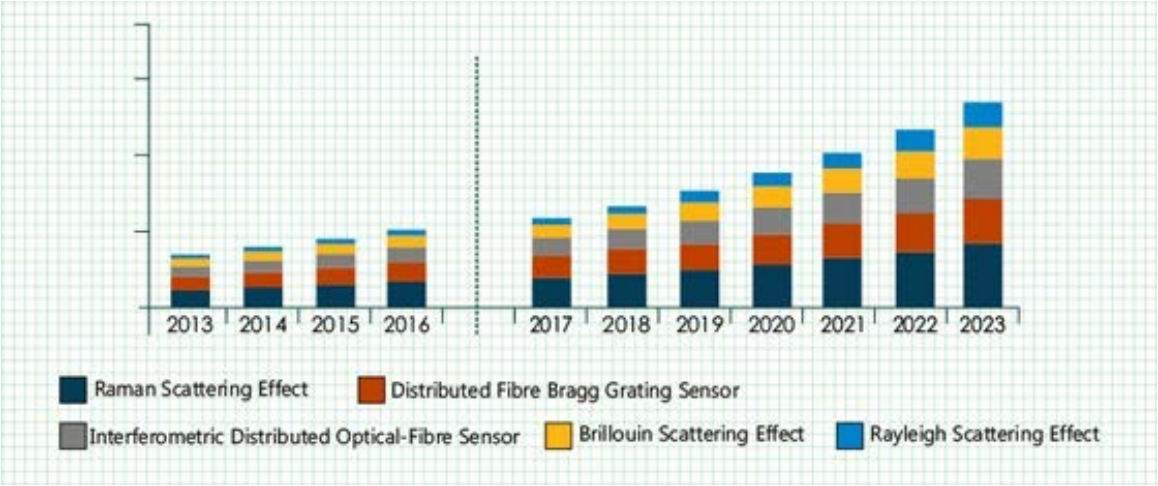

Figure 2-3 : Distributed fiber optic sensor market evolution (2013–2023)[7].

The most important part of my research activities at the ifsttar are related to the needs of the different partners inside the institute and the vast domain of applications in civil engineering and geotechnical applications. Different published books presents the details concerning the distributed optical fiber sensors [8-10], for that I'll present only the headlines, then the main results of my works.

2.2 Optical Fiber

The starting point of the subsequent remarkable progress in optical communication were triggered in 1966 by Kao[15] [11, 12], he predicted that a low-loss glass fiber waveguide of around 20dB/km would be needed to realize a larger information capacity than the coaxial cable and radio systems available at that time. Three years later, Robert Maurer, Donald Keck, and Peter Schultz of Corning succeeded in developing a length of 29 meters of glass fiber exhibiting an attenuation lower than 20 dB/km at 632.8nm [13, 14]. Major improvements were made by the original inventors and others, like Bell Laboratories, during an intensive period of research and development before optical fibers went into mass production in the early 1980s. The attenuation loss of silica glass-based fibers was greatly reduced in the to 0.154dB/km at 1.55μm by reducing the impurities in silica glasses with the vapor phase deposition technique in 1986 [15], which is close to the theoretically predicted value. In 2015, the attenuation record was set by Corning, with 0.1460 dB/km at 1.550μm[16]. A new record was realized 2017 by Sumitomo Electric Industries[16], with 0.1419 dB/km at 1560 nm [17].

The optical fibers are dielectric waveguides which can have many propagation modes. The standard structure of optical fibers, used in sensing or telecom application, includes three parts: The core, cladding, and coating. The cladding has a refractive index, which is slightly lower than the refractive index of the core.

[15] Charles Kuen Kao was awarded the Nobel Prize for physics in 2009 for groundbreaking achievements concerning the transmission of light in fibers for optical communication.

[16] http://global-sei.com/company/press/2017/03/prs029.html

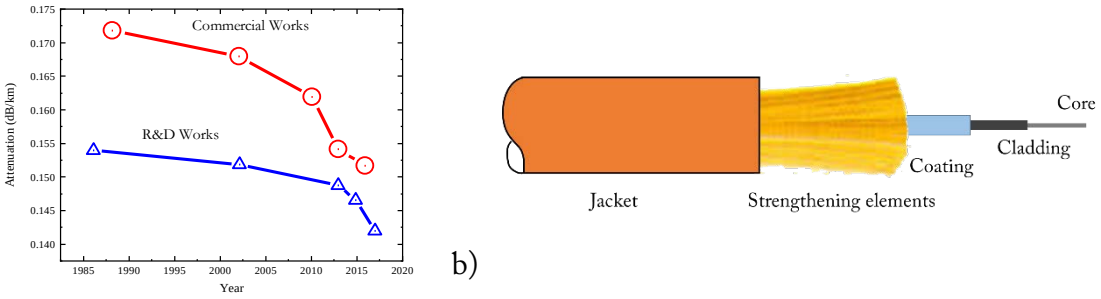

b)

Figure 2-4 : (a) Evaluation attenuation in ultra-low loss fibers [16, 17]; and (b) General structure of all types of optical fibers.

The lower attenuation was due in part to improved fabrication techniques that reduced impurities, but it also stemmed from the development of supporting technologies (e.g., lasers, detectors, and other components) that operated at higher frequencies where intrinsic loss in silica fibers was lowest.

Using optical fibers for distributed sensing has different main advantages, compared to any other sensors. The main advantages of optical fiber sensors can be summarized as[8, 18]:

-Low Signal Attenuation: as mentioned in the previous section.

-Electromagnetic interference immunity: Noise immunity is one of the most useful features of optical fibers in industrial applications. In environments where electromagnetic interference is prominent and unavoidable, optical fibers are unaffected. While cables are normally contained in protective sheaths and often run inside conduit, there is no need to physically isolate fiber-optic cables from electrical cables. This makes optical fiber routing simpler.

-No crosstalk: Since fibers is non-electrically conductive, they do not pick up electromagnetic interference, and signals on adjacent cables are not coupled together. Different sensing parameters on different fibers in the same cable is possible.

-Inherent Signal Security: for applications where signal security is a concern, optical fiber is an excellent solution. Fiber-optic cables do not generate electromagnetic fields that could be picked up by external sensors and don't perturb the work of these sensors.

-Lightweight, small diameter: makes the fiber less intrusive, without any modification to the infrastructure behavior, and this makes installation easier.

-Safe for use in hazardous areas: Fiber-optic can be used to realize measurements into potentially inflammable and explosive environments without a risk to delivering or storing sufficient energy to ignite an explosion. This makes fiber-optic technology particularly useful when designing intrinsically safe systems and remote sensing in inaccessible sites or harsh environments and multi-sensing.

-High chemical and thermal stability: silica based optical fibers have high chemical and thermal stability, comparable only with platinum, over a wide spectral range from ultraviolet to mid infrared.

2.2.1 Optical Fibers classifications:

The simplest form of the optical fiber consists of a cylindrical core surrounded by a cladding layer whose index is slightly lower than that of the core. Both core and cladding use silica as the basic material, the difference in the refractive indexes is realized by doping the core or the cladding or both. The major designs of the optical fibers are related to the refractive-index profile, the type of dopants, concentration of dopants, the core and cladding dimensions, their numbers and dimensions.

2.2.1.1 Materials:

Historically, glass or silica material was utilized to create the optical fiber. Advancements in technology and the new applications, called for the use of new materials. A complete description could be found in literature [19-21].

1- Glasses (Silica Glass Fibers, Halide Glass Fibers, Rare-Earth-Doped Glass Fibers, Chalcogenide Glass Fibers).
2- Photonic Crystal Fibers (PCF)
3- Plastic Optical Fibers (POF)
4- Nano-Fibers.

We will be interested by “Silica Glass Fibers”, as part of Glasses. Most studies about glasses and their applications have been carried out on silicate and quartz glasses, which transmit the radiation in visible range of the electromagnetic spectra. The glasses can be used for the preparation of optical fibers both for passive and active applications. Specifically, the Silica

Glass Fibers has wide wavelength range with good optical transparency. In the near-infrared spectral region, particularly around 1.5 μm wavelength, the spectral limits of the optical transmission for glasses are shown in Figure 2-8. They are the most used for optical fiber sensing applications. Silica glass can be doped with various materials. Refractive index modification is realized by the formation of dopants from the non-silica starting materials. These dopants include TiO_2, GeO_2, P_2O_5, $A1_2O_3$, B_2O_3 and F. The variation of the refractive index of silica is presented on the Figure 2-5.

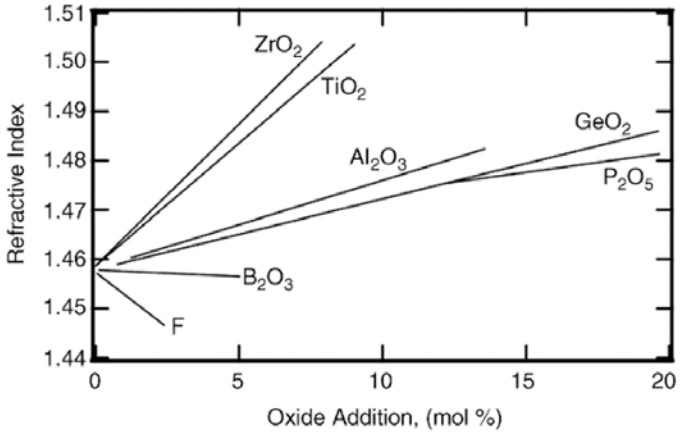

Figure 2-5 : The variation in the refractive index of silica using various dopants [22].

2.2.1.2 Geometry

Based on the geometrical dimensions of the optical guiding structure, we distinguish two main groups: single mode fibers (SMF) and multi-mode fibers (MMF) fibers, they are the mostly used fiber designs which are basically the same, only differing in the core diameter. In single mode (or mono mode) fibers, outlined in Figure 2-6, the diameter of the silica fiber core is usually between 8 to 10μm. The cladding is also made of silica with a slightly lower refractive index than the fiber core to allow the reflection of the light that propagates through the core on the interface between core and cladding. A primary coating protects the fiber from the intrusion of water and chemicals that could be harmful to the optical core. When many fibers are used to form a cable, each coating can be in a different color, which allows distinguishing one from another. The coating is made from plastic material, which is applied on the fiber directly after manufacturing with a standard diameter of 250μm. The refractive index of the primary coating is considerably larger than of the cladding to prevent light that leaves the fiber core into the cladding to be reflected back into the fiber core, causing dispersion. It's possible to have multiple

spatial paths in one optical fiber. The first approach is to use multiple different modes in a fiber by increasing the core diameter to standard values like 50µm or 62.5µm. There are two families with controlled number of modes can be obtained by increasing the diameter of the core of the fiber: few mode fiber and Large effective area fiber

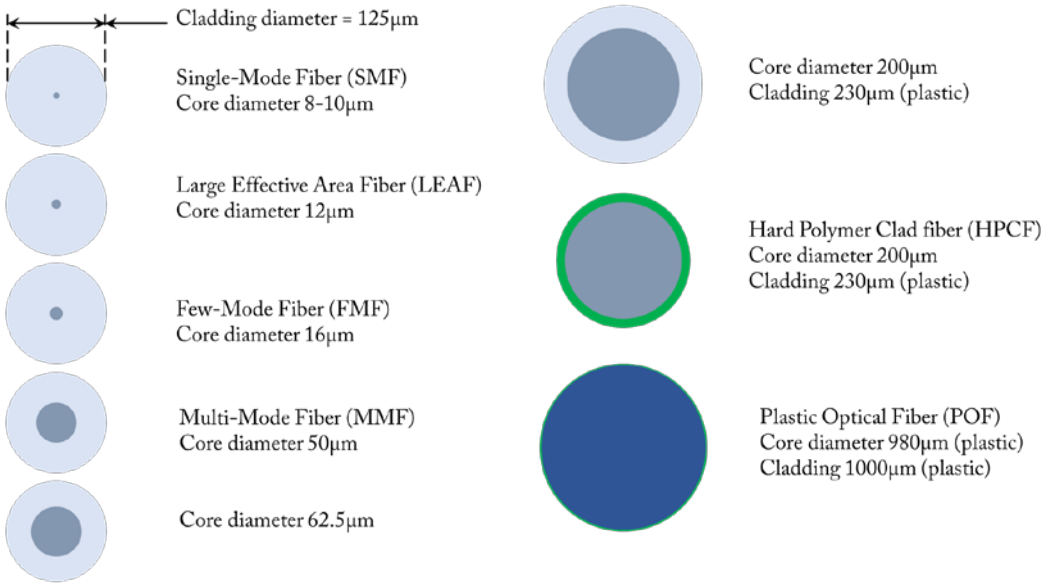

Figure 2-6 : Sketch of common single core optical fibers profile, from single mode glass fiber to multimode plastic fiber [23].

The second approach to have multiple spatial paths in the same fiber is to include multiple separate cores in the same cladding. The Multi-Core Fiber (MCF) structure has been proposed to increase the capacity per cross-sectional area of the fiber [24]. In MCFs we can find two families: uncoupled MCFs and coupled-MCFs. In the uncoupled MCFs, each core has to be arranged for keeping the inter-core crosstalk sufficiently small for long-distance transmission applications. On the other hand, in the coupled MCFs, several cores are placed to realize optical coupling among them (Figure 2-7). We can add that specialty optical fibers with high built-in birefringence, which preserve optical polarization is designed by:

-Changing the geometrical symmetry of the core (elliptical core) or the cladding (elliptical cladding)[25, 26].

-Adding some residual internal stress into the fiber core (PANDA/Bow-Tie)[27].

The different types of single core optical fibers were studied for sensing applications [28-30]. New applications related to the 3D shape construction use the MCF[31-33].

The single mode fibers are the most common used in sensing applications, for different reasons related to the long transmission length due to weak attenuations, the compatibility with telecom installed fibers, and the low cost-effective fabrication. I used single mode fibers in all the applications. The main studied parameter was related to the study of strain transfer through the cabling and coating layers.

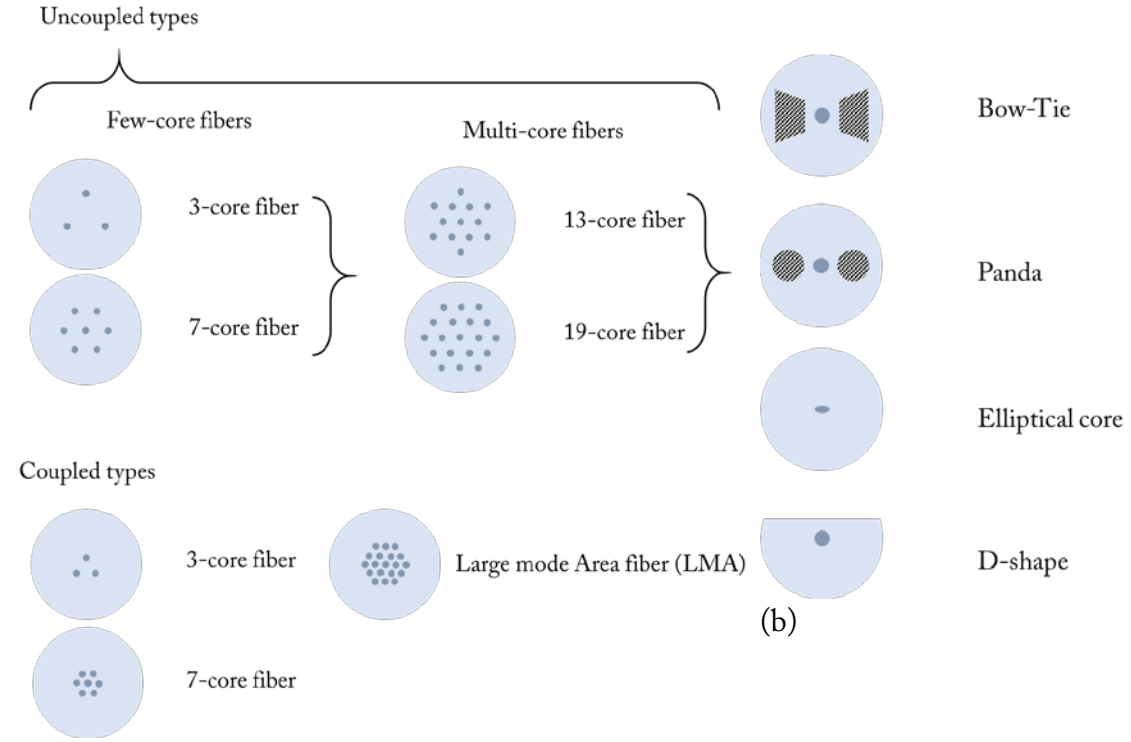

Figure 2-7 : a) Sketch of different multicore fibers; b) Basic design of a single mode optical fiber for specific applications.

2.2.2 Light interaction with glass

Different mechanisms can be observed when light proceeds into any material. These mechanisms could be simplified in four categories:

1- Reflection: part of the light can be reflected by the surface.

2- Absorption: part of the light can be absorbed by coupling into the material.

3- Scattering: part of the light can be scattered by the atoms and defects in the material.

4- Transmission: part of the light can be transmitted through.

Silica based glasses low attenuation window is limited in the short wavelength region (below 300 nm) by absorption of electronic origin or intrinsic defects, and the long wavelength limit (above 2μm) by multi-phonon absorption of molecular dipole origin.

Within these limits the material can be considered transparent. For long propagation distances, as in the case for long distance transmission in silica based optical fibers, losses due to Rayleigh scattering become significant, as shown in Figure 2-8.

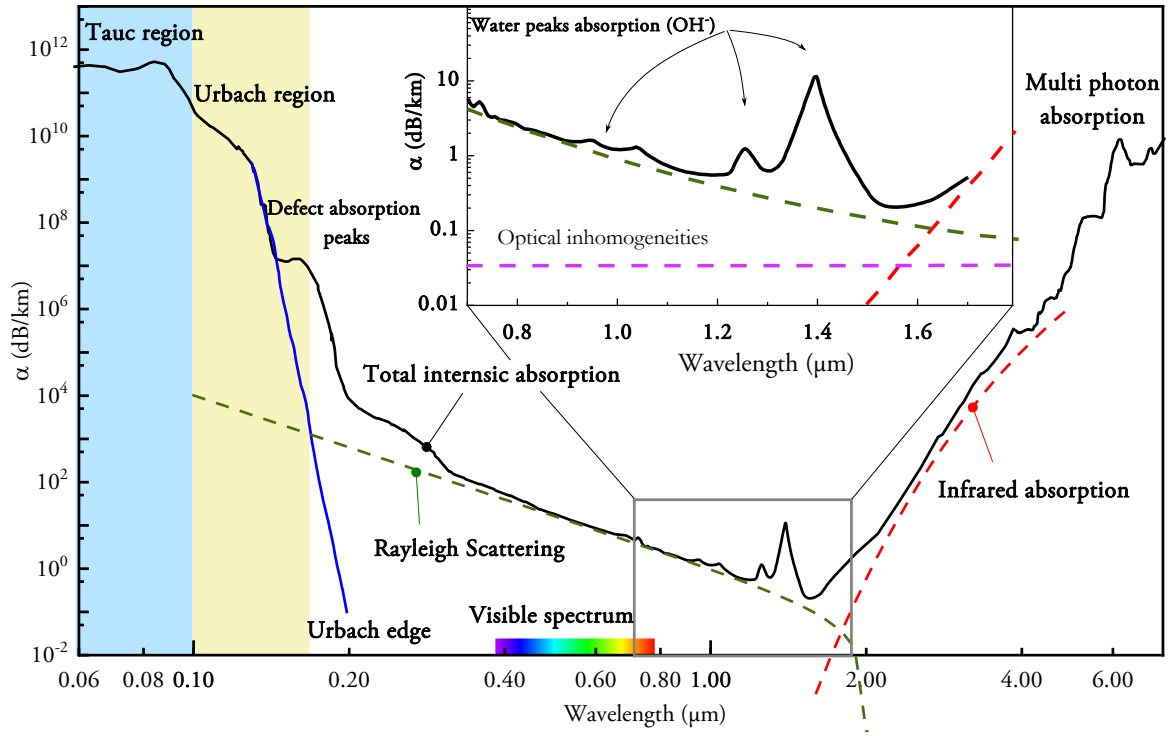

Figure 2-8 : Attenuation with wavelength in a typical silica optical fiber [13, 19, 34, 35].

As shown in the equation (2.1), the total fiber attenuation can be divided into two categories: material attenuations and fiber induced attenuations.

Material attenuations include Rayleigh scattering, ultraviolet (UV), infrared (IR) absorption, and hydroxyl (OH) absorption losses. Material losses are the limiting losses in optical fibers:

$$\alpha = \alpha_{SC} + \alpha_{OH} + \alpha_{UV} + \alpha_{IR} + \alpha_{IM} + \alpha_{im} \qquad (2.1)$$

where α_R is the scattering mechanism loss, α_{OH} the OH^- absorption loss, α_{UV} the ultraviolet absorption loss, α_{IR} the infrared absorption loss, α_{IM} the imperfection loss and α_{im} the absorption loss of other impurities.

2.2.2.1 Light absorption in optical fibers

The three mechanisms of light absorption in optical fiber are:

2.2.2.1.1 Ultraviolet absorption

In glasses the absorption in the ultraviolet region, is characterized by three different regions (as shown in Figure 2-8): the Tauc region, the Urbach region and defect or impurity related absorption [14, 15, 16].

-Tauc region: The absorption in the Tauc region is related to electronic transitions in high probability states (not contributing to band tails, see next paragraph, Urbach region). The optical bandgap, e.g. of a material is typically derived by extrapolating the absorption in the Tauc region to zero.

-Urbach (tail) region: The disordered structure of the glass, which can be viewed as a non-perfect crystal structure, causes a broadened distribution of bond angles, primarily between SiO2 units, leading to band tails. The Urbach energy is a measure of the width of the band tail, or disorder, in an amorphous dielectric. The absorption mechanisms are the same as in the Tauc region although less probable.

-Defects/impurity absorption: Defects and impurities can give rise to strong absorption bands typically located in the ultraviolet to visible wavelength region. This absorption is directly linked to the structural and compositional properties of the material. A common defect is oxygen deficiency with an absorption band located in the ultraviolet region (λ~190 - 250 nm). Absorption due to impurities is often related to transition metals ions with wide absorption bands extending from ultraviolet to visible wavelengths.

Ultraviolet absorption in optical fibers results from electronic absorption bands in the ultraviolet region. The electronic absorption bands are associated with the band gaps of amorphous glass materials. Absorption occurs when a photon interacts with an electron in the valence band and excites it to a higher energy level. For example, the ultraviolet absorption can be expressed as a function of the mole fraction x of GeO_2 and the wavelength as [19]:

$$\alpha_{uv}(x,\lambda) = 10^{-2}\frac{1.54.2\cdot x}{46.6\cdot x+60}\exp\left(\frac{4.63}{\lambda}\right) \tag{2.2}$$

2.2.2.1.2 OH-radical absorption

The OH radical of H_2O molecule vibrates at a fundamental frequency corresponding to IR light wavelength of λ~ 2.8μm. The OH absorption lines are found at different wavelengths λ= 1.39, 0.95, and 0.725μm, which are the second, third, and fourth harmonics of fundamental frequencies respectively, and broad peaks can appear [35].

OH absorption can be characterized by fitting the absorption lines by Gaussian or Lorentzian function [19, 22]:

$$\alpha_{OH_{Gauss}}(\lambda) = \sum_i A_i \exp\left(-\left(\frac{\lambda-\lambda_i}{\sigma_i}\right)^2\right) \tag{2.3}$$

$$\alpha_{OH_{Lorentz}}(\lambda) = \sum_i \frac{A_i}{1+\left(\frac{\lambda-\lambda_i}{\sigma_i}\right)^2} \tag{2.4}$$

In these two equations, A_i is amplitude, λ_i is absorption peak position, and σ_i is the width of the i-th absorption line. Using up to seven absorption lines fits the OH absorption spectrum here. In contemporary state-of-the-art fibers the hydroxyl-group absorption is greatly reduced, and only the peak at 1.38-1.39μm still retains some practical importance [36-38].

2.2.2.1.3 Infrared absorption

Infrared absorption in optical fibers is associated with the characteristic vibration frequency of the particular chemical bond between the atoms of which the fiber is composed. An interaction between the vibrating bond and the electromagnetic field of the optical signal results in a transfer of energy from the field to bond, thereby causing absorption.

The IR absorption expression for $GeO_2 - SiO_2$ glass is[19]

$$\alpha_{IR}(\lambda) = 7.81 \cdot 10^{11} \exp\left(\frac{-48.48}{\lambda}\right) \tag{2.5}$$

In the long wavelength range, 2-14μm, coupling occurs between incident photons and phonons. Phonons are quanta of the vibration in a crystal lattice. In glass, the concept of phonons can be viewed as a distribution of energies, and not a single one as for quantized particles. The coupling to phonons occurs when the electric field produced a change of state of dipole moment

2.2.2.2 Scattering phenomena in optical fibers

These intrinsic scattering effects, due to the structure of the glass itself, are the ultimate limiting factor to the transmission of a given type of glass. Light scattering occurs as a consequence of fluctuations in the optical properties of a material medium.

We refer to the scattering process as spontaneous or linear, when the optical properties of the medium are unmodified by the presence of the incident light beam. Additionally, if the energy of the scattered photons is conserved, and hence there is no frequency shift induced by the process, the scattering is considered to be elastic, whereas if an energy exchange occurs

within the medium during the process, the scattered photons undergo a frequency shift and the scattering is considered to be inelastic.

Under the most general circumstances, the spectrum of the scattered light has the form shown in Figure 2-9, in which Raman, Brillouin, and Rayleigh are present [39]. By definition, the components that are shifted to lower frequencies are known as Stokes components, whereas the components that are shifted to higher frequencies are known as anti-Stokes components. The different features in the scattered spectrum are generated by different processes, depending on the particular type of interaction between the radiation and the matter.

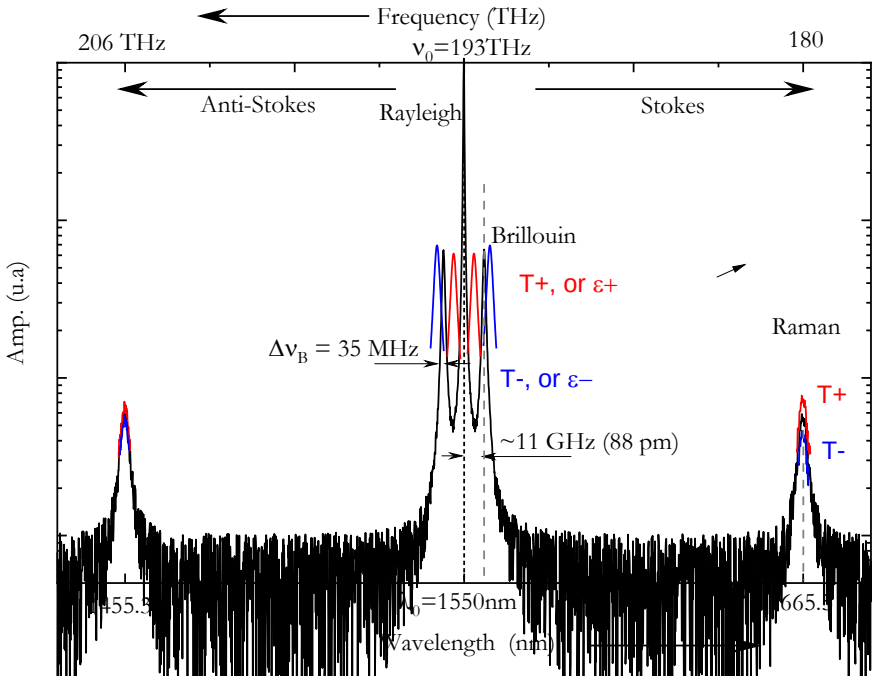

Figure 2-9 : Illustration of the typical optical spectrum of the scattering phenomena in silica (SiO2) optical fibers, for an injected laser wavelength of 1550 nm. [34, 40, 41].

2.2.2.2.1 Rayleigh scattering

Rayleigh scattering is an elastic process of light introduced by Lord Rayleigh (John Strutt) in order to explain the blue color of the sky. He refined his theory of scattering in different papers that were issued from 1871 to 1899. Questions of both the cause of this elastic scattering and the impact of thermal molecular motion on Rayleigh's scattering remained an issue for physicists.

Formally, it can be described as the scattering from fluctuations of the medium entropy (i.e., variations of the degree of molecular organization state).

Spontaneous Rayleigh scattering is a fundamental scattering mechanism arising from density fluctuations frozen into the fused silica during manufacture. The involved scattering centers are fixed, not traveling, into the medium. Therefore, this scattering process does not involve any frequency shift due to Doppler effect. This elastic scattering is related to the medium entropy, i.e. its molecular organization degree.

Figure 2-10 : Lord Rayleigh (1842- 1919).

The Rayleigh scattering loss is proportional to the light intensity propagating in the fiber and is given by the light intensity $P(r)$ and Rayleigh scattering coefficient $A(r)$ in the radial distance [42, 43]

$$\alpha_R = \frac{1}{\lambda^4} \frac{\int A(r)P(r)rdr}{\int P(r)rdr} \tag{2.6}$$

In optical fibers, Rayleigh scattering phenomenon intensity dominates.

In the general case Rayleigh wing scattering does not exist in the optical fiber since silica molecule is centro-symmetric [44].

2.2.2.2.2 Raman scattering

The effect had been predicted theoretically by the Austrian theoretical physicist, Adolf Smekal in 1923 [45]. It was discovered by C. V. Raman and his student K. S. Krishnan in liquids in 1928 [46]. In parallel and in the same year, Grigory Landsberg and Leonid Mandelstam have discovered this scattering phenomenon in crystals [47, 48].

Spontaneous Raman scattering results from the interaction of light with molecular vibrations. This results in a shift of the scattered light frequency with ~13THz in silica optical fibers.

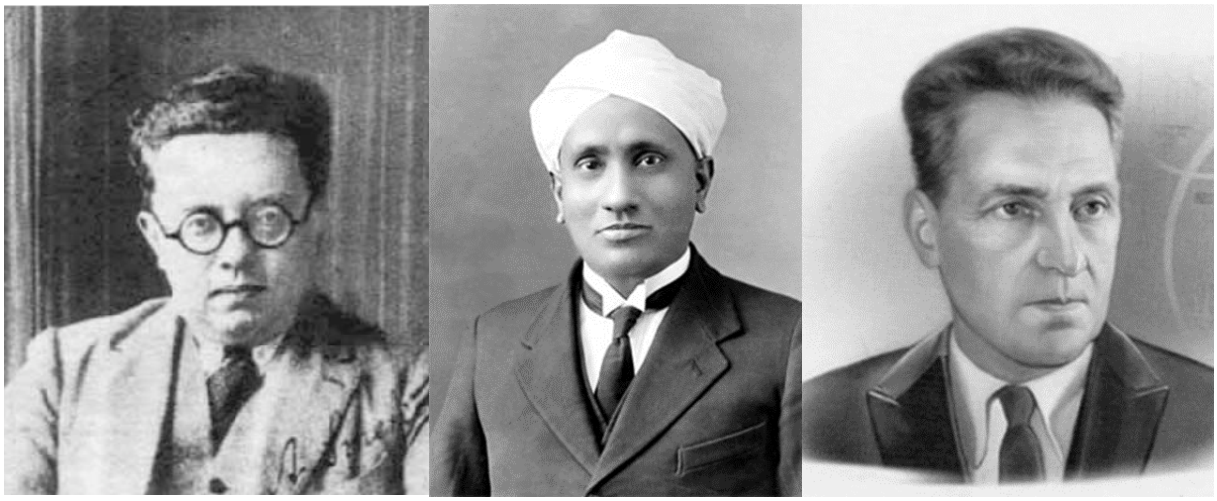

(a) (b) (c)

Figure 2-11 : (a) Adolf Smekal (1895 –1959); (b) Chandrasekhara Venkata Raman (1879-1944); and (c) Grigory Landsberg (1890-1957).

This inelastic scattering, is due to the interaction of photons with the phonons caused by vibrations of molecules and atoms of the material, comes in two scenarios.

-Incident photons lose part of their energy and create optical phonons. The rest of the photon energy is emitted as new photon (Stokes waves) of lower energy/frequency) than incident one.

-Creation of anti-Stokes photons from energy exchange between incident photons and optical phonons. The Photons absorb phonon energy therefore the anti-Stokes photon has higher frequency and energy. The probability of anti-Stokes photons generation is lower than Stokes photons generation, therefore the anti-Stokes wave is weaker than Stokes wave [49, 50].

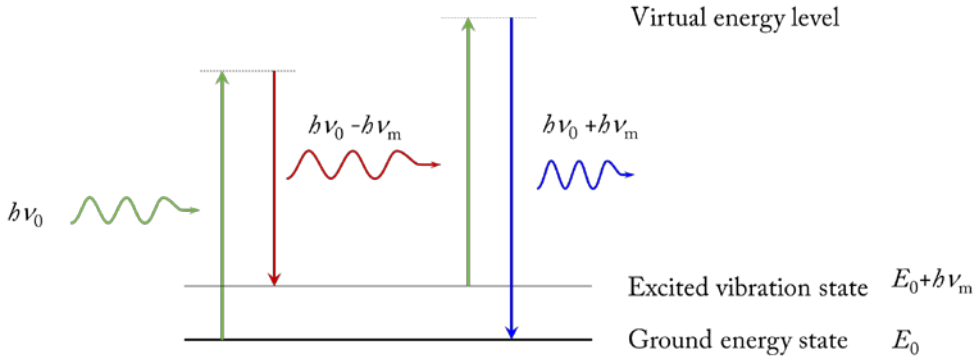

Figure 2-12 : Energy-level diagram showing Stokes and anti-Stokes Raman scattering mechanisms.

Based on the previous information, anti-Stokes wave is more dependent on the temperature changes. The temperature variation is calculated using anti-Stokes wave as detection signal and Stokes wave as the reference signal.

The basic approach to calculate the temperature distribution along the optical fiber is calculate directly the rate between the Stokes and Anti-Stokes signal amplitudes[51]:

$$R(T) = \frac{A_{AS}}{A_S} = \left(\frac{\lambda_S}{\lambda_{AS}}\right)^4 \exp\left(-\frac{hcv}{kT}\right) \tag{2.7}$$

For Raman scattering the interaction is with optical phonons, while interaction with acoustic phonons is called Brillouin scattering.

2.2.2.2.3 Brillouin scattering

Historically, Brillouin scattering is named after Léon Nicolas Brillouin (1889-1969). A French physicist who first predicted the inelastic scattering of light (photons) by thermally generated acoustic vibrations (phonons) in 1922. The soviet physicist Leonid Mandelstam (1879-1944) is believed to have discovered the scattering as early as 1918, but he published it only in 1926. For that reason, the Brillouin-Mandelstam light scattering may be used in some references. Spontaneous Brillouin scattering comes from density fluctuations associated to pressure (acoustic) waves propagating within the medium. Molecular thermal agitation sets off these acoustic waves. The scattered light frequency is Doppler-shifted, the frequency shift being related to the velocity of acoustic waves in the medium (this shift is in the order of some GHz in silica optical fibers). Although spontaneous Brillouin scattering is very weak in optical fibers (30 dB weaker than Rayleigh scattering), it is of importance when acting as an initiation process for stimulated Brillouin scattering [52].

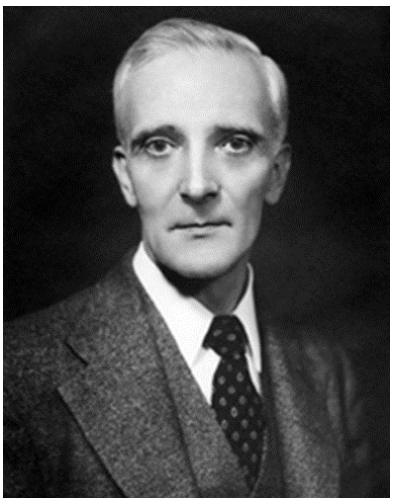

a

b

Figure 2-13 : a) Léon Nicolas Brillouin (1889-1969), b) Leonid Mandelstam (1879-1944)

When an optical pulse (pump wave) propagates along the optical fiber, the electrical field interacts with the material by changing the material density through the electro-striction effect. The striction pattern then generates vibration waves (phonons), at the expense of the energy of the pump light that gets its energy reduced. The effect also implies that an acoustic wave which is present in the material interacts with the electromagnetic field through energy exchange[53]. The mechanical deformation pattern interacting with the pulsed light lifetime is less than 10 nanoseconds[54, 55]. This energy exchange between vibrations and the optical pump gives rise to the generation of photons with different frequencies. Light-waves frequencies are shifted with respect to that of the pump light[56].

Brillouin scattering process has two mechanisms:

- "Stokes" interaction in which the pump light loses energy and create the mechanical waves (phonons), and the scattered light has lower optical frequencies with respect to the pump frequency.

- "Anti-Stokes" Brillouin interaction, in which a pump photon gets energy from a pre-existing mechanical wave (excited phonon) increasing the photon energy. The scattered light has higher optical frequencies with respect to the pump frequency, with lower probability.

In order to efficiently generate Brillouin scattering, the spectral purity combined with the intensity of the pump light must create a regular and strong pattern of electrostriction. This translates into some constraints on the pump light wave in terms of maximum linewidth and minimum power threshold.

The Brillouin effect arises from a pump-probe process in which a part of the energy is temporarily stored in a short-lifetime mechanical form, and it can turn back into electromagnetic energy spontaneously, as well as a stimulated effect[57, 58].

The characteristics of Brillouin scattering depend essentially on the optical fiber glass properties (e.g. refractive index, density etc.). Since these are strongly influenced by optical fiber temperature and deformation, it is then straightforward that by measuring the fiber Brillouin scattering characteristics it is possible to reliably estimate the optical fiber temperature and deformation conditions[59].

Strain and temperature changes cause the Brillouin frequency shift to change linearly according to the following relation[60]:

$$\nu_B(T,\varepsilon) = C_\varepsilon \cdot (\varepsilon - \varepsilon_0) + C_T \cdot (T - T_0) + \nu_{B0}(T_0, \varepsilon_0) \quad (2.8)$$

With C_ε and C_T as the strain and temperature coefficients respectively, ε is the strain value represented in $\mu m.m^{-1}$, and T the temperature. ε_0 and T_0 are the strain and temperature values at the reference Brillouin frequency shift, ν_{B0}.

We can summarize the main characteristics f scattering phenomena in the next table.

	Rayleigh scattering	Brillouin Scattering	Raman scattering
Typical Frequency shift (GHz)	0	11-13	~13000
Linewidth (MHz)	~15	35-100	~150
Relaxation time (n·sec)	10	1	~0.001
Gain in the stimulated case (cm/MW)		10^{-9}	5×10^{-3}

Table 2-1 : Different parameters of scattering phenomena at wavelength of 1550 nm [61]

2.2.2.3 Optical losses in optical fibers

There are two main families of losses in optical fibers:

2.2.2.3.1 Bending

We distinguish two contributions to bending loss known as macro-bending loss and micro-bending loss as shown in the Figure 2-14.

-Macro-bending loss: This occurs when fibers are bent with a “macroscopic” radius of curvature. The critical radius at which radiative loss begins must be proportional to the bend radius of the fiber.

-Micro-bending loss: is a radiative loss, resulting from mode coupling caused by random micro-bends, which are repetitive small-scale fluctuations in the radius of the curvature of the fiber axis. An approximate expression for the attenuation coefficient has been studied in [62].

The distinction between macro and micro-bending has been discussed and could be estimated as presented in the Figure 2-14 [63].

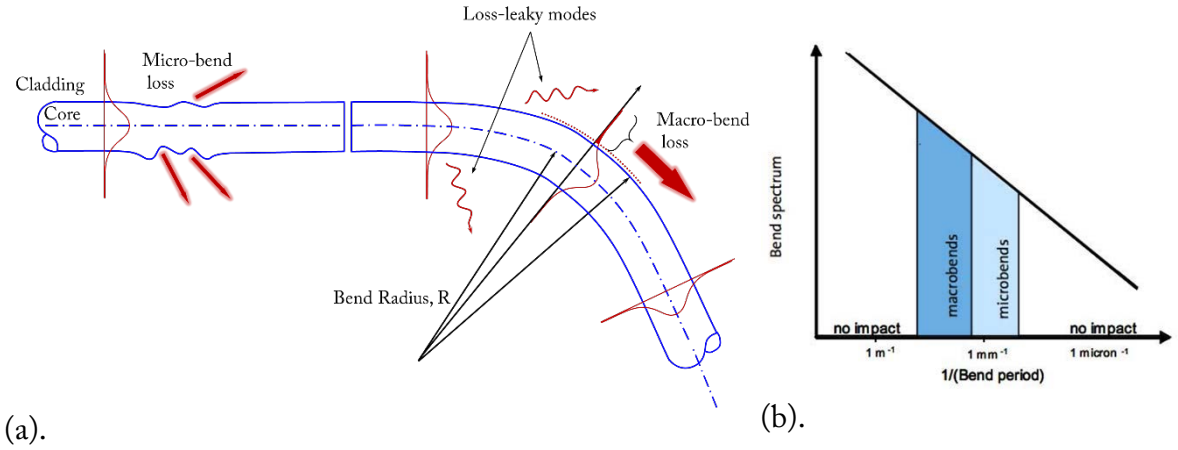

(a). (b).

Figure 2-14 : Optical fiber bending: (a). Illustration of bend loss mechanisms; (b). micro- and macro bending radius.

2.2.2.3.2 Optical connection/splicing loss

The connection between two fibers must be mechanically strong enough to withstand pulling force and bending moments and guarantee high transmission of light. Accordingly, the fiber cores must fit together exactly. Connection types can either be temporary (connector) or permanent (splice).

A splice is the dielectric interface between two optical fibers. Any index-of-refraction mismatch at any point in this interface will produce reflection and refraction of the light incident at that point. For splicing calculations, we assume that the mode field of single-mode fibers is nearly Gaussian. The coupling losses for the splicing connectors can be calculated by evaluating the coupling between two misaligned Gaussian beams.

Based on the above model, the optical connection (splicing) loss between two single mode fibers can be given by a simplified equation [64, 65]:

$$\alpha_{Con} \simeq -20 \cdot \log\left(\frac{2 \cdot w_1 \cdot w_2}{w_1^2 + w_2^2}\right) \tag{2.9}$$

Where w_1 and w_2 are mode field radii of the two connected/spliced fibers. The mode field radius is defined as half of the spatial extend of the fundamental mode through a larger volume, including the inner fiber cladding, where the mode intensity level is at $1/e^2$.

1- Splices:

Fusion splicing is the most frequently used technique to realize permanent fiber connections. It is achieved by an electric arc ionizing the space between the aligned fibers which

eliminates the air and heats the fibers to a temperature of 1100°C. The softened fiber ends are then moved together with precise alignment to form the fusion joint. A perfect fusion splice results in a single fiber, with no indication that this is the result of two joined fibers. The tensile strength of a fusion splice is comparable to that of the original fiber. In general, a heat-shrink sleeve, is provided to replace the removed section of coating, for better mechanical protection.

Figure 2-15 presents different images for splicing standard single mode fiber: a) successive steps during a fusion splice of ordinary single-mode fiber. Core and cladding regions of the fiber are visible. The timing of these images from top to bottom: *i*) Fiber tips aligned, *ii*) Fiber tips following hot push during joint formation, *iii*) Completed splice with a loss less than 0.05dB. Some splicing defaults are shown in the same figure: b) Upper image presents the two fiber ends before splicing during alignment, the lower image is after splicing. The cleave angle of the right fiber tip was about 3-5°. The visible geometric deformation of the core induced about 0.3dB loss at 1550 nm. c) A splice with an incompletely formed seam at the joint. Image of a bubble at the fusion splice between two ordinary SMF fibers. Bubbles such as this one cause extremely high splice loss but often do not significantly reduce the tensile strength of the splice. This bubble resulted from dirt on the fiber tip end face.

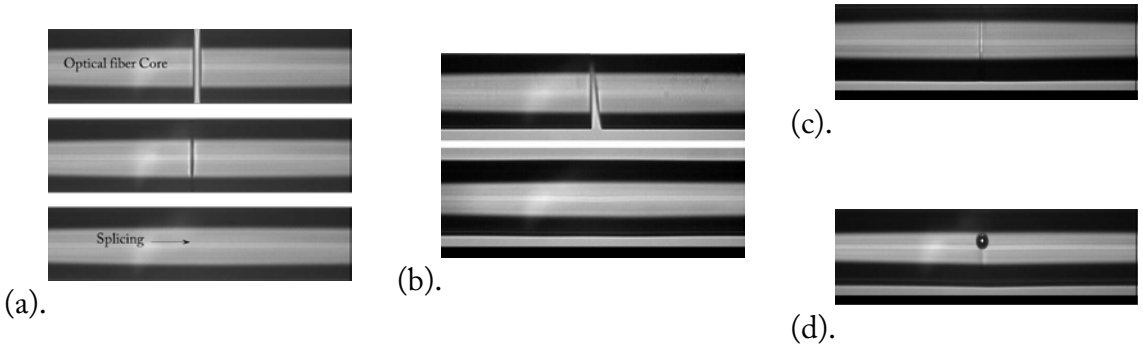

Figure 2-15 : a) successive steps during a fusion splice of ordinary single-mode fiber. Some splicing defaults are shown in: (b). Upper image presents cleave angle of the right fiber tip was about 3-5°, the lower image is after splice; (c). A splice with an incompletely formed seam at the joint; (d). Image of a bubble at the fusion splice between two standard SMF fibers.

2- Connectors:

Nowadays awide variety of connector types are available, with different dimensions and different methods of mechanical coupling. The connector is produced by gluing a fiber into a ferrule. Then, the end is cut and polished to be even with the face of the ferrule. A connector

can be polished flat, with a slightly rounded dome for “Physical Contact” (PC), or an angled face “angled PC” (APC), usually 8°. The PC reduces the back reflection caused by air gap between the fiber ends, while the angle minimizes the back reflections at the point of connection, in some specific applications, a precise polishing is done to obtain high flatness on the surface of the fiber core, this is called Ultra-Physical Contact (UPC). The mechanical body of the connector may have different names based on producer norms and classifications:

-SC Standard Connector, developed by (NTT) in the mid-eighties, has a push-pull coupling end face with a spring loaded ceramic ferrule.

-LC (Lucent Connector) Introduced by Lucent Corporation, it is a push-pull connector, the LC utilizes a latch as opposed to the SC locking tab and with a smaller ferrule. It is known as a small form factor connector.

-FC was the first optical fiber connector to use a ceramic ferrule, but unlike the plastic bodied SC and LC, it utilizes a round screw-type fitment made from nickel-plated or stainless steel.

-E2000: It looks like a miniature SC connector. It is easy to install, with a push-pull latching mechanism which clicks when fully inserted. It features a spring-loaded shutter which fully protects the ferrule from dust and scratches. The shutter closes automatically when the connector is disengaged, locking out impurities which could later lead to network failure, and locking in potentially harmful laser beams. When it is plugged into the adapter the shutter opens automatically.

These different connectors are not compatible. As a precaution, different colors distinguish connector types, as presented in the Figure 2-16.

Figure 2-16 : Different Fiber-optic connectors and adapters.

In general, splices offer a lower attenuation than connectors and are more economical. However, within a strain sensing system, only temporary connections are desired and a connector offers this flexibility

2.2.3 Optical Fibers by ITU Standards:

The ITU Telecommunication Standardization Sector (ITU-T), coordinates standards for telecommunications. The characteristics of fibers for telecom applications were specified in its recommendations. Each type has its own area of application and the evolution of these optical fiber specifications reflects the evolution of transmission system technology from the earliest installation of single mode optical fiber through to the present day[17]. We will be interested more in single mode fiber for sensing applications. This choice is based on the dimensions of the fiber, its sensitivity to strain and temperature variations, and it's compatibility with the different instrumentations systems and acquisition units.

We present here the list of the main types:

ITU-T G.651: Multimode fiber standard

ITU-TG.652: Standard Single mode fiber with 4 different categories (A, B, C, D). The G.652C and G.652D standards have been developed to specifically reduce the water peak at the 1383nm wavelength range (low-water-peak).

The most kwon is ITU-TG.652D

ITU-T G.653: Zero Dispersion Shifted Fiber (ZDSF), having zero dispersion around the 1550nm window.

ITU-T G.654: cut-off shifted and low attenuation single-mode optical fiber, designed mainly for submarine applications.

ITU-T G.655: Non-zero Dispersion Shifted single mode Fiber (NZDSF), having low dispersion in the 1550nm and 1625nm windows, the DWDM region. Suited for long-haul and backbone applications.

ITU-T G.656 Medium Dispersion Fiber (MDF), designed for local access and long-haul

ITU-TG.657 Latest standard for FTTH application. Designed to bend at small radius of down to below 10mm radius.

[17] https://www.itu.int/net/ITU-T/cdb/Test-Specifications.aspx

Bend-insensitive fiber standards appeared inNovember 2006 with the last release (ITU-T G.657). This standard divides these new fibers into two very distinct categories of fiber performance: Class A and Class B.

Class A is referred to as “bend tolerant” fiber, better macro-bending performance when compared to previous single mode fiber standards. This type is fully compatible with G.652D, commonly referred to as the low water peak single mode fiber specification.

Class B fibers are the truly bend-insensitive class, providing the highest known bending performance. It has 10 times better performance than the Class A products. The backward compatibility has not been required since one of the implementations included in Class B is a fiber design that uses very low mode field diameter (MFD), about 6 to 8.5μm. Still, some Class B products do comply 100% with G.652D.

Reducing the bending loss of single-mode fibers was realized using different approaches. The first approaches were focusing on changes to the cladding. Recent approaches include reducing the mode field diameter (MFD)[66] depressing the cladding, adding a low index trench, and adding a ring of symmetric holes within the cladding. Figure 2-17 shows schematics of these fiber designs.

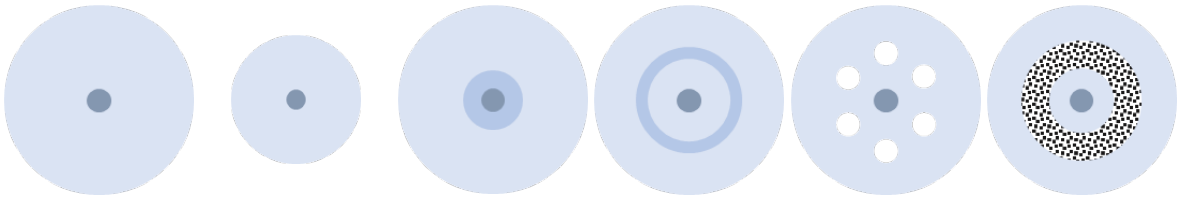

(a). (b). (c). (d). (e). (f).

Figure 2-17 : Illustration of optical fiber designs for reducing bending loss: (a). reduced mode field diameter (MFD) design; (b). reduced cladding; (c). depressed-cladding design; (d). trench assisted fiber design G.657A2; (e). hole-assisted design; and (f). nano-structured design G.657A3.

A better view of the influence of polishing the different fiber profiles is shown in the Figure 2-18. The major difficulties using two different types are related to the splicing/connection difficulties and physical strength of the splicing region.

What I have chosen in the different works of instrumentation: IUT G.652D for all sensing applications with low bending curvature. IUT G.657A3 for applications with high curvature diameter. In all the used sensing fibers I have worked in 1.55µm spectral window.

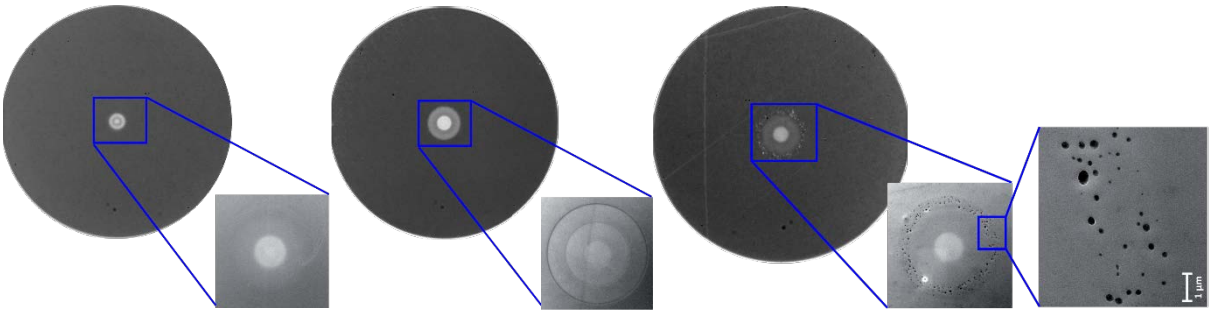

(a). (b). (c).

Figure 2-18 : Microscope picture of the fiber end faces in the assembled ferrules (300× magnification), and SEM pictures of the core region of the three types of fibers: (a) Standard SMF fiber G.652D; (b). depressed-cladding design; and (c). nano-structured design.

2.3 Intrinsic distributed optical fiber sensors

The distributed measurement technique should deliver full field strain/temperature measurement along the fiber with zero-dead zone. That means, along a specified sensing length of the optical fiber, we should obtain high sensibility, with minimum spatial resolution and short gauge length [18, 40, 41, 67]. These different parameters are illustrated on Figure 2-19. Gauge lengths and sampling intervals combination along the fiber sensing length should be optimized for every sensing fiber installation. If long gauge lengths are chosen, strains along the optical fiber appear smooth, and the strain concentrations are smoothed out and may not be detected. And, if gauge length and sampling intervals are too small, the measured strain shows much noise, the amplitude noise values depend on the optical signal quality in the optical fiber.

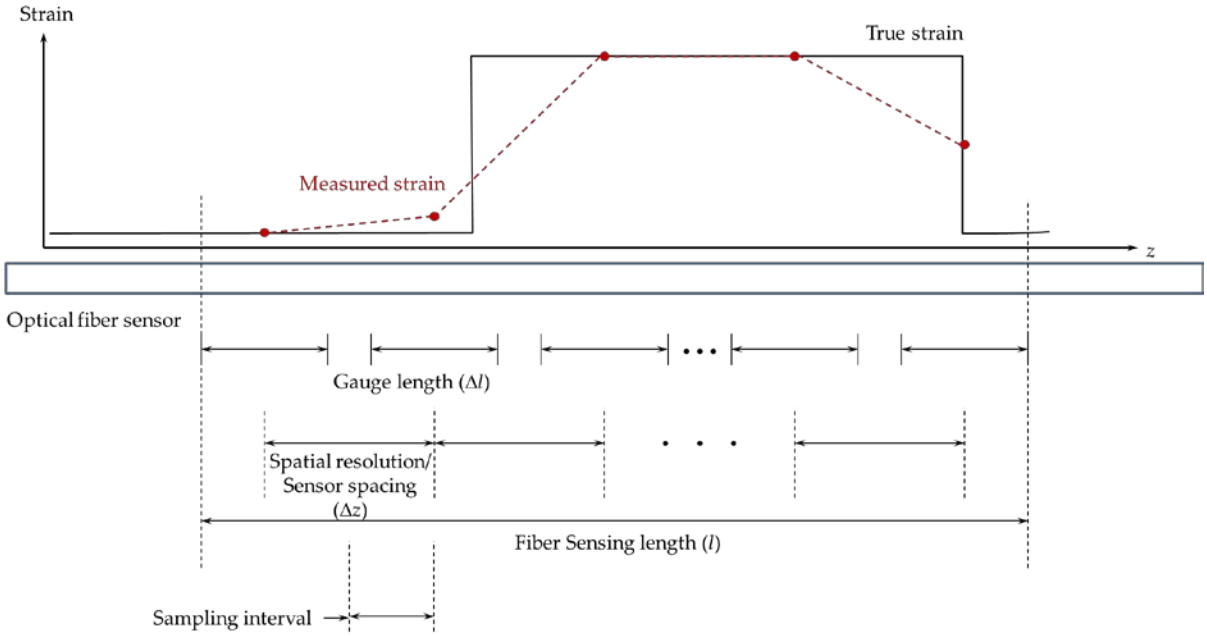

Figure 2-19 : Illustration of distributed sensing parameters: sensing length, sampling interval or gauge length and sensor spacing.

If an optical fiber is perturbed mechanically, it will suffer a deformation proportional to the amplitude of the perturbation force. This approach is valid for perturbations values lower than the elastic limit of the optical fiber, where the mechanical perturbations are reversible. So, we can try to investigate the variation of the mechanical properties of the fiber using the characteristics of light as shown in Figure 2-20. Where we study the polarization variation, the optical modes variations, wavelength variation, or intensity fluctuation with time.

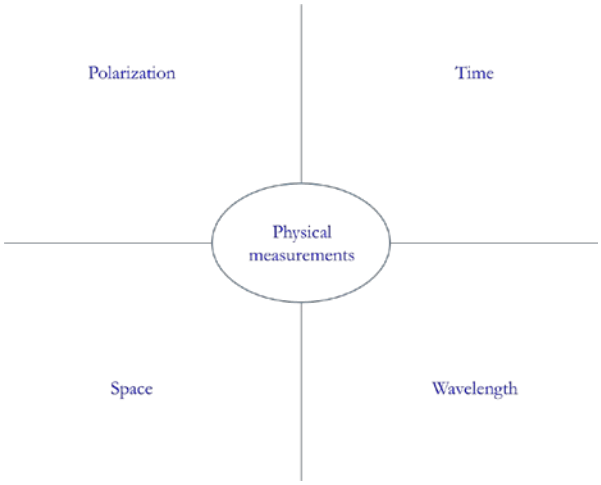

Figure 2-20 : Four main solution to obtain a physical measurement. Decorrelation the effect should be realized using two solutions.

In the case of external mechanical deformation. A pressure will be created at the correspondent position, which will result in changes in: -the optical fiber length (strain effect), -the optical fiber core diameter (Poisson effect), and -the refractive index of the optical fiber core (photo-elastic effect). The three changes are correlated, the global measured parameter in general is the variation of length, and it will be measured in $\mu m.m^{-1}$. The Hooke's law expresses the relation between the perturbation force and the produced deformation, the proportionality is given by the material elastic constant. The Hooke's law is given by the following expression, along the longitudinal axis of the fiber:

$$K = \frac{|F|}{|\Delta l|} \tag{2.10}$$

Where K is the elastic constant, F is the applied perturbation force and Δl is the relative deformation created by F. The Young modulus of the optical fiber, E_{fib}, is the proportionality constant between the perturbation force per area and the relative deformation:

$$E_{fib} = \frac{F}{A} \cdot \frac{1}{\left(\frac{\Delta l}{L}\right)} \tag{2.11}$$

Where A is the cross section of the fiber and L is length the optical fiber under perturbation.

That means, measuring the variation of length of the fiber will give us a clear idea about the applied force in the elastic region. The analysis of this variation could be treated using the optical reflectometry techniques.

2.4 Optical reflectometry techniques

Optical reflectometry is the best technique for the characterization of optical fibers. By analyzing the backscattered light, the magnitudes and locations of faults and reflections could be determined and the propagation characteristics of the fiber are estimated. The distance for fiber optic reflectometry analysis is limited. This limitation of the range is founded in the attenuation losses that occur in the optical fiber and the limited amount of light (power) that can be coupled into the fiber core. Especially in long range applications, the losses in the connecting splices and the connectors have to be kept at a low level of usually less than 0.1dB per connection in order to assure a strong and distinguished signal for good measurement results.

2.4.1 Optical Time-Domain Reflectometer based techniques

The principle of the OTDR is based on the detection and analysis of light scattered from imperfections and impurities in the optical fiber. The fundamental phenomenon investigated by this technique is Rayleigh scattering. The earliest works to measure the backscattered light in optical fibers using a time-domain method reported in early 1976[68-70].

The evolution of OTDR development could be summarized in four phases: The first was the invention and early development of the OTDR. The second phase consisted of the years in which OTDRs were brought from the laboratory into commercial development and gradually refined. The third phase was the period in which the OTDR was transformed from basically a refined oscilloscope to a monolithic instrument designed specifically for testing optical fiber and capable not only of measuring the fiber waveform data but also of interpreting them. The latest phase has been the reduction of the OTDR into a form factor that is small and portable.

The OTDR injects an accurately timed light pulse into the fiber and the optical detector observes the backscattered light. The backscattered light intensity is -79dB.

2.4.1.1 Theory of OTDR

It is necessary to understand the basics of intrinsic fiber measurement using an OTDR. In simple description, an OTDR consists of: a pulsed laser source and an optical detector, together synchronized using an electronic and software driven controls. An optical circulator (or coupler).

The launched pulse width, typically in the order of some nanoseconds. The amplitude of the scattered light seen by the OTDR detector, together with the corresponding time delay (from when the input pulse was triggered), is recorded. The time delay is converted into distance travelled using the known refractive index along the optical fiber. The refractive index depends on fiber type and measurement wavelength[18]. The spatial resolution is directly related to the pulse-width of the laser A 10-ns pulse corresponds to roughly 1m spatial resolution [18]. Following figure shows the typical OTDR trace from the oscilloscope and we present the main performance on it.

Figure 2-21 shows how light travelling along a single-mode fiber may be reflected back towards the OTDR detector due to: a) Rayleigh Scattering due to non-homogeneous structural changes of the fiber, b) variations caused by glass geometrical changes or differences (called

[18] Refractive index values are generally provided in product information sheets available from supplier.

mode field diameter (MFD), c) Reflections due to localized changes in the refractive index of the glass, d) Fresnel peaks, where there is a sudden change in material density, e.g. from glass-to-air transitions at near-perpendicular cleaved fiber ends. In general, OTDR traces can be used to locate extrinsic events such as splices, cable joints, and connectors.

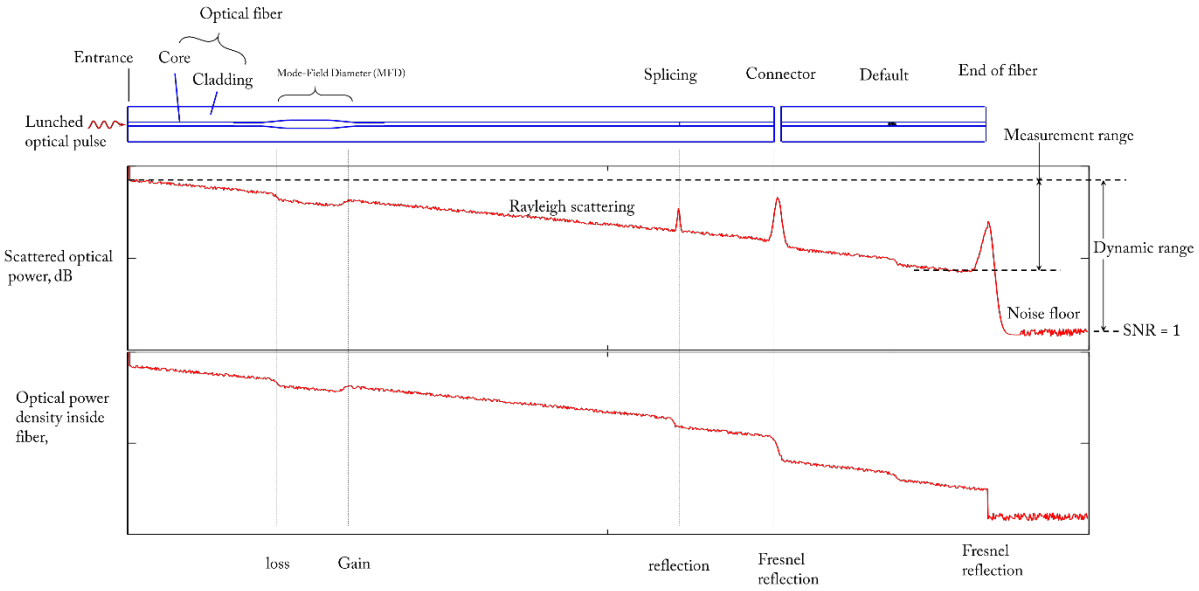

Figure 2-21 : Illustration of an OTDR trace sample, interpretation of events along the fiber. Optical power density inside the fiber is shown also.

2.4.1.2 Schemas of OTDR (X-OTDR)

In all common OTDR solutions, the optical fiber is probed by sort optical pulses, and the measured spatial resolution can be improved as the pulses are shortened and the measurement bandwidth is broadened (Figure 2-22). However, it results in the increase of noise level, which will reduce the dynamic range (trade-off between dynamic range and spatial resolution)[71-73]. To solve this problem other approaches to optical reflectometry in time domain were investigated, like the correlation OTDR based on the use of pseudorandom probe signal [74], photon-counting OTDR [75, 76], the use of complementary Golay code probe signal [77], and the low correlation OTDR [78, 79]. Each of these OTDR modifications are characteristic by some advantages that determine the field of their utilization. The low-correlation OTDR, has the highest spatial resolution (~10μm) with a very high sensitivity (below -180dB), with very high sensitivity and space resolution is used for the characterization of miniature integrated optical waveguides[80].

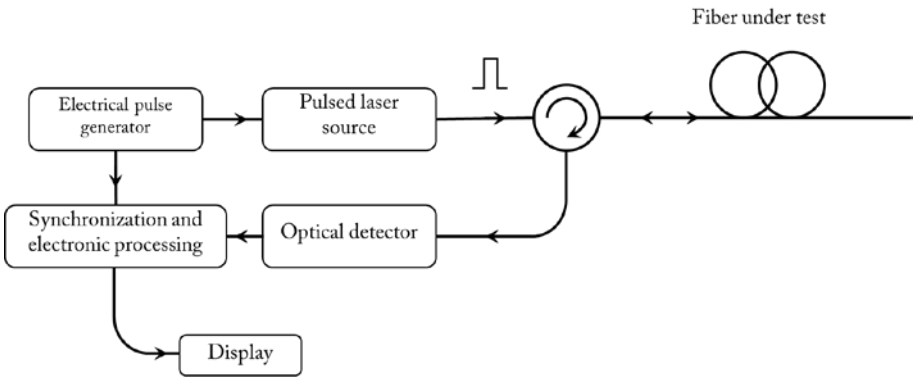

Figure 2-22 : Illustration of OTDR system configuration.

The principle of this modified OTDR configuration is based on the fact that the backward Rayleigh scattered light in a single-mode fiber contains additional information about the variation of the polarization state along the fiber (Figure 2-23). This modified OTDR configuration investigate the polarization properties by placing a polarization analyzer is in front of a detector, this method has been designated as the polarization optical time-domain reflectometry (P-OTDR) [81].

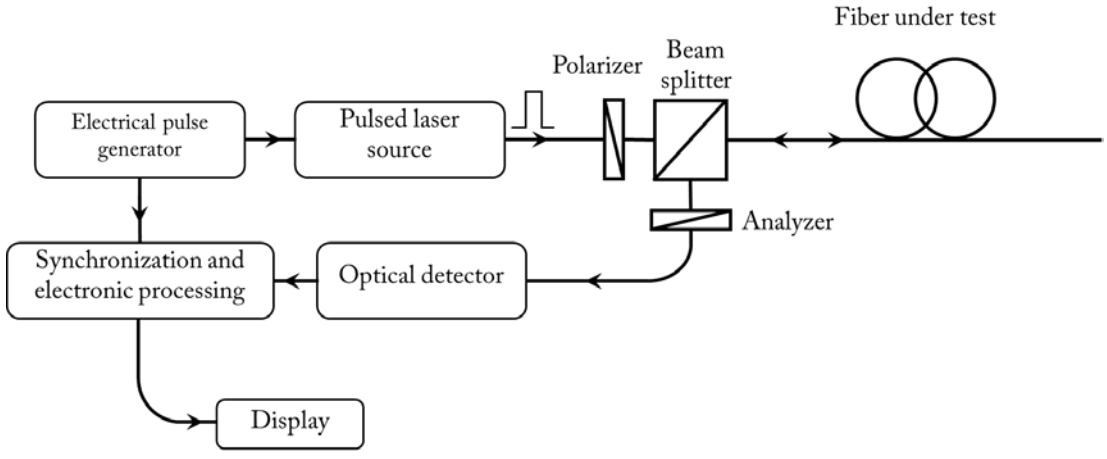

Figure 2-23 : Illustration of P-OTDR system configuration.

To increase the performance of the OTDR system, it's possible to use the coherent detection schematic as shown in the Figure 2-24. The coherent OTDR (C-OTDR) uses the same stabilized laser to inject light pulses in the fiber and measure realize the detection.

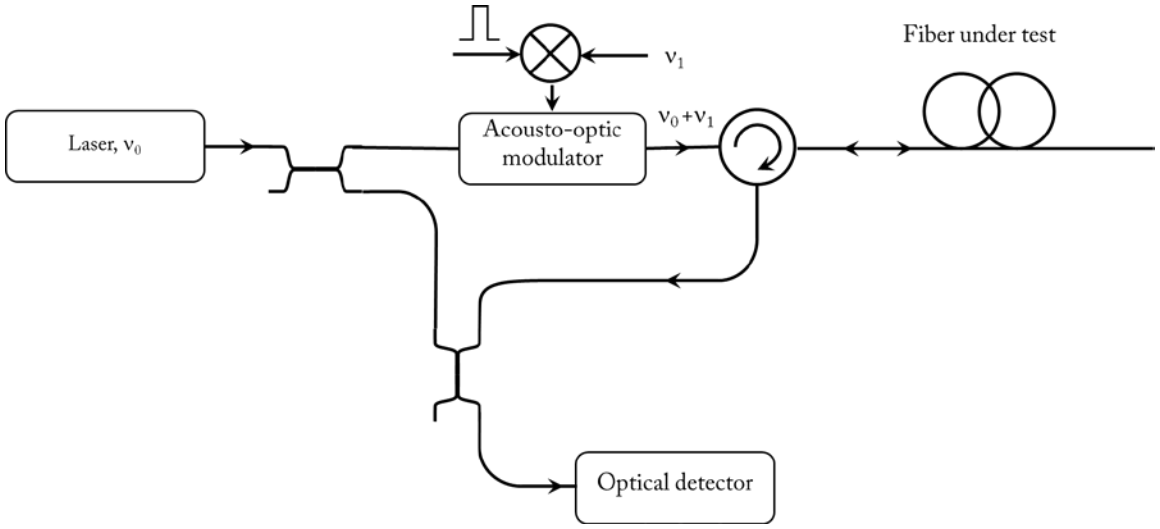

Figure 2-24 : Illustration of C-OTDR system configuration.

The OTDR configuration has undergone a long process of development, and still the fundamental configuration used in distributed sensing applications. The continuous development of new technologies for the optical fiber production and new components, makes it possible to develop new sensing solutions with increased dynamical range and space resolution.

2.4.2 Optical Frequency-Domain Reflectometer based techniques

One of the most progressive variations of the conventional optical reflectometry based on the Rayleigh back scattering is coherent frequency-domain optical reflectometry. It combines the advantages of the coherent detection and simultaneously provides very high spatial resolution. In this configuration, the spatial resolution is given mainly by the tuning interval of the frequency and its linearity, and also by the frequency bandwidth of the optical receiver.

2.4.2.1 Theory of OFDR

Optical frequency domain reflectometry (OFDR) used in optical fiber networks[82-84], is inspired from Frequency Modulated Continuous Wave (FMCW) technique of radar systems [85, 86]. The Figure 2-25 present a simplified description of this technique. A sweep frequency bandwidth f_1-f_2 is generated in a specific time T_s. The received signal is then mixed with the

emitted signal and due to the delay caused by the time of flight for the reflected signal, there will be a frequency difference that can be detected as a signal in the low frequency range (f_b). This signal could be measured to determine distance:

$$t_d = T_S \frac{f_b}{B_{sweep}} \tag{2.12}$$

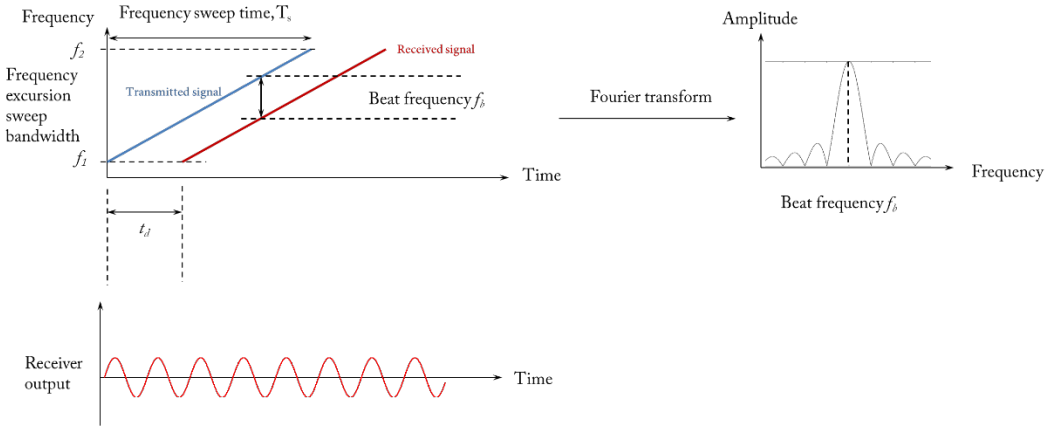

Figure 2-25 : Operation principle of Frequency Modulated Continuous Wave (FMCW) technique

The interest OFDR for optical systems have increased with the evolution of the laser sources and optical components. There are two ways to realize the frequency modulation: adding it directly to the optical frequency or, it could be added to the outgoing light intensity.

2.4.2.2 Basic schemas of OFDR (X-OFDR)

OFDR methods are divided into two main categories: coherent OFDR (C-OFDR), and incoherent OFDR (I-OFDR), the two cases will be briefly presented.

2.4.2.2.1 Coherent OFDR (C-OFDR)

This technique was reported in single-mode fiber for the first time in 1981 [87], as a method to measure the spatial distribution of the Rayleigh backscattering and the fiber loss, and it has been used in multimode fibers too[88]. It enables to measure complex Rayleigh backscatter signatures that can be used to identify specific sections of fiber within parallel optical networks [89].

In this C-OFDR case [90, 91], as presented in the Figure 2-26, the optical carrier frequency of the tunable laser source is swept linearly in time without mode hops. Then, the frequency-modulated optical signal (probe signal) is split into two paths, one of which probes

the sensing optical fiber whereas the other is used as reference signal (considered as local oscillator). The reference signal returning from the reference mirror and test signal returning from the reflection sites in the test fiber coherently interfere at the coupler. This interference signal contains the beat frequencies which appear as peaks at the network analyzer display after the Fourier transform of the time-sampled photocurrent. Using a linear optical frequency sweep, the measured beat frequencies can be mapped into a distance scale (the proportionality factor between beat frequency and the corresponding distance is determined by the rate of change of the optical frequency), while the squared magnitude of the signal at each beat frequency reveals the reflectivity of each reflection site [4].

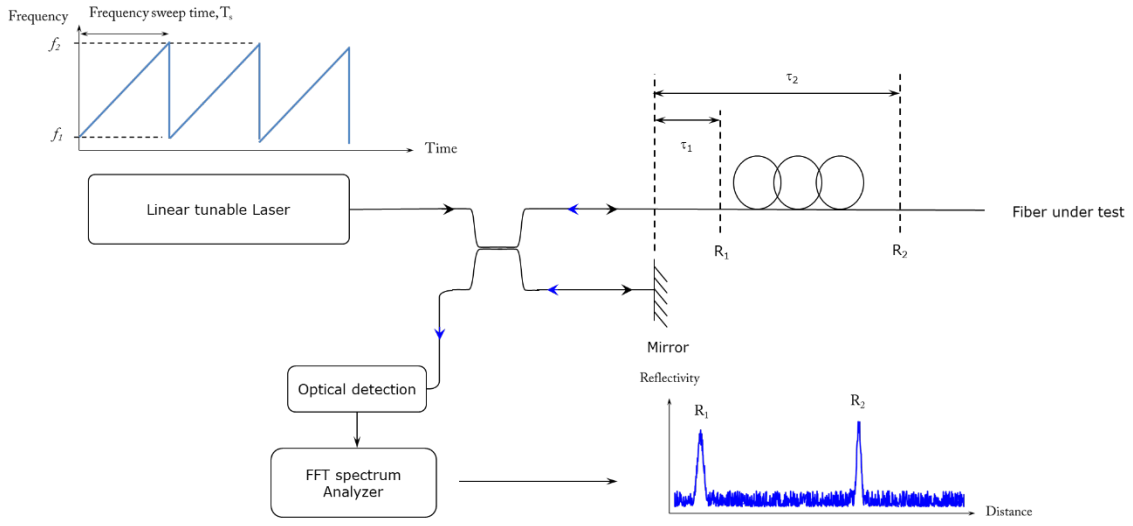

(a).

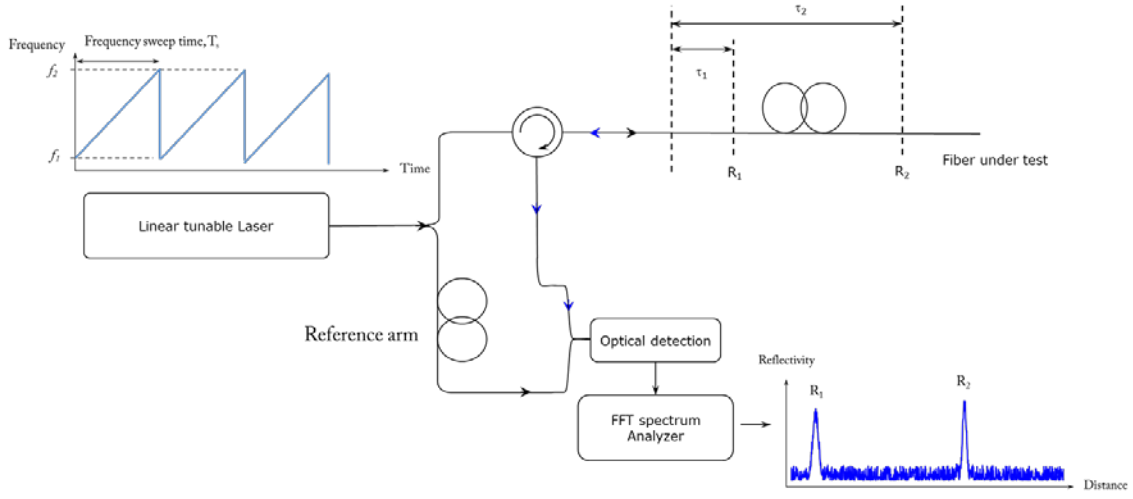

(b).

Figure 2-26 : Operation principle of C-OFDR: (a) Michelson interferometer implementation of the FMCW, (b) Mach-Zehnder interferometer implementation of the FMCW.

C-OFDR has got some advantages of the coherent detection scheme [4]: First of all, the measured photocurrent is not proportional to the reflected optical power but to the square root of it, which permits the system to measure signals with large amplitude differences. Secondly, the receiver bandwidth (RF frequencies) is lower compared to the OTDR techniques reducing the noise level and increasing the dynamic range. Moreover, C-OFDR systems have got the ability to measure active devices (e.g. optical amplifiers) without saturation since only low power CW signals are used. Finally, no dead zone is observed in C-OFDR since the receiver does not saturate as in pulsed OTDR methods. However, C-OFDR has a problem in dealing with long measurement distances.

2.4.2.2.2 Incoherent OFDR (I-OFDR)

In this method, a continuous wave (CW) optical carrier is intensity modulated by a constant amplitude RF signal whose frequency is changed periodically over a defined frequency range either stepwise (step-frequency method) [92] or continuously (sweep frequency method) [93].

The CW signal is then launched into fiber. Back reflected optical signals and Rayleigh backscattered signal are detected as a function of modulation frequency and processed in a vector signal analyzer to obtain frequency response of the fiber. This is the reason why the group including step-frequency and sweep-frequency methods is called as Network Analysis OFDR (NA-OFDR).

Fourier transform of the frequency response then gives the time-domain impulse response provided that the scanned frequency range is sufficiently large. In an alternative sub-group called Incoherent Frequency-Modulated Continuous Wave (I-FMCW), the modulating RF signal is swept in frequency and the detected probe signal is mixed with the modulating RF signal in the electrical domain [3]. Resulting output that contains mixing products is then observed by means of an electrical spectrum analyzer. The frequency axis represents the delay times experienced by the probe signal. Knowing the speed of light within the fiber, time axis is converted into physical distance.

2.5 Distributed sensing configurations:

Fiber-optic distributed sensors deliver a precise information about two basic parameters: the first is the magnitude of the strain or temperature variations, and the second is to resolve the position where strain or temperature change is applied. The methods to resolve the position were presented in the paragraph 2.4. We present here the basic configurations of distributed sensors based on the scattering phenomenon.

2.5.1 Rayleigh based sensing configurations

The Rayleigh backscattering in optical fiber is caused by the random fluctuations in the refractive index profile along the fiber length, these fluctuations are the result of the imperfections in the fiber fabrication [94]. For an optical fiber, the amplitude of the optical backscatter signal is a random static property as a function of fiber length, but it may be considered as long, weak fiber Bragg grating with a random period. Any changes in the local period of the Rayleigh backscattering modify the locally reflected spectrum.

Schematically, the Figure 2-27 presents the measured OTDR signal, for a 345m single mode fiber. We can see the fluctuation in the amplitude between Figure 2-27 (a) and (b), acquired with a time shift, the Figure 2-27 (c) shows the effect of the pulse width on the spatial resolution, and we can see less details of the scattered light compared to previous traces.

(a).

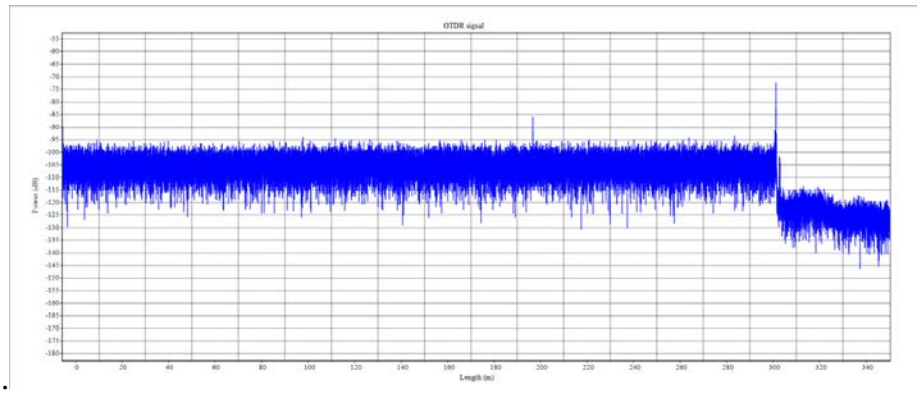

(b).

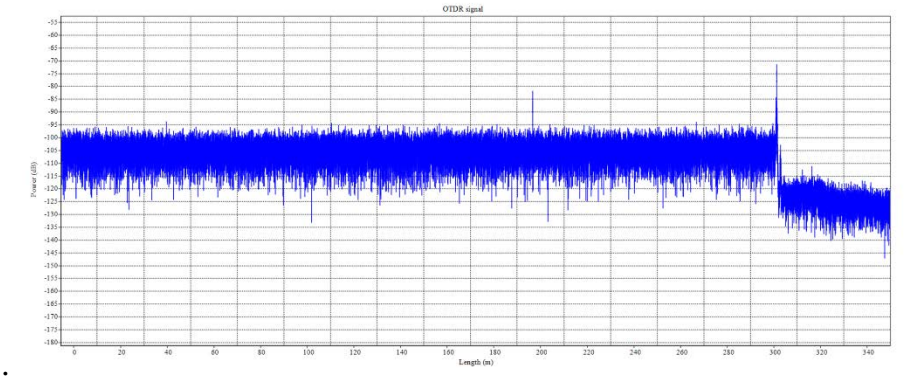

(c)

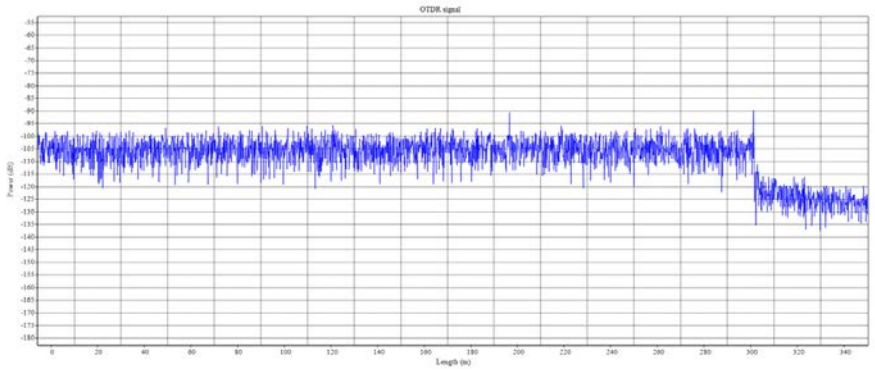

Figure 2-27 : Set of Rayleigh backscatter power measurements made for 345m fiber length, (a) and (b) has been taken with time shift, using pulse width <1nsec; and (c) with 5nsec pulse width.

2.5.1.1 Time-domain technique

Strain measurements in time domain are based on the analysis of the OTDR signal. The conventional COTDR was used [95, 96]. Another configuration was demonstrated using a time division multiplexing scheme where an optical pulse was used [97]. In the different configurations what was measured is the variation of the local intensity or the phase variations. These solutions have opened the way for the distributed measurements of vibration and acoustic waves[98-104].

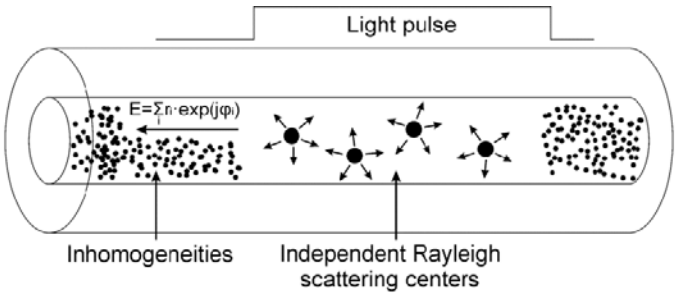

Figure 2-28 : Phase variations with Rayleigh backscattering.

2.5.1.2 Frequency-domain technique

The C-OFDR technique enables the measurement of the complex reflection coefficient of an optical fiber as a function of wavelength, and the Rayleigh backscattering as a function of

the fiber length is obtained via the Fourier transform. Any modification could be qualified as a spectral shift, and then calibrated to form a distributed sensor. The optoelectronic interrogation technique choice is based on two main parameters: highest spatial resolution with the smallest gauge length, and highest strain sensibility. The frequency tuning range and chromatic dispersion of the laser source determine the spatial resolution of C-OFDR system[105], and the phase noise limits the maximum sensing length[87].

The sensing gauge is formed by first measuring and storing the Rayleigh backscatter signature of the fiber as a baseline state. A new profile is then measured in a modified state. The Rayleigh backscatter profiles from the two data sets are then compared along the sensing length of the fiber in increments of Δl, each segment represents a discrete sensing element. When a segment has any change in state, the backscattered spectrum shifts proportionally to the change. To determine the equivalent spectral shift, a complex cross-correlation is performed between reference data and measurement data for each fiber segment. A shift in the correlation peak will present the change in state. Therefore, to make a distributed measurement one simply measures the shift in the cross-correlation peak for each segment along the fiber.

The wavelength shift, $\Delta\lambda$, (or frequency shift, $\Delta\nu$) of the backscatter pattern due to the strain along the fiber axis, ε, or the temperature change, ΔT, is similar to the response of a fiber Bragg grating:

$$\frac{\Delta\lambda}{\lambda_C} = -\frac{\Delta\nu}{\nu_C} = C_T.\Delta T + C_\varepsilon.\Delta\varepsilon \tag{2.13}$$

where λ_C (ν_C) are the central optical wavelength (frequency) of the tunable laser source, and C_ε (C_T) are the strain (temperature) calibration coefficients, respectively. These coefficients are somewhat dependent on the dopant species and concentrations in the core of the fiber, but also on the composition of cladding and coating. The characteristic values for Ge-doped silica fibers are $C_\varepsilon \sim 0.8\ \mu\varepsilon^{-1}$ for and $C_T \sim 6.5\cdot10^{-6}\ ^\circ C^{-1}$ [106-108].

2.5.2 Brillouin based sensing configurations:

Distributed optical sensors based on Brillouin scattering are used widely in civil engineering, and pipe lines monitoring. These sensors still the most promising for multi parameters sensing[109], in spite of the significant improvements of these sensors[110]: spatial resolution over two kilometer sensing length is 2 cm and the longest reported sensing length is 150 km with 2m spatial resolution and 1°C temperature resolution[111]. I'll present here the basic configurations, more details related to the evolution in every technique could be found in different published works [112-115].

2.5.2.1 Time-domain techniques

The first concept of Brillouin scattering-based distributed sensing named Brillouin optical time-domain analysis (BOTDA) was demonstrated using the stimulated Brillouin scattering [60, 116, 117]. In this configuration (as presented in Figure 2-29-a), a short pump pulse is launched into one end of the fiber, and a continuous wave probe beam with a frequency offset corresponding to the nominal Brillouin shift frequency is launched into the other end of the fiber. The continuous light wave probe amplifies the Brillouin gain at the locations in the FUT where the frequency offset is matching the peak Brillouin gain. Measurements should be carried out with a wide range of frequency offsets to obtain a full picture of the Brillouin frequency for each location in the optical fiber. As a consequence, the distribution of strain and temperature can be derived within the spatial resolution limited by the width of the pump pulse.

Spontaneous Brillouin scattering-based fiber-optic distributed sensors (as presented in Figure 2-29-b), called Brillouin optical time-domain reflectometry (BOTDR). In this technique, we can be distinguish two detection configurations: Direct detection [118], and the coherent detection [119].

In coherent detection case, a narrow-linewidth reference oscillator derived from the pump optical wave is used. An excellent electrical selection of the Brillouin component beside a wide dynamic range could be obtained using this reference oscillator. The wide bandwidth (25 GHz or higher) and high sensitive photodiodes have simplified the sensing without using the acousto-optical modulator. So, nowadays it's necessarily to make frequency shift in the reference path.

As was explained in the case of BOTDA [45, 46], the spatial resolution of basic BOTDR is also limited to 1 m, because the BGS broadens rapidly as the optical pulse width decreases below 10 ns. However, a "double-pulse BOTDR (DP-BOTDR)" system was recently proposed by Koyamada et al. [60-62] to enhance the spatial resolution further, where double optical pulses are transmitted into the FUT instead of a conventional single optical pulse. So far, they have experimentally obtained 20-cm resolution. To enlarge the measurement range, Raman amplification was employed to BOTDR with the coherent detection, resulting in 150-km range [63]. A new BOTDR system based on optical-pulse coding has also been proposed and studied [64, 65].

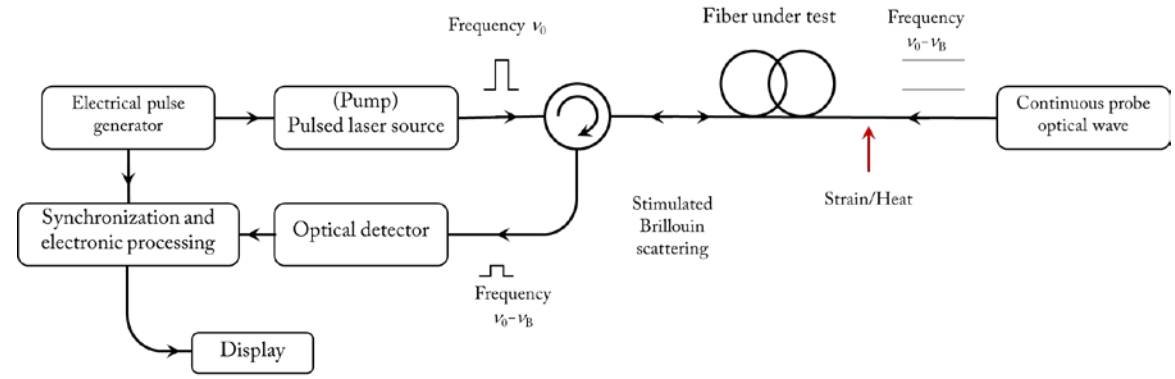

(a)

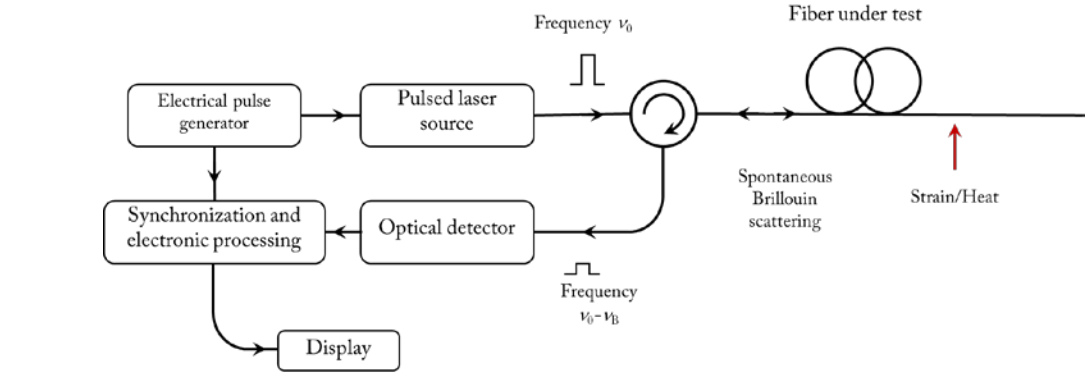

(b)

Figure 2-29 : (a) Schematic of basic BOTDA system; (b) Schematic of basic BOTDA system.

2.5.2.2 Brillouin optical frequency-domain analysis (B-OFDA)

This technique employs a continuous probe optical wave and a pump optical wave with sinusoidal amplitude modulation[120-122]. When the stimulated Brillouin scattering occurs, the probe signal acquires an intensity modulation at the same frequency of the pump, and the induced modulation is measured by a vector network analyzer for a range of modulation frequencies. The baseband transfer function provides information similar to the pulse response measured in B-OTDA or B-OTDR. This frequency-domain approach improves the signal-to-noise (S/N) ratio due to a synchronous detection, but the data analysis is still performed in the time domain after an inverse Fourier transform of the measured data.

2.5.2.3 Brillouin optical correlation-domain analysis (B-OCDA)

The correlation-domain technology named Brillouin optical correlation-domain analysis (B-OCDA) was proposed to overcome the limitation of the spatial resolution and the measurement time in two previous techniques[123-126]. It is based on the technique called the

synthesis of the optical coherence function, where the correlation between frequency-modulated optical waves is controlled [127, 128].

In B-OCDA technique, the frequencies of counter-propagating pump and probe are sinusoidally modulated. They are synchronous in phase because the two optical waves are obtained from the same source except for a frequency difference, which can be expressed as

$$\begin{aligned} f_{pump} &= f_0 + \Delta f \cdot \sin\left(2\pi f_m t\right) \\ f_{probe} &= f_0 - f_B' + \Delta f \cdot \sin\left(2\pi f_m t\right) \end{aligned} \tag{2.14}$$

where f_0 is the optical frequency of the laser source without frequency modulation, f_m the sinusoidal-modulation frequency, Δf the sinusoidal-modulation amplitude, and f_B' the frequency difference between pump and probe optical waves, which is close to the Brillouin frequency shift of the tested optical fiber.

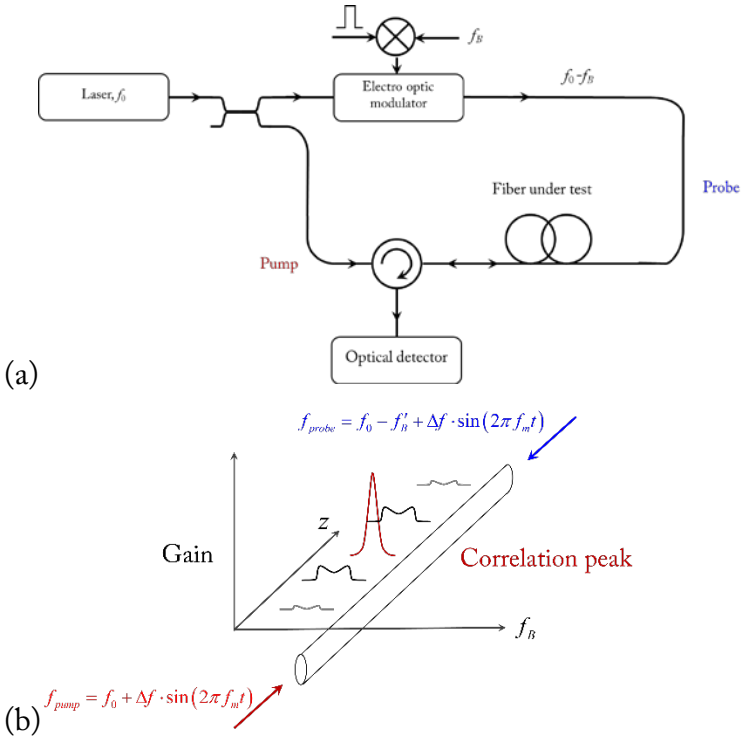

Figure 2-30 : (a) Schematic diagram of conventional B-OCDA system; and (b); Schematic of the correlation peak in B-OCDA

The beat power spectra generated by the synchronized pump and probe optical waves, will intensify the acoustic phonons due to electrostriction effect that interact with the probe amplification from the pump. The beat spectra have a delta-function-shaped distribution along the fiber due to the synthesis of the optical coherence effect. The observed Brillouin gain spectrum is written as 2-dimensional convolution of the beat spectra and the local Brillouin gain spectrum concerning frequency f and position z [123]:

$$G(z, f) = B(z, f) \otimes g(z, f) \tag{2.15}$$

With $B(z, f)$ as the synthesized beat spectra:

$$B(z, f) = FFT\left[\left|E_{pump}(z,t)E^{*}_{pump}(z,t)\right|^{2}\right] \tag{2.16}$$

and $g(z,f)$ is a local intrinsic Brillouin gain spectrum :

$$g(z, f) = \frac{g_{B0}}{1+4\left(\frac{f - f_B(z)}{\Delta\nu_B}\right)^{2}} \tag{2.17}$$

The spatial resolution Δz is determined by the relation between the broadened beat spectra and the Brillouin gain spectrum. And the measurement range L is determined by the interval between two correlation peaks:

$$\begin{aligned} \Delta z &= \frac{v_g \cdot \Delta\nu_B}{2\pi f_m \Delta f} \\ L &= \frac{v_g}{2 f_m} \end{aligned} \tag{2.18}$$

Distributed measurement is done by sweeping f_m, thus the position of the correlation peaks can be scanned along the optical fiber.

2.5.3 Raman based sensing configurations:

As Stokes and Anti-Stokes waves have different frequencies (~26 THz separation in optical glass fibers), they propagate along the fiber with different attenuations. Therefore, to obtain a temperature profile that reproduces properly exact values of the measured temperature, this difference must be taken into consideration [50, 129]. It's possible to summarize in the next bloc diagram the techniques to obtain the temperature profile along the sensing fiber.

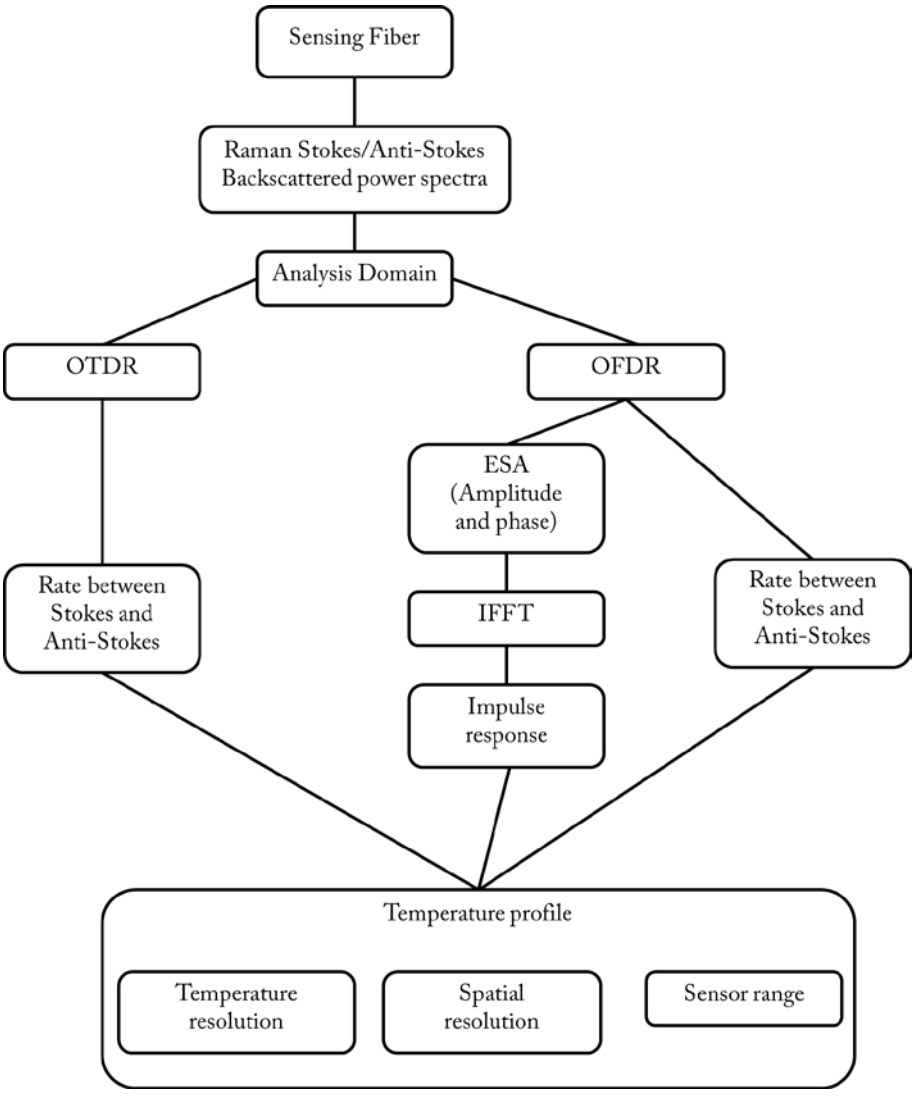

Figure 2-31 : Bloc diagram of the possible steps to obtain the temperature profile based on Raman scattering.

2.6 New solutions for distributed sensing

The main elements used in the distributed sensors are the sensing cable fiber itself, the laser, the detection technique, and the processing algorithms behind all that. My work was oriented in the first place to have good experience with different sensing equipment and increase my experimental experience in the instrumentation domain in mechanically Heterogenous and homogenous structures, from concrete structures to composite.

At first, I will start with work related to the key element in the interrogation systems, which is the laser itself.

2.6.1 The laser

Dual frequency lasers could be applied to distributed optical fiber sensors based on Brillouin scattering, aiming at operating such systems in a low-frequency detection range [130]. Indeed, if the generated frequency difference is close to the Brillouin frequency shift ($\Delta\nu_B$ ~ 11GHz for silica based optical fibers), one laser frequency may act as a local oscillator for the detection of the Brillouin scattering spectrum. Optical heterodyning with the backscattered signal performs the detection at the lower frequency ($\Delta\nu - \Delta\nu_B$), where $\Delta\nu$ is the difference between the two laser frequencies and $\Delta\nu_B$ is the Brillouin frequency. Such a system has been proposed using two phase-locked fiber lasers [131]. Using a dual-frequency source in which the two frequencies share the same cavity may simplify the stabilization scheme. Based on this idea we are interested in the demonstration of a dual-frequency vertical external cavity surface emitting laser (VECSEL) emitting at 1.5µm with a frequency difference close to the Brillouin frequency.

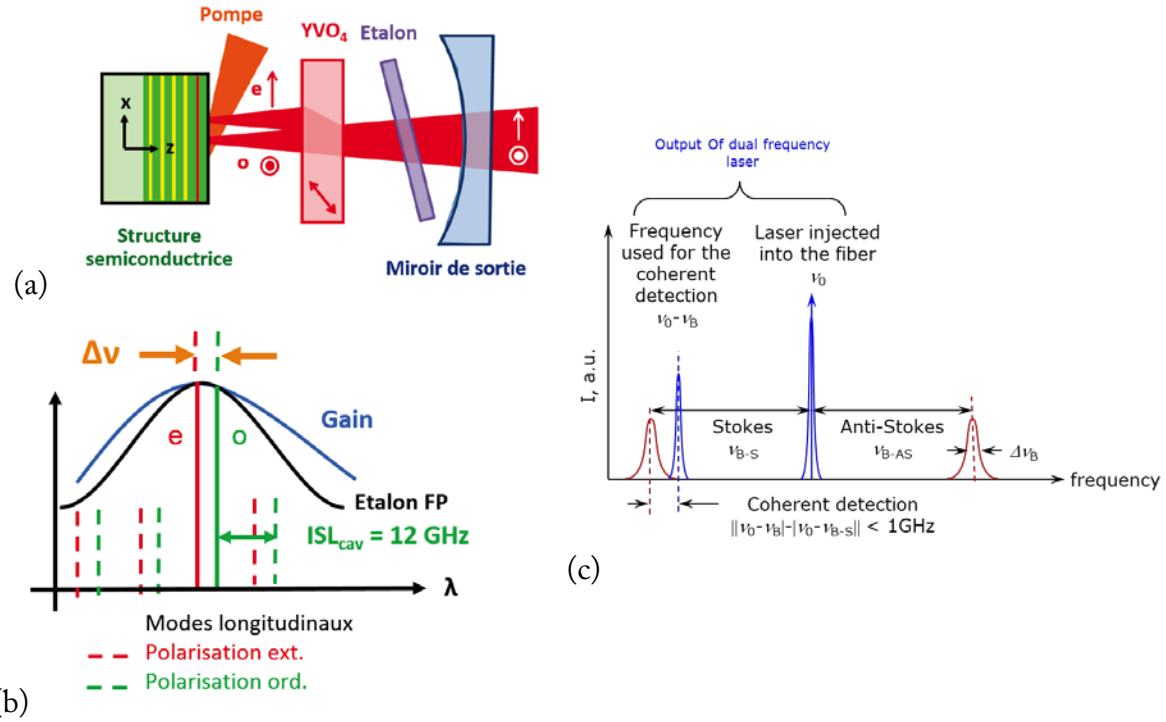

Figure 2-32 : (a) The laser cavity with the elements intracavity to obtain dual frequency laser; (b) selection mode technique using the Fabry-Perot etalon. (c) spectral components used in the spontaneous Brillouin scattering sensing.

The main results related to the output spectrum are showed in the Figure 2-33. Frequency separation was close to 11GHz.

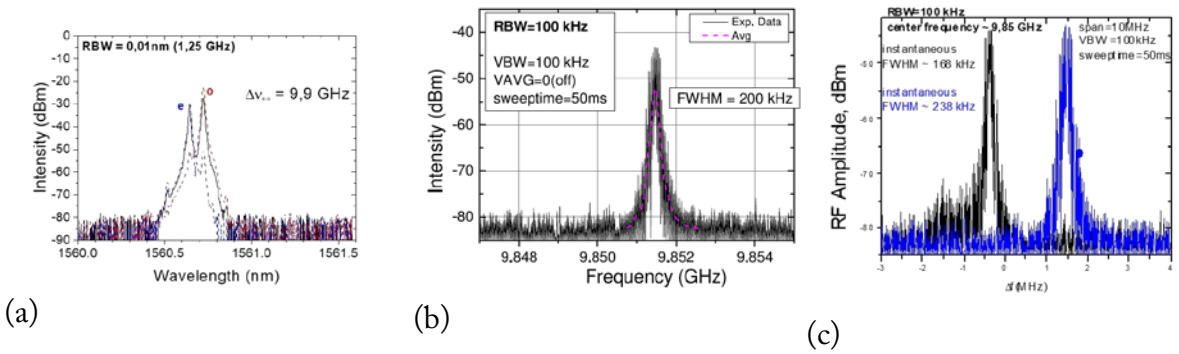

(a) (b) (c)

Figure 2-33 : a) The optical spectrum of the dual-frequency laser emission obtained with a 50µm thick SiO_2 Fabry-Perot etalon, o- ordinary component, e-extraordinary component; (b) Electrical spectrum recorded with the electrical spectrum analyzer (ESA) for a cavity length of ~8.8mm and an YVO_4 plate thickness of 500µm. The ESA resolution bandwidth (RBW) and video bandwidth (VBW) were set to 100 kHz. No video averaging (VAVG) of the trace was used; and (c) Evolution with time of the electrical spectrum recorded with the electrical spectrum analyzer for 5mins.

Frequency instabilities were detected, we have distinguished three different levels:

-Cooling and heating: It is a slow process, it will modify the gain of the VECSEL beside that cavity length is impacted. The output frequency is slowly modified.

-Environmental mechanical vibrations, related to the different mechanical elements appear to be the main cause.

To resolve these two previous problems, we worked on a short cavity design on Solidworks. The simulations realized that we had again some vibrations close to 5-8 Hz in horizontal and vertical directions. Now a new work on the design of monolithic cavity inspired bibliographic work is in progress [132]. It should be simulated and fabricated in 2018.

-The last problem was related to the optical pumping non-stabilities. Where the fluctuation in power and the variation of the polarization has impacted the high frequency stability of the dual frequency laser.

The design of the new monolithic cavity adds a polarization splitting for the pump. In this case we should pump every resonator mode (o-, e-) with one polarization.

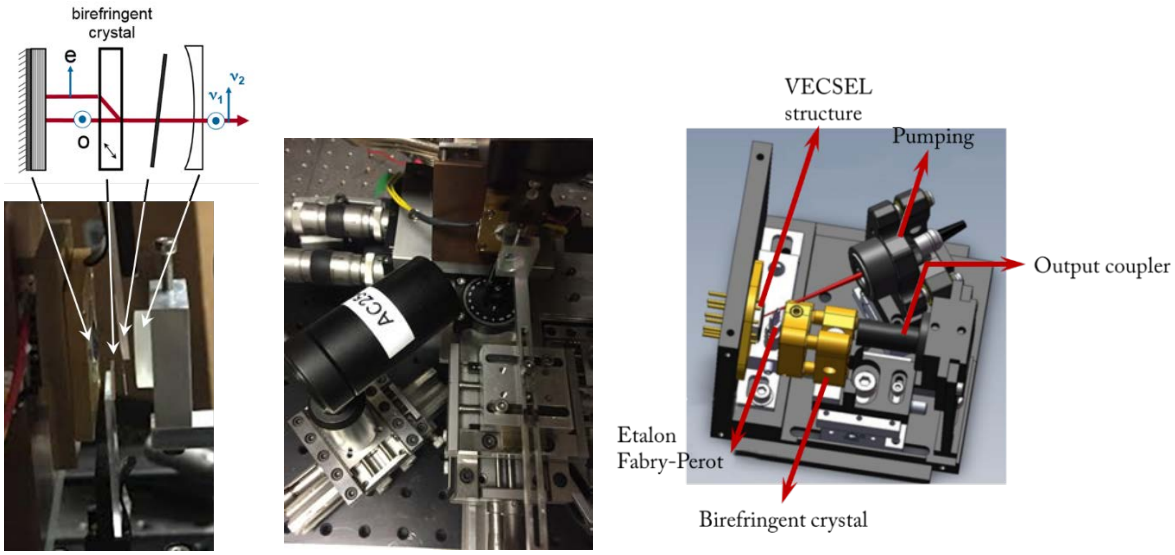

(a) (b) (c)

Figure 2-34 : Dual frequency VECSEL: (a) The laser cavity in lab. with the four elements: -VECSEL structure, birefringent crystal YVO_4, Etalon Fabry-Perot, and the output coupler. (b) the complete cavity in the lab; and (c) A proposed version of compact dual frequency VECSEL cavity on Solidworks.

2.6.2 The sensing schema

The proposed sensing schemas for Brillouin optical fiber sensors based on the dual frequency laser is presented in the Figure 2-35. It is possible to investigate Brillouin scattering, in spontaneous and stimulated processes. The important benefits from dual frequency lasers, is the coherence de phase between the two generated frequencies. This coherence of phase will increase the detection efficiency, which will very attractive for fast acquisition of Brillouin gain spectrum.

We tried in the thesis of M. Salhi to investigate the laser parameters on the detection performance. For that reason, a simplified electrical circuit has been used to simulate the optical fiber and generating the Brillouin frequency shift from random thermal fluctuations in the fiber itself. We simplified the sensing configuration by using the electric field and working on spontaneous Brillouin scattering at the first phase as shown in the Figure 2-36.

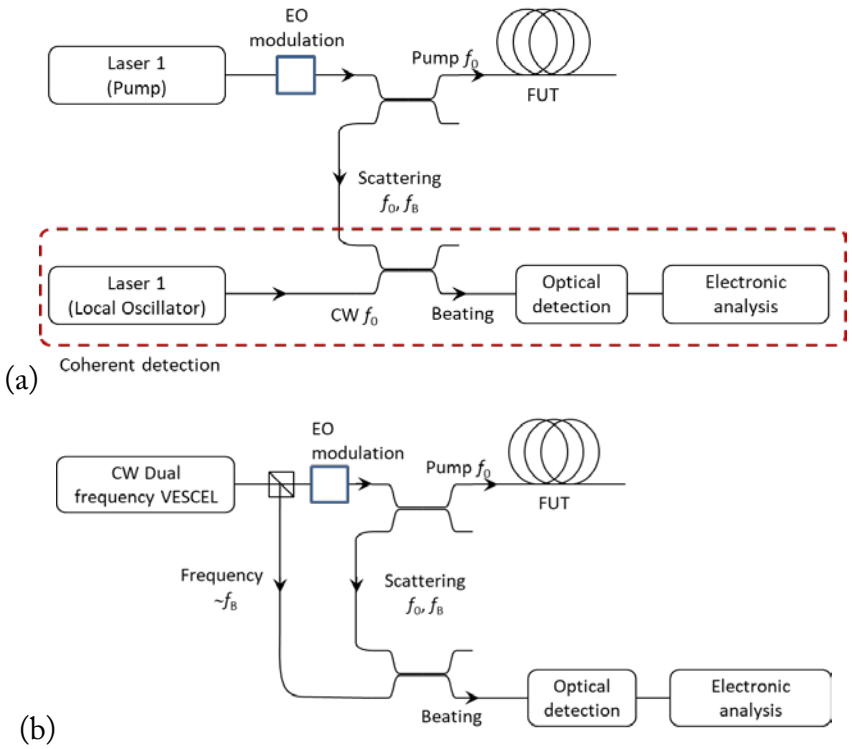

Figure 2-35 : a) sensing schema used in B-OTDR systems, b) proposed schema using dual frequency sensor laser.

The next step, is to use this model and work on the simplification of the sensing schema.

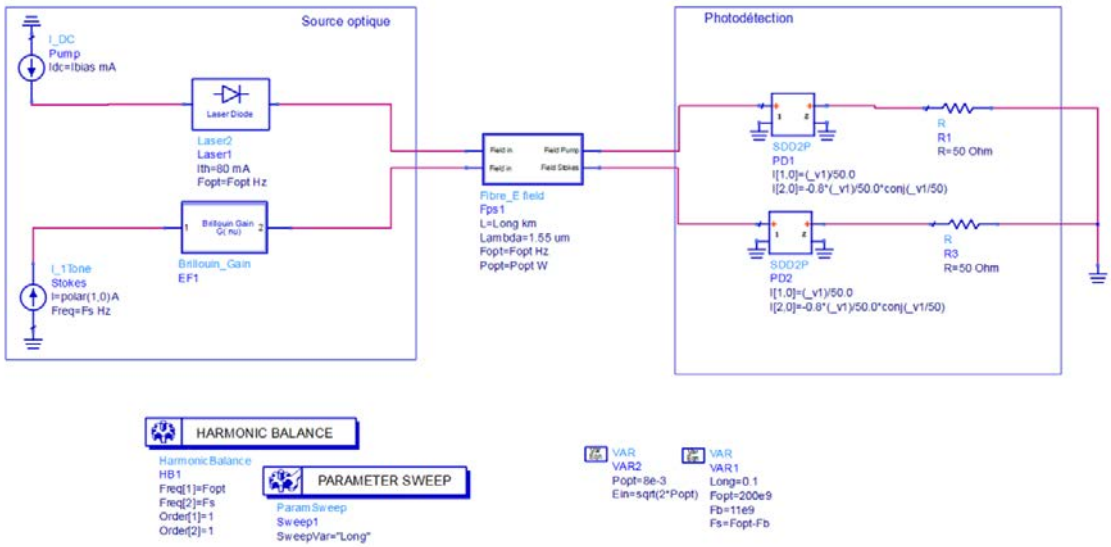

Figure 2-36 : Electrical circuit studied to simulate Brillouin scattering.

2.7 Optical fiber sensing cables

The quality of load transmission between the different interfaces from the matrix material to the optical fiber determine its ability to measure strain precisely. The stresses that appear in an optical cable when axial stress is applied can be illustrated as in the Figure 2-37. The coating layer is applied on the fiber during its fabrication process, which can usually be considered as perfect, and the bond can be described by $\tau_{c,f}$ [133]. Where the other interfaces depend on the cable design and its production procedure.

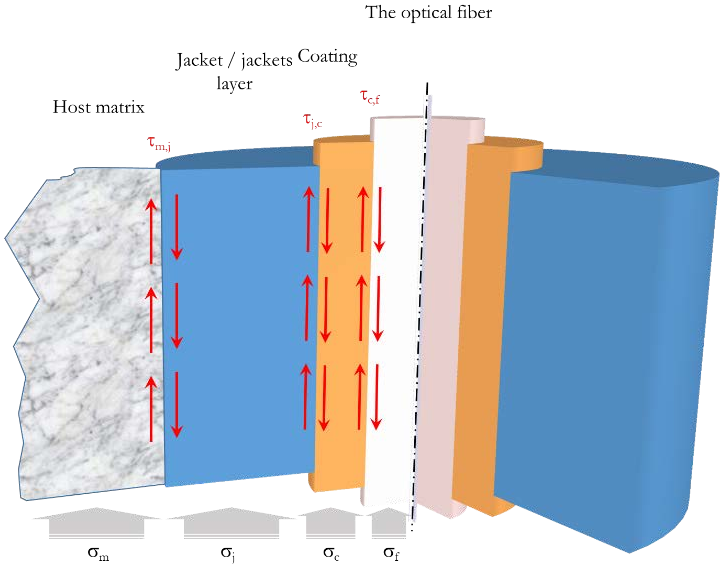

Figure 2-37 : Normal stresses and shear stresses inside an optical fiber cable.

Apart from the bonding between different layers, the strain transmission is dependent on the mechanical properties of the different elements: optical fiber, the protective coating, the jackets and the length of the optical fiber [134, 135]. A part of the strain in the host matrix material is always absorbed in the coating and the jackets layers, because they have in almost cases, Young's moduli lower than of the fiber[136]. The relationship between the axial deformation of the different cable layers can be described using the equation:

$$\delta_m(x) = \delta_f(x) + \delta_c(x) + \delta_j(x) \tag{2.19}$$

With δ_m axial deformation of matrix material [m]

δ_f axial deformation of the optical fiber [m]

δ_c axial deformation of the protective coating [m]

δ_j axial deformation of the jacket layer [m]

Theoretical modeling and mechanical tests showed that in assumption of perfect bond: strain decaying effects occur especially in the end regions in the transition from loose cable to installed one [137]. The same phenomena observed in regions of fast variation of strain [138].

The best obtained results for load transmission are achieved when the optical fiber was directly embedded into the host matrix. The research works stated that the effect of strain decay due to load transmission, depends strongly on the overall length of the fiber. It has an effect especially in the last few cm of the fiber, which is for most measuring setups beyond the spatial resolution.

Optical fiber sensing cable designs depend on the boundary conditions and their specific needs, thus a basic cable design, which fits all requirements, will be very complicated to be designed. Therefore, different cable designs for different monitoring applications have been developed to fit the needs for best possible data quality. Strain sensing cables should satisfy completely different requirements than standard telecommunication cables,that have extensively been studied and can be used for distributed temperature sensing, for example. The main needs for the optical fiber cables design are the mechanical protection, the bonding between the different layers of the cable, temperature cross-sensitivity measures and specific project-requirements.

The optical fiber sensing cable designs can basically be separated into three different groups:

-Cables for external installation thus cables that are attached onto the structure to be measured, we have studied such type of cables (Figure 2-38).

-Cables for the installation inside of concrete, we have used different types of such cables and the results depends on PH, stability of the host medium. We present some results in the next paragraph.

-Cables for the installation into natural soils.

Some cable designs are possible to install into multiple surrounding materials thus cannot strictly be categorized in one group.

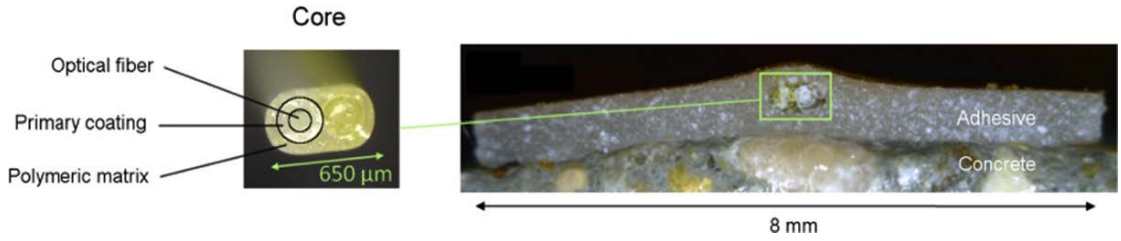

Figure 2-38 : cross-section of the cable stuck to a concrete surface, including a zoomed view of the cable core, where two optical fibers and their primary coatings are embedded in a polymeric matrix.

2.8 Distributed optical fiber sensors applications

I present in this part some applications related to specific integration of the optical fiber into the structure. Other results considered confidential by the industrial partners are not presented.

2.8.1 Distributed optical fiber sensors concrete structures

I present here some main results which has been validated in laboratory tests, and in the real conditions outside of laboratory tests. I start with tests done on reinforced-concrete structures made of ultra-high-performance fibrous concrete (UHPFRC) which is an interesting case in structural health monitoring applications. Then I present works done on older structures, to show that optical fiber sensor integration into existed structure is working very well. At last I present some results from tests still going on in the Great Paris construction of new train stations. Works on concrete shrinkage and swelling of concrete are not presented in this dissertation.

2.8.1.1 Instrumentation of UHPFRC structures

The structural health monitoring of reinforced-concrete structures made of ultra-high-performance fibrous concrete (UHPFRC)[139, 140] is an attractive application for distributed optical fiber sensors applications, that is investigated in this study. Using DOFSs to monitor such type of structures, where high spatial resolution appears very attractive due to their small transfer length (minimal length to transfer forces from the rebar to the concrete) is proposed in this study. Different solutions were proposed for Optical Fiber sensors integration into naked rebars and into rebars embedded in a RC member: (1) The optical Fiber sensors can be potted into the drilled cavity in the rebar using suitable adhesive. Then the short rebar with embedded sensor can be welded with the primary rebar [141]. Using this technique, point strain measurements could be measured, which is not very suitable for strain measurements along all rebar. (2) The sensor is aligned in a trench (1 mm wide, 2 mm deep) that is cut along the entire length of the tendon. Optical Fiber sensors is continuously fixed with a two-component epoxy inside the trench [142, 143], or in the center of the reinforcement steel rebar [144].

But some questions will stay to be investigated: -effect of rebar cross section reduction, and the preparation processes of trench. The strain transfer characteristics into Optical Fiber sensors should be evaluated to determine the maximum strain experienced by the host structures. In addition, the mechanical properties of the adhesive, which display material nonlinearity and plastic features, can influence the force equilibrium of the Optical Fiber sensors system, and thus they can also alter the quantity of strain transfer characteristics. Moreover, we

cannot accurately predict the maximum host strain from the residual strains without consideration of mechanical and geometric properties of the adhesive layer. We should mention that concrete mix used in this work derives from the mix used in the cooling towers of Cattenom nuclear power plant [145].

The Young's modulus of bare standard silica optical fiber is ~72GPa, and for a polymer coated silica optical fiber it is reduced to 15-20GPa [146-149], due to the low Young's modulus of polymers. The adhesive has a substantial influence on strain measurements. The viscosity and shear strain are factors that are important when dealing with optical fibers. The adherents and adhesive interact and should have a good compatibility in order to obtain correct bonding of the optical fibers into the rebar and ensure its mechanical protection. The DOFS was embedded into a U-groove using two-component Methyl Methacrylate adhesive (HBM Germany, Darmstadt, Germany) [150]. This adhesive was chosen for its mechanical and thermal characteristics, Working temperature -200°C up to +60°C for HBM X60, and-55°C up to +120°C for HBM X120.

The Figure 2-39 presents all the details related to the DOFS integration into the rebar: (a) the design of the U-groove, (b) the image of the U-groove realization with, (c) the embedded fiber into rebar where the input/output leads of the optical fiber (unbonded parts) were protected by means of a fiber plastic jacket, and: (d), an image of the U-groove with the output cavity where it is possible to see the adhesive in contact with the surface of the U-groove. The DOFS is surrounded by the adhesive and it's possible to see its trace in yellow after the cutting the rebar. The groove has a depth of 2mm with a width of 0.5 mm.

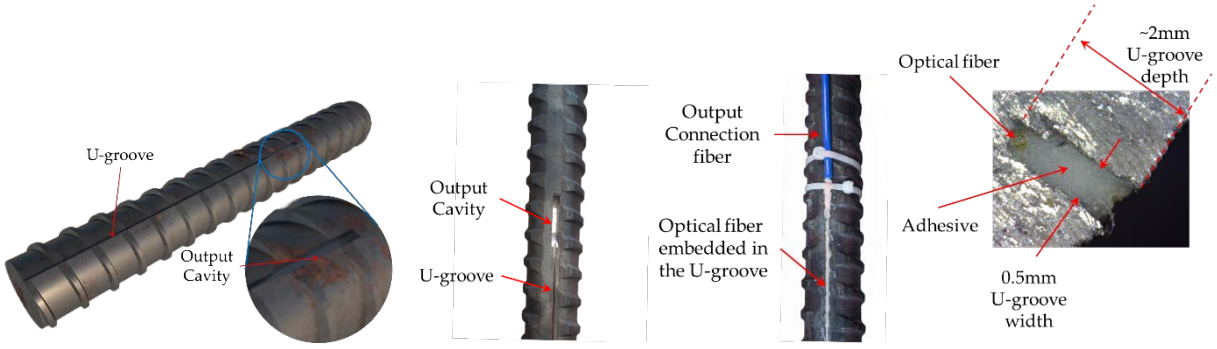

Figure 2-39 : distributed optical fiber sensor embedded into a rebar: (a) view of the U-groove geometry with the output cavity, (b) an image of prepared reinforcement rebar with U-groove and output cavity, (c) the image of the DOFS embedded into rebar with adhesive, the end of the bonded zone with the connection fiber; and (d) detailed profile view with adhesive inside the U-groove showing perfect contact with all faces.

In the first evaluation test, load-controlled direct tensile tests were performed on 60-cm long steel rebar (diameter = 8mm; characteristic strength at yielding 500 MPa). The FOS integrated into the rebar was 45 cm long. The bar had two U-grooves in opposite positions with respect to the centroid of the section. The two grooves were 0.5 mm and 1 mm wide. The purpose was to check the geometrical effect of the U-groove on the integrated FOS signal.
To test the sensor-equipped rebar, a hydraulic uniaxial tension press was used. The rebar is inserted between the jaws of the press and blocked by friction at both ends. Any uniaxial force (in tension or compression) or displacement can be applied. During loading process, both the load (with an accuracy of 0.5% of the total applied load) and the axial displacement can be monitored. In addition, the strain on the surface of the rebar can be measured by means of a conventional strain gauge or a Linear Variable Differential Transformer (LVDT), to make comparisons with FOS results.

The instrumentation setup and the strain distribution obtained by means of the FOS integrated into the rebar under different loadings, compared with LVDT and gauges is shown is presented in Figure 2-40.

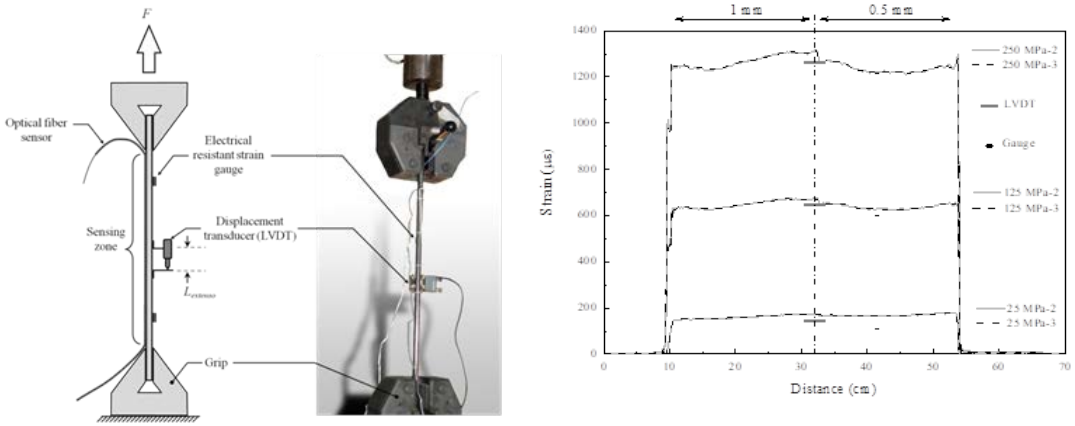

Figure 2-40 : Strain distribution obtained by means of the FOS integrated into the rebar under different loadings, compared with LVDT and gauges (two different widths of the U-groove, 1mm on left side and 0.5 mm on right side).

Load/displacement-controlled tests in direct uniaxial tension were performed on reinforced UHPFRC dog-bone specimens with a length of 160 cm. The rebar diameter was 12

mm and the FOS length integrated into rebar was 96 cm. The U-groove had a width/depth equal to 0.5/1 mm, respectively. The characteristic strength at yielding of the steel f_{yk} was 500 MPa. The geometry of the UHPFRC specimens is depicted in Figure 2-41. During the tests, specific attention was paid to protect FOS connections.

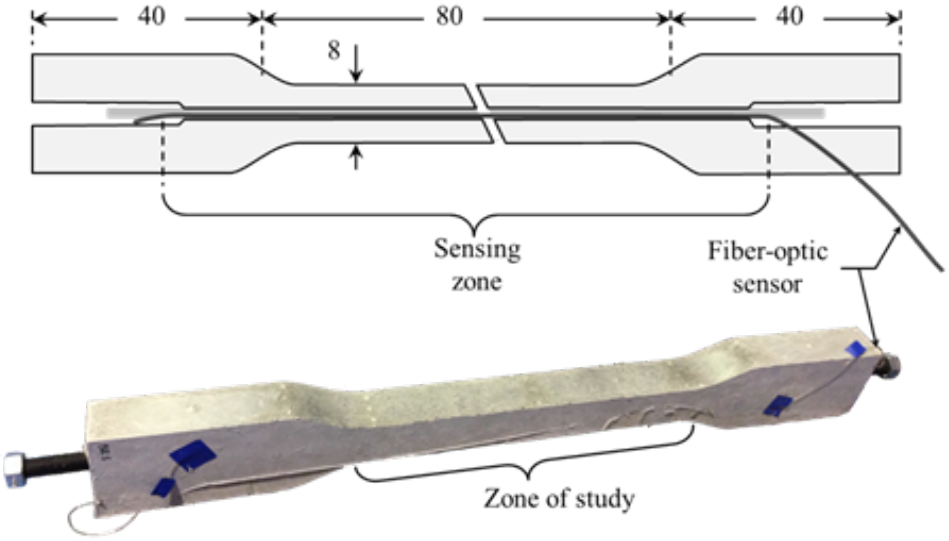

Figure 2-41 : UHPFRC dog-bone specimen tested in uniaxial tension (in cm); the cross-section is 80×80 mm2 in the central zone.

The FOS enables to describe the strain profile in the elastic regime and also to detect first cracking, as shown in Figure 2-42 a). When the load increases, new cracks appear and the width of the existing cracks increases. The FOS then enables to describe completely the strain profile of the rebar induced by cracking (Figure 2-42 b)). Close to the maximum load, some cracks localize with the yielding of the rebar. The FOS detects this localization with a sizable strain increase at this point (Figure 2-42 c)).

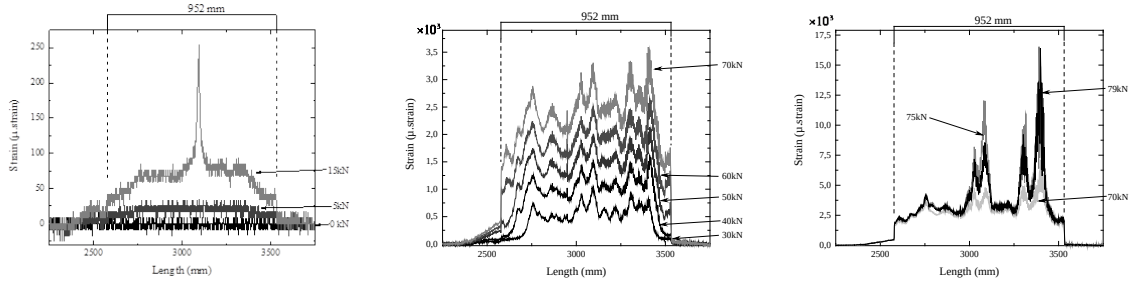

(a) (b) (c)

Figure 2-42 : FOS-evaluated strain distributions along the bar under different load histories: a) non-stabilized cracking with progressive cracks initiation, b) non-stabilized cracking with progressive cracks initiation. c) strain localization, with local bar yielding

To further evaluate the performance of the developed sensing chain when implemented in RC structure, pullout samples were fabricated. The pull-out test is a traditional bond test that consists of the extraction of a bar partially embedded in a concrete block (Figure 2-43). In this research, two embedding lengths were tested (EL=30mm and EL=90mm) in order to experiment the sensing chain when facing two different strain profiles. A single Ultra-high-performance fiber reinforced concrete (UHPFRC) test block containing six embedded rebars was cast for each studied embedding length.

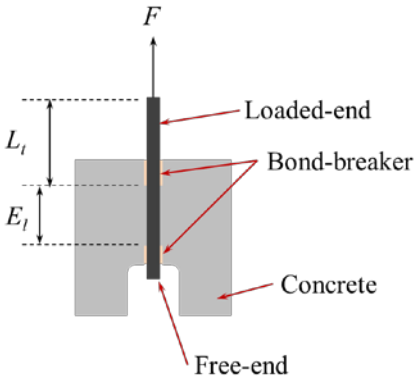

(a)

(b)

Figure 2-43 : Direct tension pullout bond test: (a) Principle of the test (Lt Length under pure tension, El rebar embedded length); (a) and overall photo of the loading setup (b) overall photo of the loading setup

Measurements were performed while tensile loading was imposed to the deformed rebar, but during measurement, it was necessary to maintain the load to a constant value. Results presented on Figure 10 and Figure 11, demonstrate that OF sensors can not only survive the concreting process, but can also acquire strain measurement. Indeed, a near constant value of the tensile strain was recorded along the length of the rebar under pure tension (the small fluctuations can be explained by the variation of the rebar diameter due to the ribs). Moreover, the typical strain profiles of embedded rebars are recorded whatever is the embedded length.

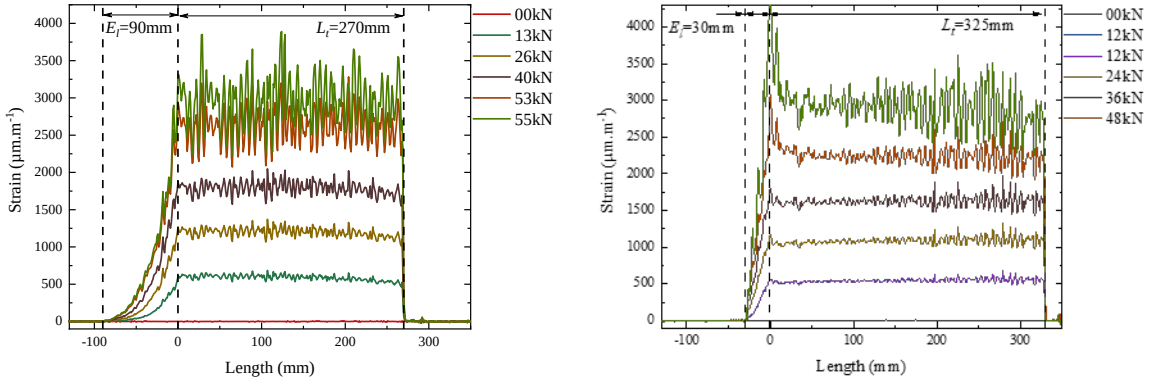

(a) (b)

Figure 2-44 : Measured strain profiles along the rebar for different loading steps: a) rebar embedded length EL=90mm, b) rebar embedded length EL=30mm

This technique of optical fiber integration into rebars has been used to study the interface (rebar-concrete) in push-in tests. We have added some fibers around the steel rebar to study the evolution of the measured strain in the concrete. The fiber configuration with the experiment is shown in (Figure 2-45).

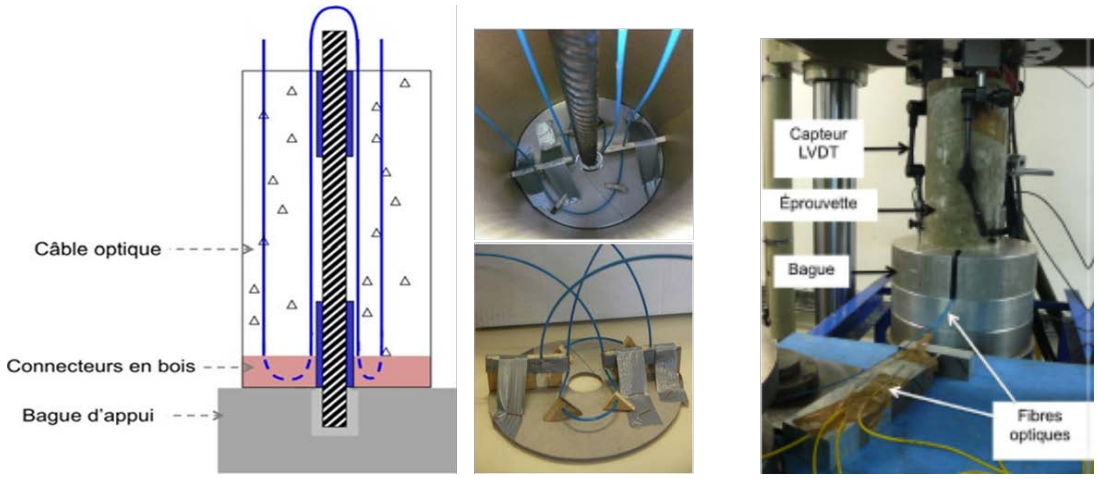

Figure 2-45 : optical fibers installed for push-in tests.

2.8.1.2 Instrumentation of Viaduct precast prestressed concrete beam

The mechanical behavior of large scale pre-stressed concrete beam strengthened with adhesively bonded FRP was studied; using distributed optical fiber sensing technique. The sensing fibers were installed into the concrete structure and between FRP layers. The high spatial resolution strain measurement leads to measure precisely the strain profile along the strengthened beam and to identify the pre-existing cracks and the new cracks which appeared during the 3 points bending test carried-out in 2014 (Figure 2-46), and during shear test performed to the half of the beam in 2016. The role of FRP layers for strengthening and for the control of the crack openings was possible using the different fibers between the FRP layers.

The viaduct of Clerval (France) was built between 1952 and 1954 using precast, prestressed concrete beams. It was demolished in 2002 due to severe corrosion of prestressed cables. At that time, the Cerema laboratory in Autun recovered the upstream edge beam of the right-bank span (length 30m and height 1.30m). Before demolition of the bridge, two flexural cracks, with a maximum opening of 0.2mm were observed in this beam.

Different loading tests were carried out on the beam, before and after the strengthening phases. In 2014, a bending test was performed up to failure followed in 2016 by a shear test performed on a remaining third part of the beam.

(a) (b)

Figure 2-46 : (a) Bending test of the Clerval beam -2014; (b) profile of the Clerval beam, with prestressed cables.

To realize high-performance measurements of strain and detect the cracks locations along the beam length, we installed two types of optical fibers:

-sensing cable to be implemented in the concrete structure,

-single mode fiber with polyimide coating between FRP plates,

We present the complete schemas in the next figure, with all fiber symbols which will be used in the text.

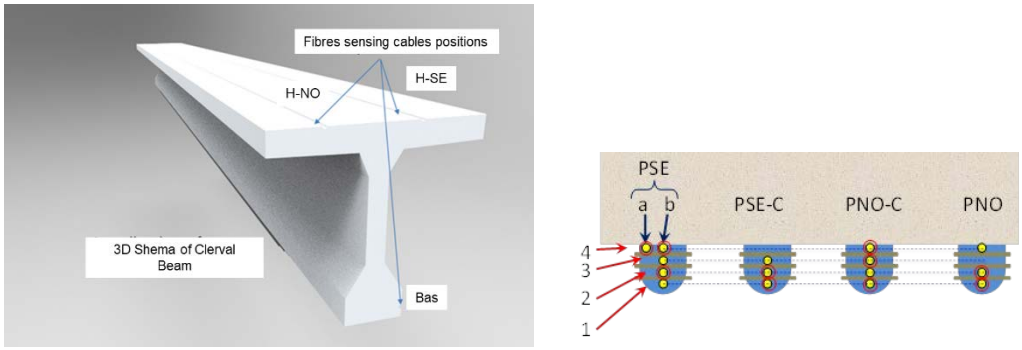

Figure 2-47 : (left) optical fiber sensing cables in concrete implemented into the beam body, (right) Optical fibers between FRP plates.

Symbols: *H-SE : Fiber cable sensor on the South-East side,*

H-NO: Fiber cable sensor on the North-West side,

Bas: Fiber cable sensor in lower part,

P-SE i : *Fibers on the South-East side (i : fiber order),*

P-SE-C i : *Fibers on the South-East side near the beam axe (i : fiber order),*

P-NO-C i : *Fibers on the North-West east side near the beam axe (i : fiber order),*

P-NO-i : *Fibers on the North-West east side (i : fiber order),*

The sensing cables in concrete and the single mode fibres between the FRP plates worked perfectly during the loading procedure. We present in the figures 7-9, the measured strain profile with increasing charge up to failure (from 0kN to 590kN), in concrete.

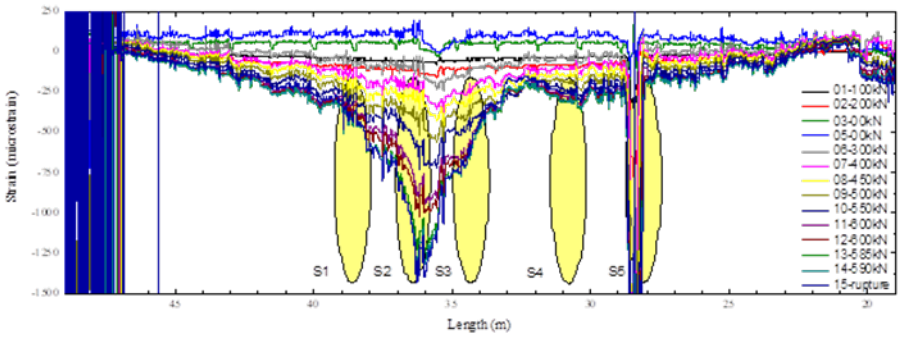

(a)

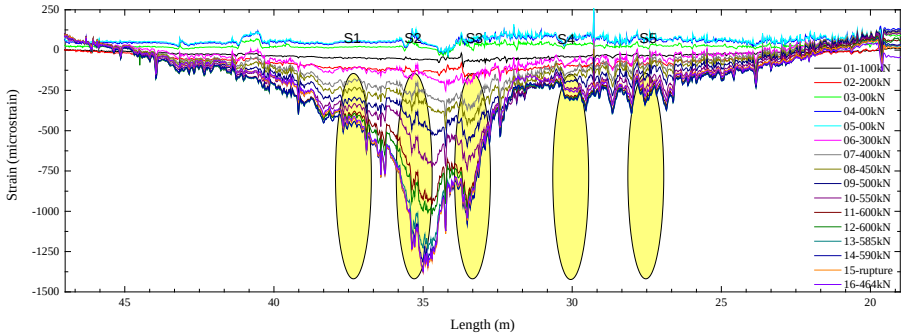

(b)

Figure 2-48 : a) Measured Strain profiles using "H-SE" fiber sensor during the loading, b) Measured Strain profiles using "H-NO" fiber sensor during the loading.

To demonstrate the applicability of the optical fiber instrumentation in the particular case of reinforcement FRP plates, we present some profiles of measured strain between FRP plates. The position of selected fiber is shown on the upper right of the graphs.

In all cases (optical fibers bonded on the FRP and in the concrete), measured values of strain were higher than 5000 μstrain at the loading stages near failure. The analysis of results showed that the error measurement was <4 μstrain. For the same loading step, the comparison of strain profiles of optical fibers bonded on the FRP and in the concrete show that strain profile of FRP exhibit a more constant shape in the central part of the beam, Moreover, it can also be noticed that the DFOS instrumentation can detect cracks when optical fibers are bonded in the concrete as well as on the FRP. The strain profiles recorded by the optical fiber bonded on the last FRP reinforcement layer is slightly different from the one recorded by the fiber closer to the concrete surface.

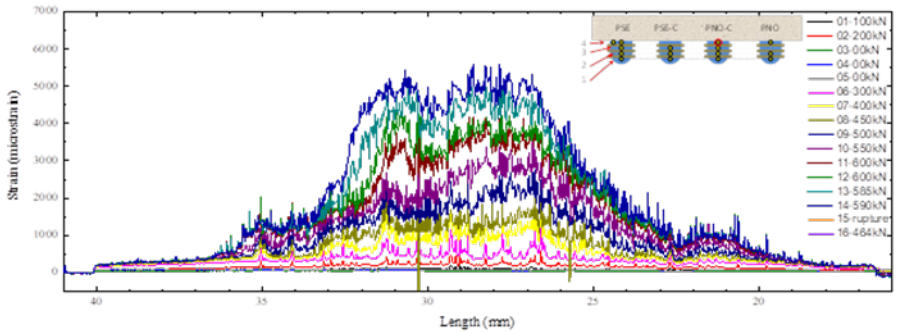

(a)

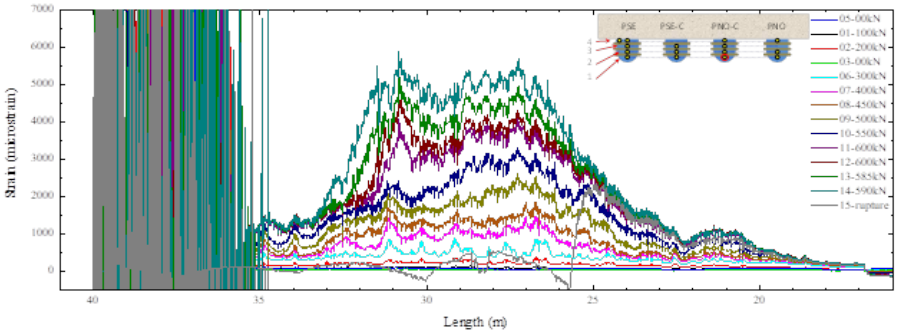

(b)

Figure 2-49 : a) Measured Strain profiles using P-NO-C 4 fiber sensor during the loading, b) Measured Strain profiles using P-NO-C 1 fiber sensor during the loading.

In the shear Test phase, a new schema of fibers between FRP plates, in the middle of the beam was realized. To demonstrate performance of the chosen instrumentation, some measured profiles of strain for different fibers as shown in the next figures:

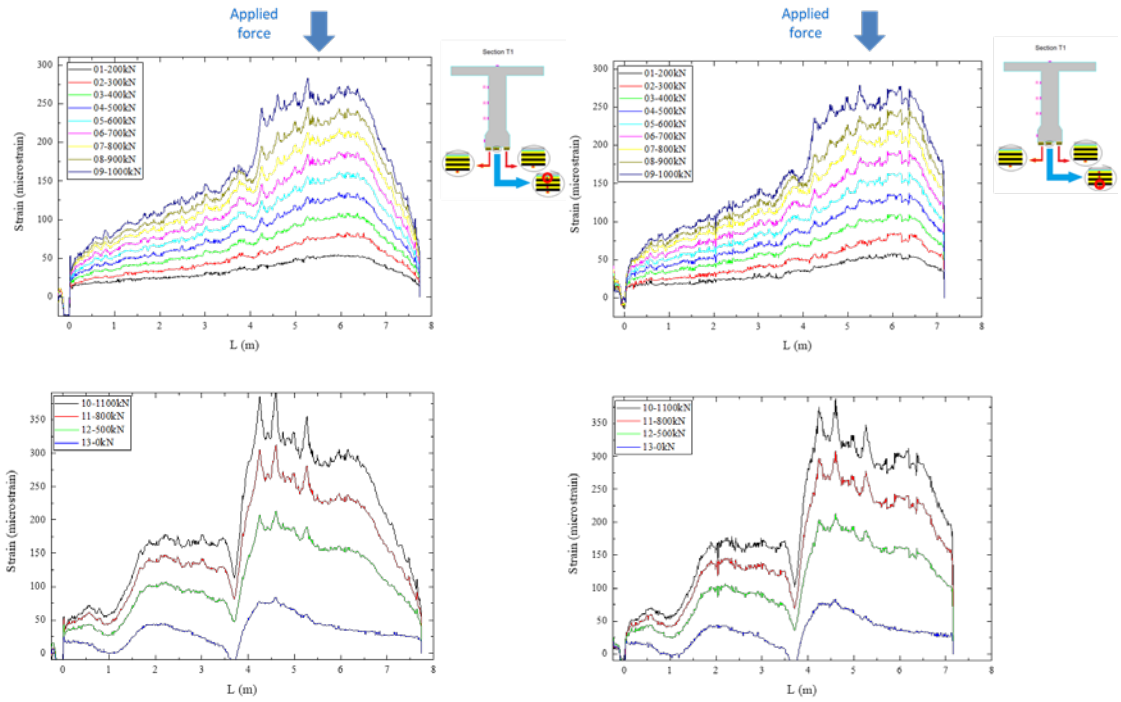

Figure 2-50 : Measured strain of optical fibers between FRP plates: -upper graphs: during loading, and before breakdown of the half beam, -down graphs: after breakdown of the half beam

It was shown that high resolution strain measurement based on C-OFDR Rayleigh scattering technique, is a suitable solution to measure the strain profile and detect the cracks appearing in an existing structure. The optical fibers between FRP plates worked perfectly with high precision strain measurements. More work is needed on the modeling to understand exactly the different problems related to prestressed cables corrosion and concrete cracks appearing, and this phase should finish in 2018.

2.8.1.3 Rock-concrete interface

In the case of hydraulic dams, the structure is supported mainly by rocks. The study of cracks developments at the interface will give an idea about the stability of the dam structure with the shear at the interface, as presented in the Figure 2-51.

We have used a large-scale shear machine, situated at Cerema labs in Lyon city. The tested bloc was formed of two parts: lower part with the rock, and the upper one with concrete.

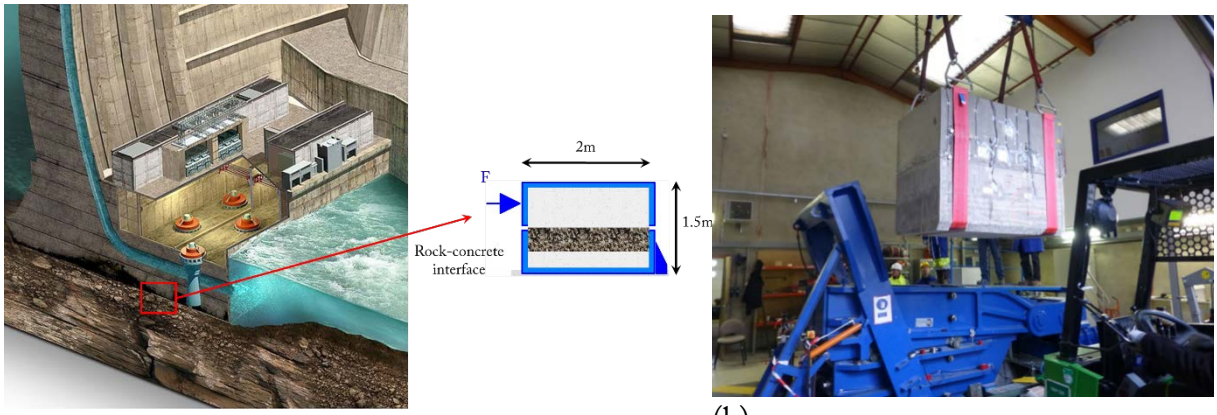

(a) (b)

Figure 2-51 : (a) Illustration for the importance of rock-concrete interface, with the idea of the shear test; (b) image of the shear machine test (at Lyon), with the rock concrete bloc. The dimensions of the bloc are 1.5×2×2.

We have installed the fiber close to the rock surface, as shown in the next photo. After the test was finished we have found that the fiber has moved during the preparation of the concrete. For that reason, we had some difficulties in the post processing to understand all the details. Then we have modified the installation technique of the optical fiber in the bloc.

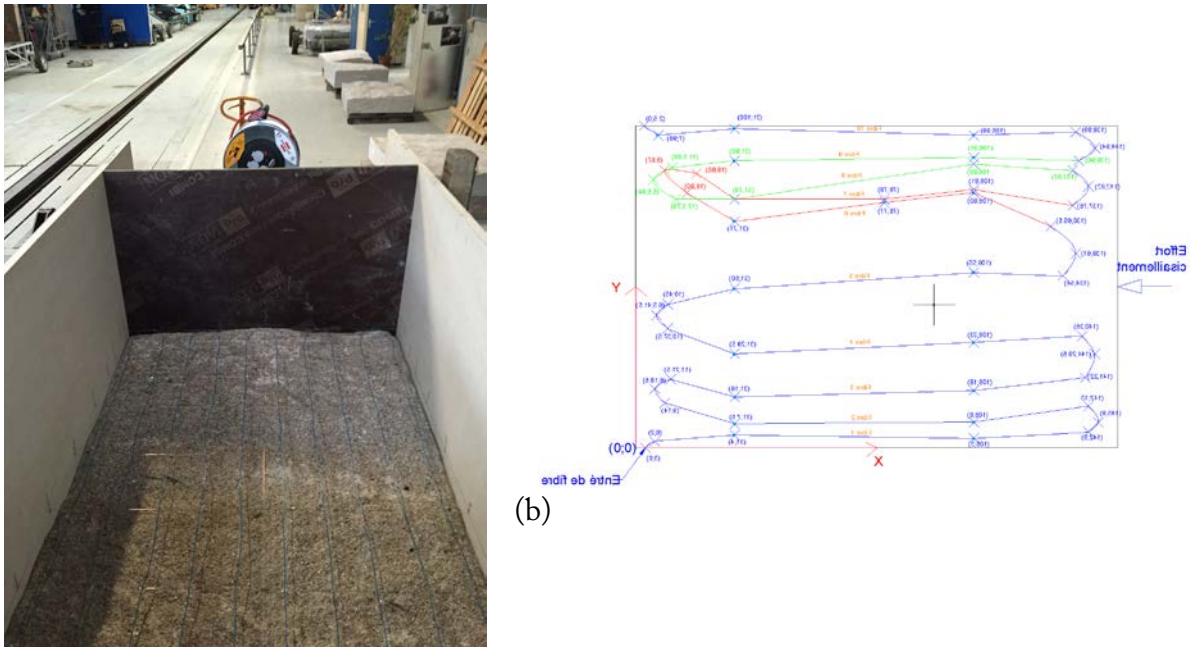

(a) (b)

Figure 2-52 : (a) Photo of the fiber sensing cables at 1-2 cm from the rock surface; (b) illustration for the real fiber position at the end of the test.

The strain measurement during the application of the shear force were registered. The projection of the strain values on an x-y grid related to the coordinates of the optical fibers is shown in the Figure 2-53. We can identify the phase of cracks appearing, propagation, and the breakdown of the interface. These tests were repeated 5 times, with different rock surface roughness. Other samples were tested on small surface scale to understand the relation between the surface roughness, the applied shear force, the initiation of cracks and their propagation. This part is not finished yet.

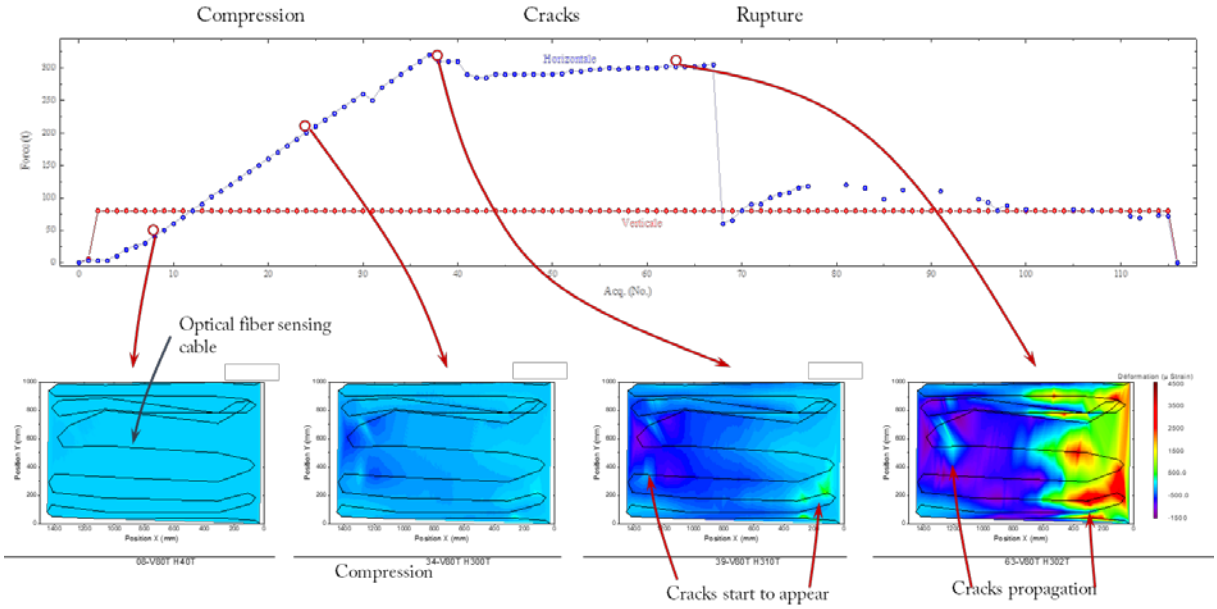

Figure 2-53 : Measured deformations by optical fibers sensors, projected and meshed on x-y plane.

2.8.1.4 Instrumentation of new train station for the project GPE (Grand Paris Express)

This project will create four new metro lines around Paris. The new lines are numbered 15, 16, 17, and 18. They are planned to open in stages through 2023. I'm working on the instrumentation using optical fiber sensors in two new train stations. The instrumentation objectives are oriented to study the evolution of the train station structure during the construction phase.

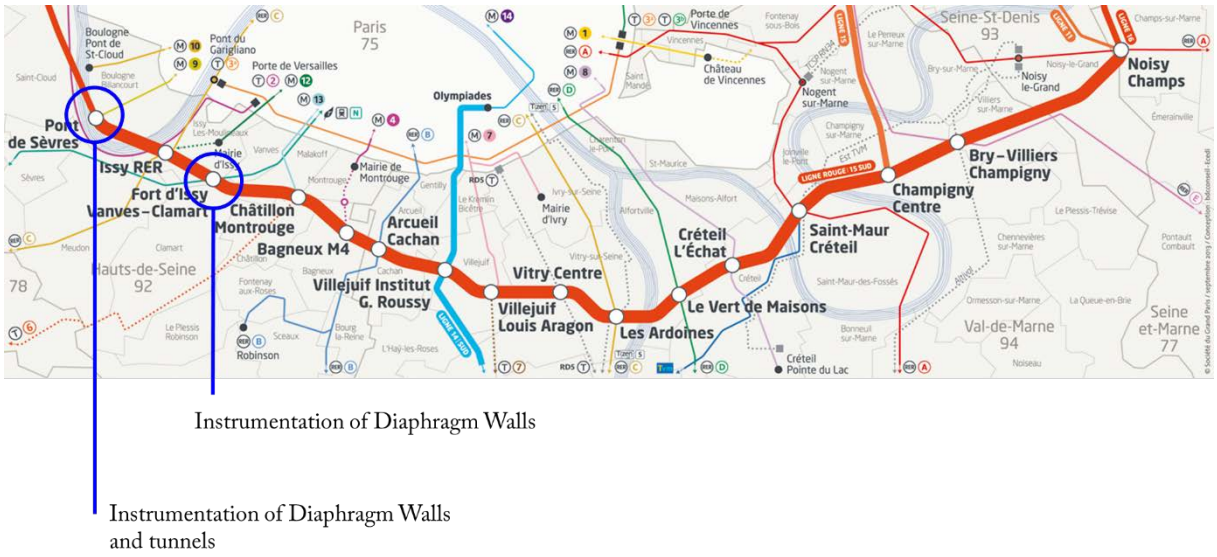

Figure 2-54 : The two train stations, where we have installed optical fiber sensors to follow the evolution of the strains during the construction phase.

Geotechnical design and construction in soft soils are usually associated with substantial difficulties. Since these types of soils are sensitive to deformations and possess low shear strength, their use may lead to structural damage during construction phase as well as throughout the life of the projects. As the metro station perimeter should constructed of diaphragm walls, our choice was to install suitable optical sensing cables along the diaphragm walls.

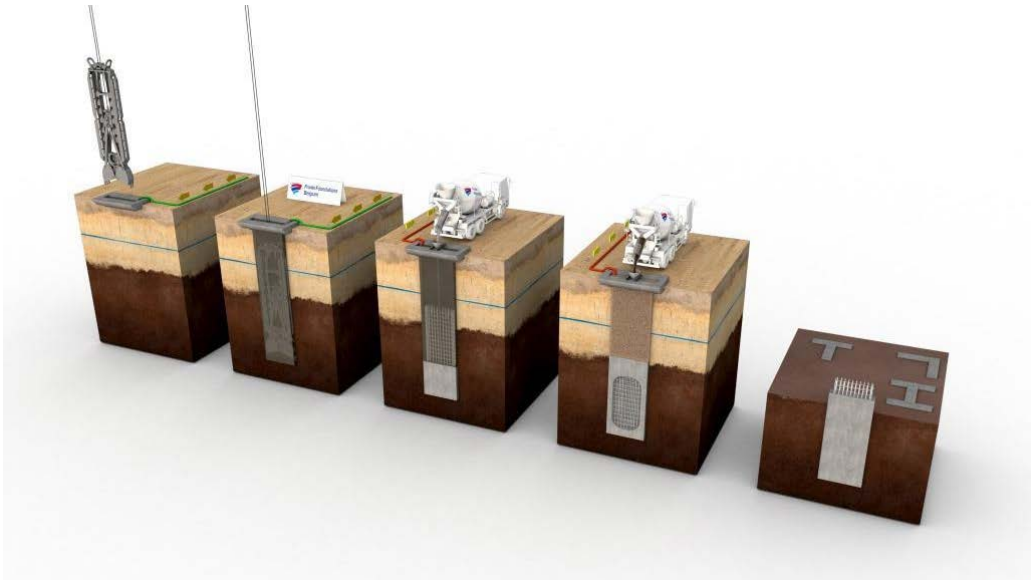

Figure 2-55 : The fives phases to realize a diaphragm wall, from left to right.

2.8.1.4.1 Instrumentation of Diaphragm Wall at FIVC new train station

New train stations are in construction phase near Paris, I present hear the first works on the train station FIVC (Gare Fort d'Issy Vanves Clamart). We have installed an optical fiber sensing cable in U-form to study what is happening in strain and temperature variations with the evolution of the train station construction. The complete length of the U-form sensing fiber was 30m. which means 15m of total depth.

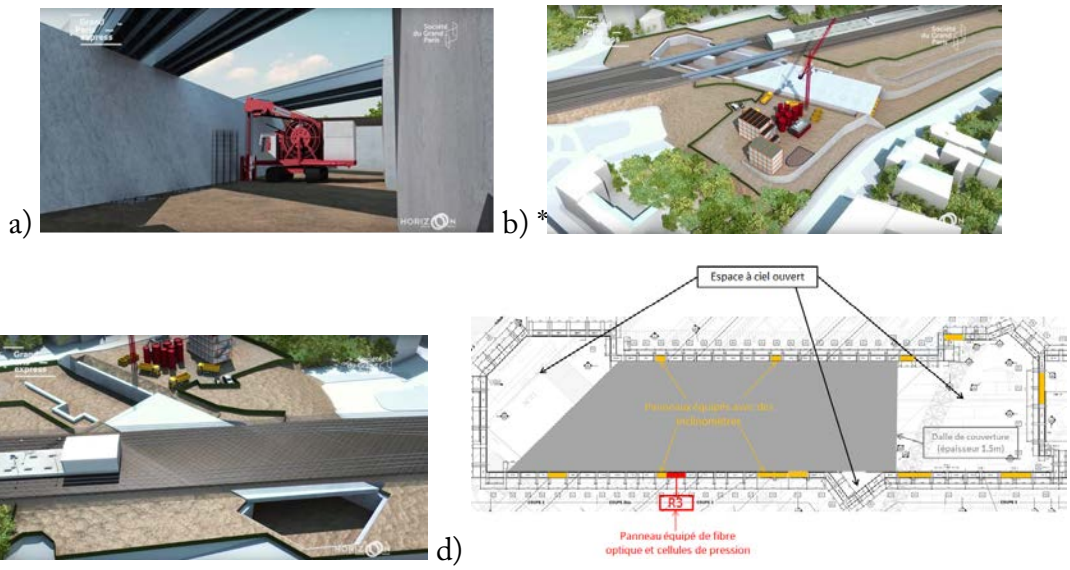

Figure 2-56 : Evolution of the works in the train station FIVC construction: a) June 2017 b) July 2017 c) August 2017, d) position of the Diaphragm Wall monitored by fiber optic sensor.

I have validated the installation, and the reference measurements. A new schema for beams instrumentation has been validated and realized in May 2018.

The Figure 2-57 presents the schema of installed fiber, and measured profiles of strain during the underground perimeter of the station is excavated

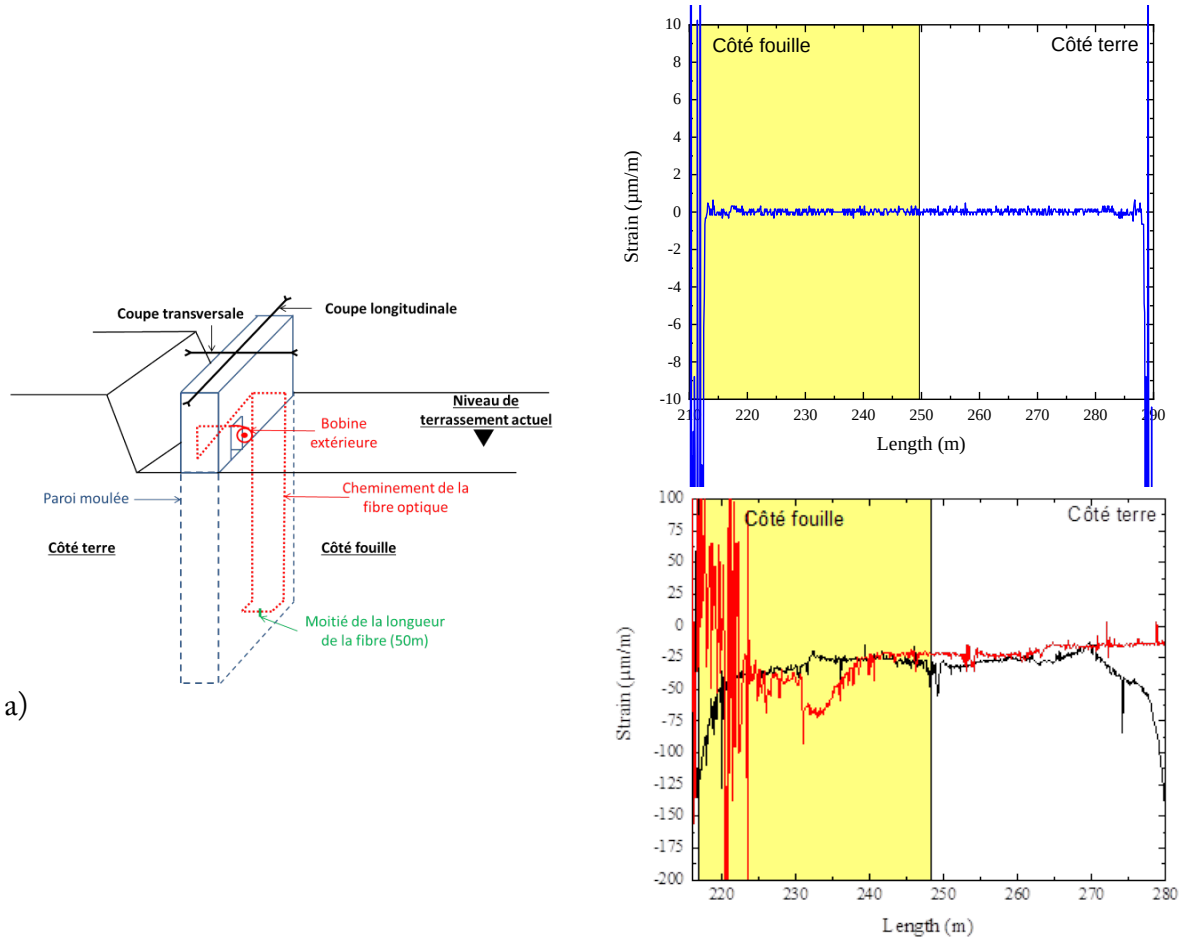

Figure 2-57 : a) Illustration of the installed fiber, b) up-strain profile on 21 July 2017 (reference), down-the strain profile on 25 October in black, and on 11 November 2017 in red.

We make a weekly measurement of strain since November 2017. The complete results will be available at the end of 2018.

2.8.1.4.2 Instrumentation of diaphragm walls and the tunnel at 'Pont de Sèvres'

In this train station, we have more complicated structure to be studies, at first the diaphragm walls: we have chosen to install the fibers in horizontal and vertical positions to monitor the strain in both directions. During the creation of the junction with the tunnel. As shown in the Figure 2-58.

The diaphragm walls have ~1.5m thick and 48 m deep. The reinforcement cage is formed of 3 elements. We have developed a specified procedure to insure the installation of the fiber sensor cable, respecting the low bent curvature diameter and we have verified the signal quality on some realized diaphragm walls.

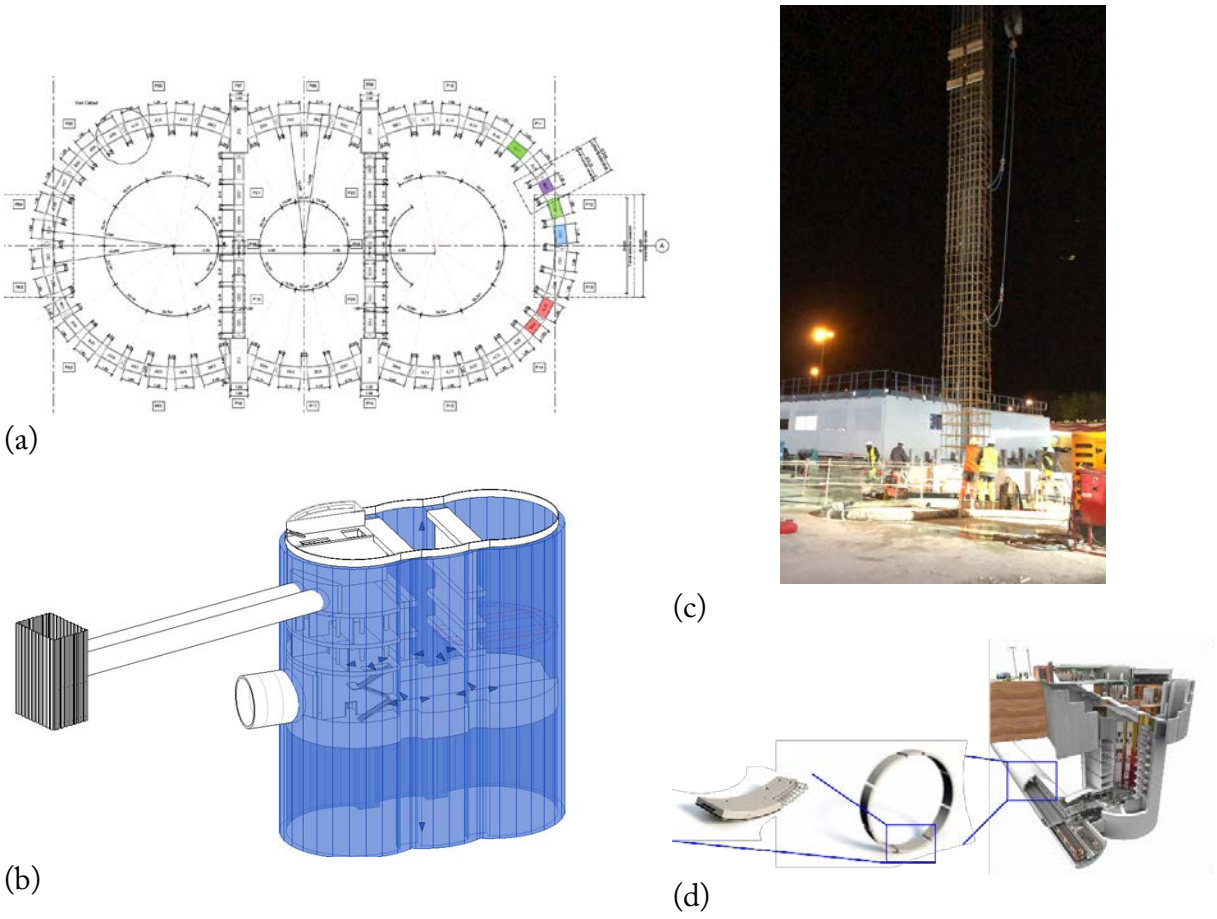

(a) (b) (c) (d)

Figure 2-58 : (a) a profile section of the train station, with the position of the first 2 instrumented diaphragm walls in red (b) 3D Illustration of the metro station, with the junction to be instrumented; (c) one reinforcement cage element during the installation in the diaphragm walls and (d) the single segment to be instrumented in 2019.

The installation was prepared in cooperation with construction site personnel, to avoid any problem. We had different difficulties, mainly: to respect the curvature diameter of the used optical fiber (4cm), we had installed metallic structures and the fibers were fixed on it (Figure 2-59).

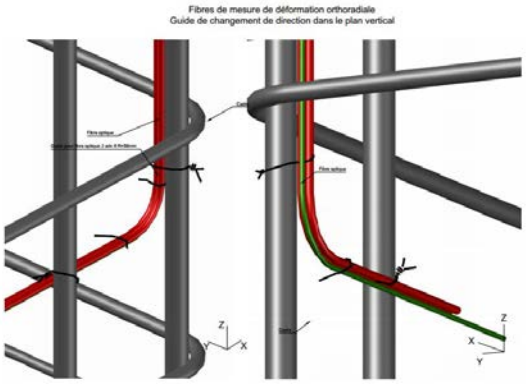

Figure 2-59 : optical sensing fibers fixed to metallic structures to respect the minimal curvature diameter.

Another difficulty was related to reinforcement cages. We had 3 successive reinforcement cages, and the optical fiber should go through all of them. For that reason, we had used different coils of optical fibers at the head of every single cage unite (Figure 2-60). First inspection of fibers has shown a high quality of the optical signal alone the 100m of every single fiber. We are working now to finish the connection network and start the acquisition from August 2018.

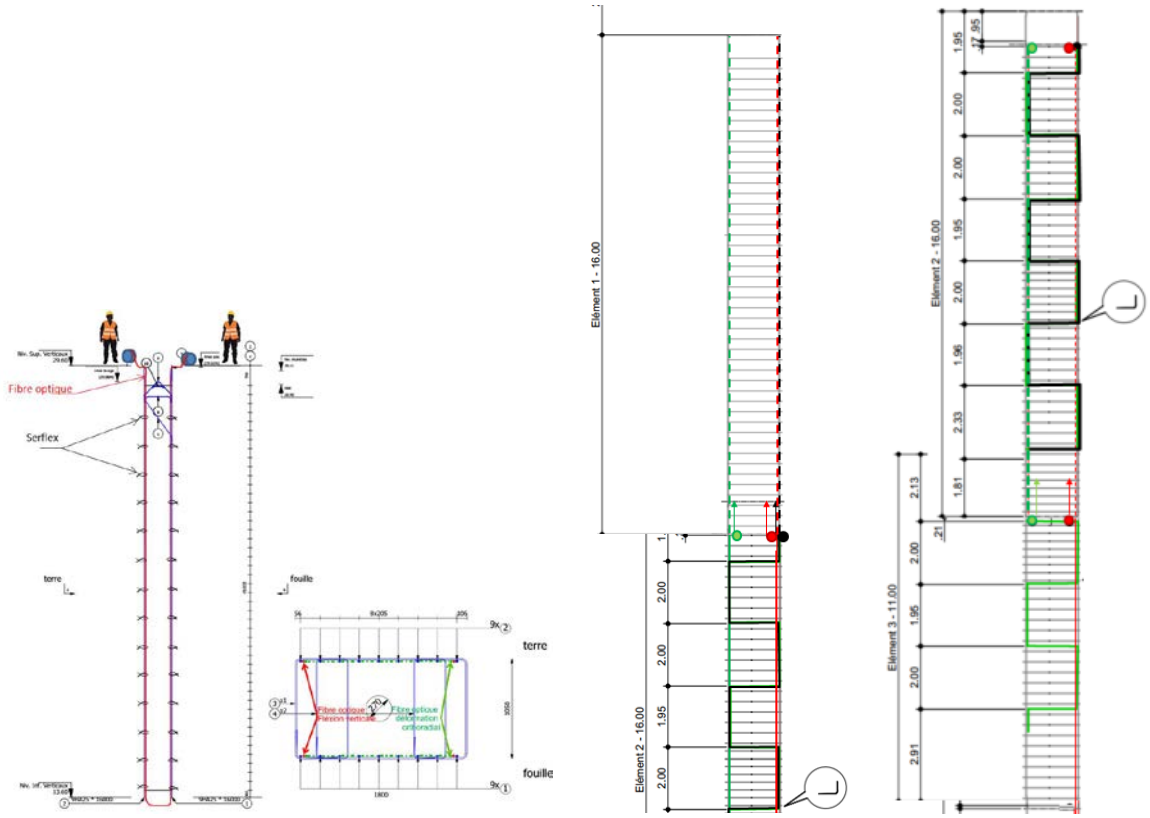

Figure 2-60 : optical sensing fibers fixed to metallic structures to respect the minimal curvature diameter.

The tunnel lining consists of twin bored single-track tunnels. Each tube has a concrete segmental lining with an outer diameter of 7m. and an inner diameter of 5.7 m. The estimated total length of sensing cables to be used in all this application is more than 1500m.

2.8.2 Distributed optical fiber sensors in composite structures

2.8.2.1 Instrumentation of rotator wind blade

In the analyzed wind-turbine configurations, high area of rotation induces extreme mass flow through the blade, so blade should with stand relative forces caused by this mass flow. Numerical analysis could provide preliminary vision about the behavior of blades with low cost of investment. The blade was configured by Python codes to achieve accurate dimensions, airfoil modeling and section splines. Each component of the blade was programmed independently

and assembled in Abaqus commercial software. The blade length is 70 m and chord length at the root corresponds to 3m. The chord length at the tip was considered as 1.5m.

The blade has a twist throughout the span, this twist is assumed to be 15° from root to tip. In other words, the root plane and tip plane are orientated by 15° from one to the other. Spar was considered as box beam section, fixed with skin. The spar contains spar cap, which is placed between 15% and 50% of chord length of the air foil, which with stand bending forces and the chord-wise inertial forces [151]. Shear webs help to with stand the shear forces acting on the largescale assembly. The Figure 2-61 shows the designed aerodynamic configurations and the final model of the blade in Abaqus user interface.

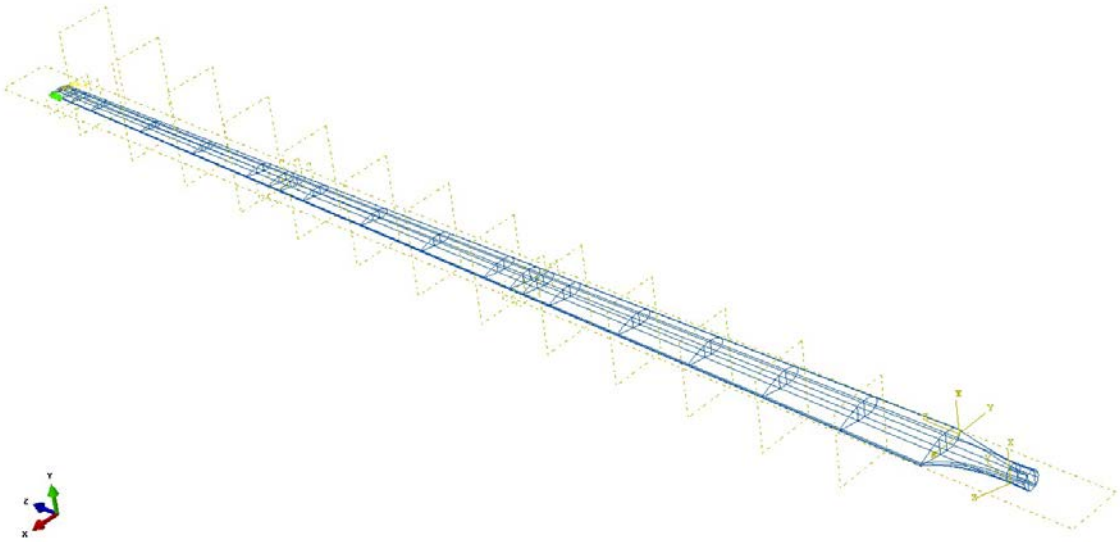

Figure 2-61 : Blade designed by several planes to maintain the air foil profile and twist angle

Embedding a fiber optic sensor FOS into a composite structure is an important issue, since the interface between FOS and surrounding material has to allow accurate measurements. One has to admit that FOSs are foreign entities to the host structure; therefore, it will always alter the stress and strain in the vicinity of the embedded sensor.

The embedment of FOS is decided by two intrusive properties: -Fiber's diameter and coating material. The coating is also known as buffer coating that surrounds the core and cladding of the fiber optics to provide the protection against the environmental impact. FOS exists in various diameters (including coating) in strain sensing applications. If needed,

additional protection is added to use them in the harsh environments [152]. But, sensing is more effective, while FOS is covered by thin coating layers. In other words, least coating is better for the sensibility of sensor

In the model, we have considered adhesive as isotropic material [153]. Thin bonding layer located between the upper and lower section is modeled with shell element from root to tip. This helps to design the bonding without affecting the leading and trailing edge geometries. The section thickness of adhesive layer is 40mm. Composite blades are bonded generally by adhesive materials with high shear modulus and tensile rigidity to avoid the separation of the blades even at the critical wind loading.

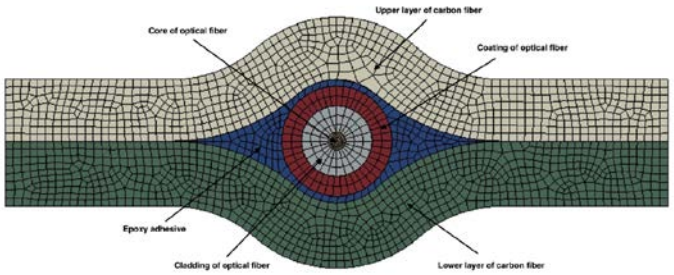

Figure 2-62 : Numerical meshed model of fiber optic sensor embedded in-between two composite plies.

The distributed FOS alignments were studied to see the effectiveness of sensor positioning for their sensitivity, the elastic range of measurements, and multi-parameters measurements (strain at bending and torsion). It is proved from the numerical simulation that linear alignment sensors are able to observe lateral stresses, but not sensible for longitudinal and shear loads (Figure 2-63). Therefore, sinusoidal positioning is considered as a better solution for the various direction strain sensing and also for the large surface area coverage from a single fiber optic sensor. To verify this, we have conducted the experiment under 3-point bending load.

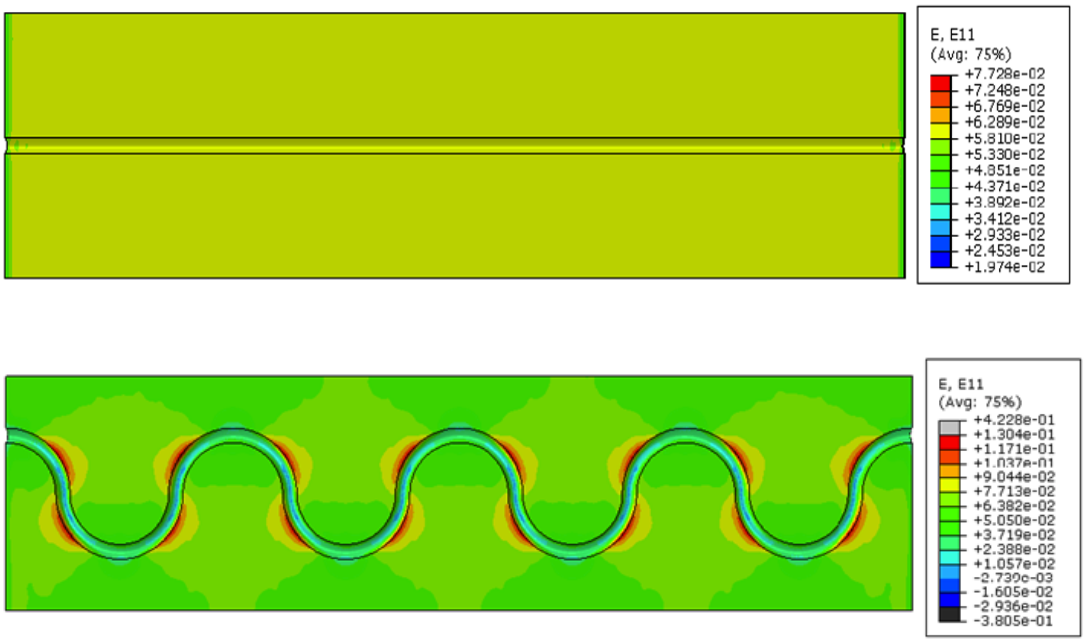

Figure 2-63 : longitudinal strain (E11) observed in epoxy region: a) in linear fiber optic senor with polyimide coating model, b) sinusoidal fiber optic senor with acrylate coating model

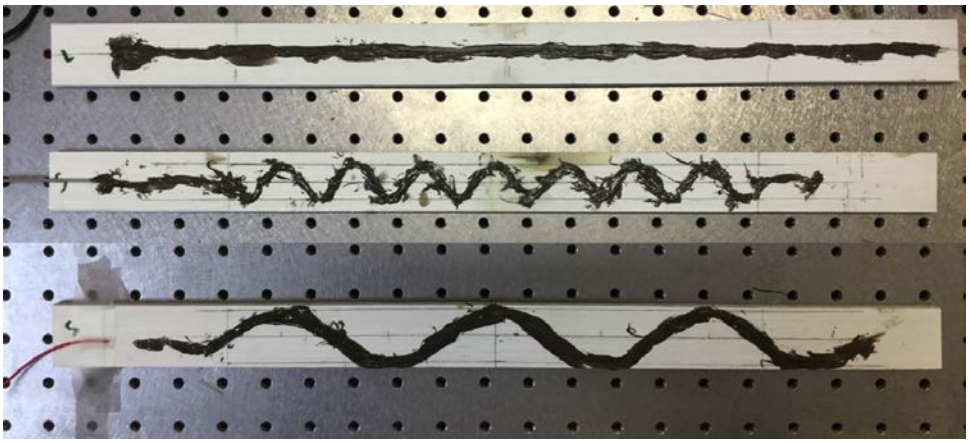

Figure 2-64 : Method of fiber optic sensor alignment in bonding zone for experimental model; linear, small sinusoidal and extended sinusoidal alignments represented from top to bottom

The obtained results, as shown in Figure 2-65 ,confirm that it is possible to recover the strain range by keeping multi-parameter sensing performance just by optimizing sensor alignment. Additionally, torsional strain is also observed with peaks variation. Therefore, sinusoidal alignment would be a better solution for monitoring such structures.

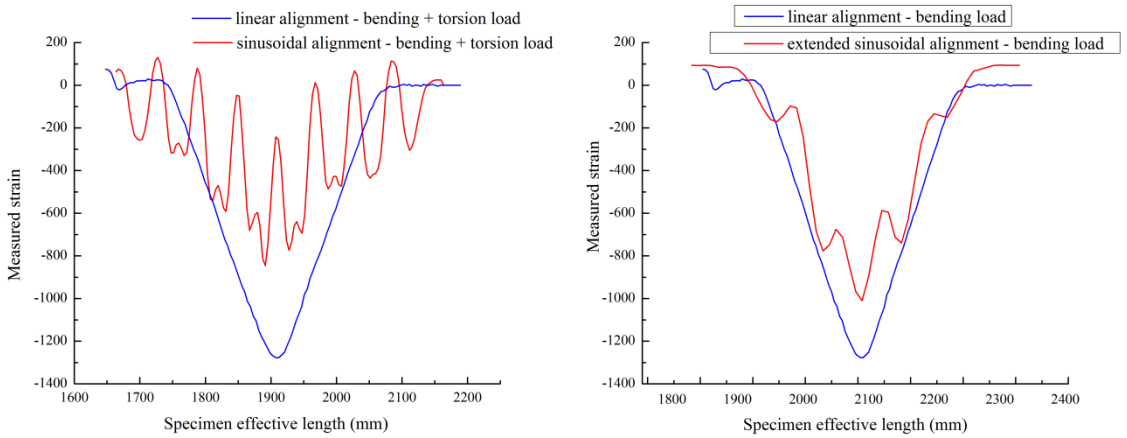

Figure 2-65 : a) Linear vs small sinusoidal alignment-Bending + torsional load; b) Linear vs extended sinusoidal alignment-Bending load.

Distributed sensors are able to measure the strain and temperature modifications in the material. We considered Rayleigh and Raman scattering method to get information about strain and temperature variation, respectively.

Critical aspect of damage initiation around sensor:

The comparative results of the quasi-static mechanical tests carried out on specimens with and without sensors, coupled with the observations under numerical microscope. The main damage begins at a very low stress in the contour zones around the optical fibers that located between the composite plies. Encapsulation in optimal case has a small initial length, and we need high energy to extend it into delamination.

This appears clearly in the micrography that the width of the contour zones is much too large, which results in delamination very easy to initiate in the early stages of mechanical loading. This explains why the mechanical behavior curves of the intelligent composite material (UD and ±45◦) are below their homologue of the composite material without fiber optic sensors. This is an extremely important point for further preliminary fatigue tests. Indeed, the first track to improve the mechanical properties of this composite material passes through the closest possible "encapsulation" of the optical fiber between the plies. If this is done finely, the initiation of delamination will require a much greater energy than in the case where the encapsulation is too extensive (Figure 2-64).

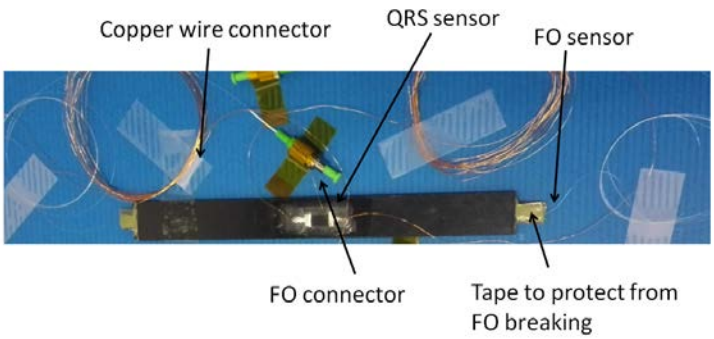

a)

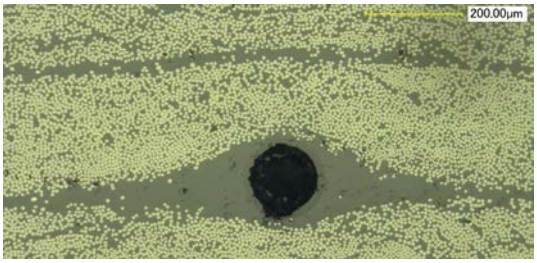

b)

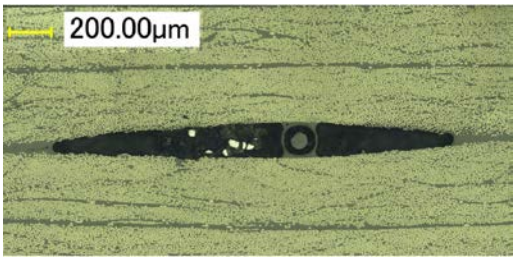

c)

Figure 2-66 : (a) 3-point bending specimen after sensor integration; (b) -Cross section of untested UD smart specimen; and (c) -Cross section of untested angle ply specimen.

The load-unload test result shown in Figure 2-67 of a unidirectional smart specimen. The ascending and descending profile of displacement was finely detected by embedded FOS and shown by red color curve. The strain range is similar to the strain values observed in quasi-static. Therefore, FOS strain values can be used directly without conversion factor.

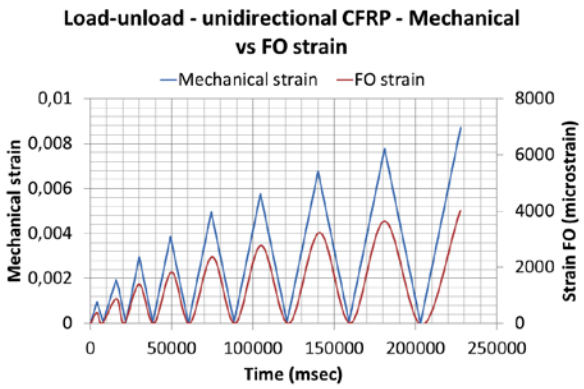

a)

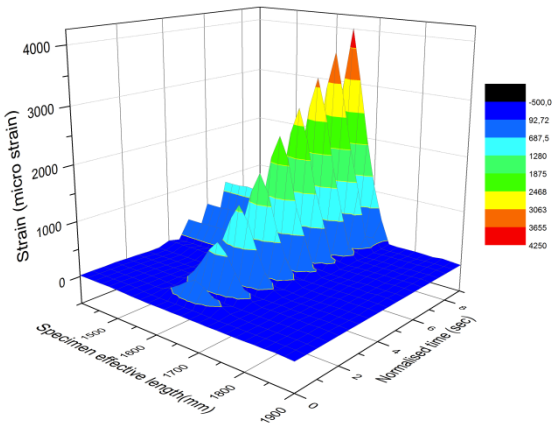

b)

Figure 2-67 : :a) -Load-unload test curve for smart UD specimen, b) -3-D load-unload test curve for smart UD specimen

We have studied two main factors, which affect the intrusive properties of fiber optic sensors when they are embedded in composites, namely, fiber-optic's diameter and its coating material. Polyimide is preferable for harsh environment conditions; whereas acrylate fits to ambient Temperature conditions. In the case of FOS diameter, the sensor of diameter 125microns was estimated to be very suitable for current industrial applications. To get the best coverage of the structure that has to be monitored, appropriate placement of sensors is critical. The use of alternative placement technique such as sinusoid alone was found to bring significant advances not only in terms of cost-saving but also regarding multi-parameter strain sensing.

2.8.2.2 Instrumentation CFRP strips for metallic bridges strengthening

Externally bonded CFRP strengthening systems for steel bridges present a reliable preventive, cost-effective and sustainable solution for their life-time extension. However, consistent assessment of CFRP to steel bonding in service condition needs to understand thermal changes effect on the behavior of bonded joints. For that reason, some tests were performed at different temperatures, on CFRP strips-to-steel bonded joints. High resolution distributed optical fiber sensor based on C-OFDR measurements was used to obtain the strain profile on both steel and CFRP junction layers. The used sensing cable was a single mode fibre SMF28, with suitable primary coating to insure high performance strain transfer into the fibre silicate structure.

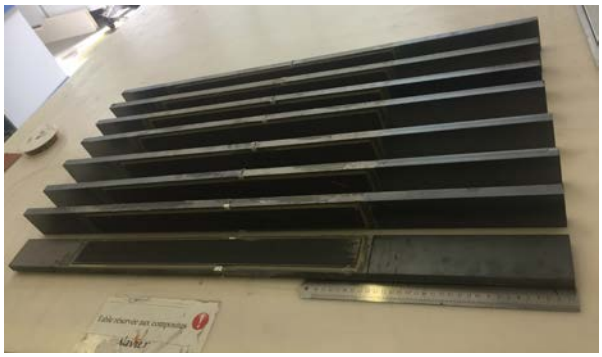

(a)

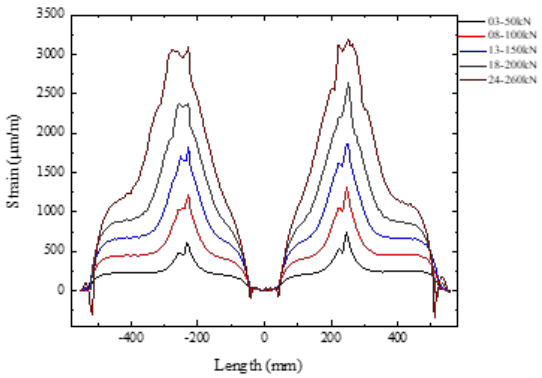

(b)

Figure 2-68 : (a) Externally bonded CFRP to steel; (b) Strain profile obtained during tensile test of CFRP strips (spatial resolution: 1 cm; measurement incertitude: 1 µm/m, Test temperature 45°C).

Other tests have been carried out in cooperation with Leoben university in Austria (Figure 2-69). We installed fibers in the composite tissue and changed the curing temperature to analyze the residual strain and its impact on the mechanical behavior of the sample. We have used a single mode fiber with carbon coating, other tests were realized using single mode fibers with Polyimide coating.

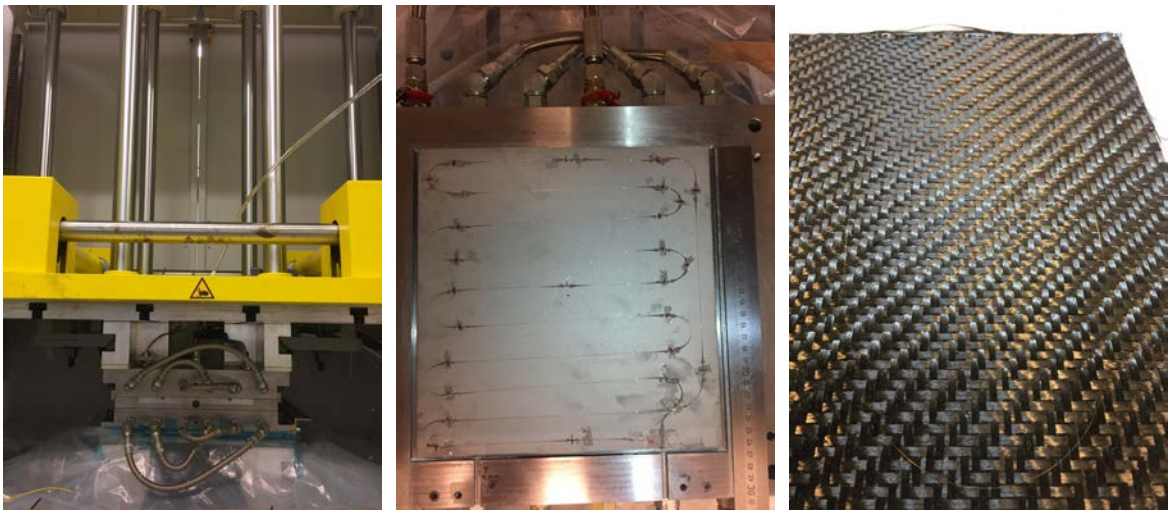

(a) (b) (c)

Figure 2-69 : (a) Curing machine of composite; (b) installed fiber on metallic layer to be integrated into composite tissue; and (c) optical fiber installed in the composite tissue.

2.8.3 Distributed optical fiber sensors for geo-science and geotechnical applications.

The results shown here are only for validated and authorized to be communicated. Different works still not finished to be analyzed.

2.8.3.1 Pile strain instrumentation

In a common project between Solétanche-Bachy and IFSTTAR, a fiber optics was installed to study the profile of strain in the Pile. The pile location was at “La Défense”, one of Europe's largest purpose-built business district, near Paris. Instrumented static pile load tests are conducted to determine the soil parameters in order to verify and optimize the design of the foundation for a structure. The instrumentation consists of placement of distributed optical fiber sensors along the test pile to determine the load for each load applied to the pile head. From the measured strain, the forces in the pile can be calculated, and thus the load distribution along pile shaft is known.

Figure 2-70 : Fiber optic sensors installation.

The total depth of the pile was ~20m. The soil profile is shown in the Figure 2-71.

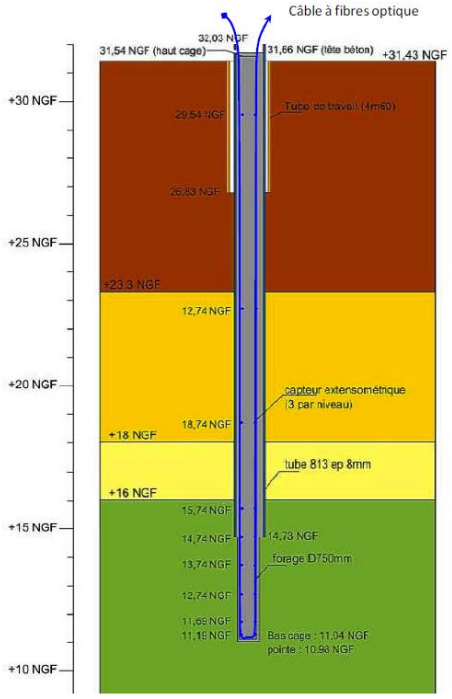

Figure 2-71 : Soil profile and instrumentation details, closed-ended pipe pile (dimensions in m)

Figure 2-72 presents a complete profile of measured strain, some points relative to the strain gauges installed for comparison.

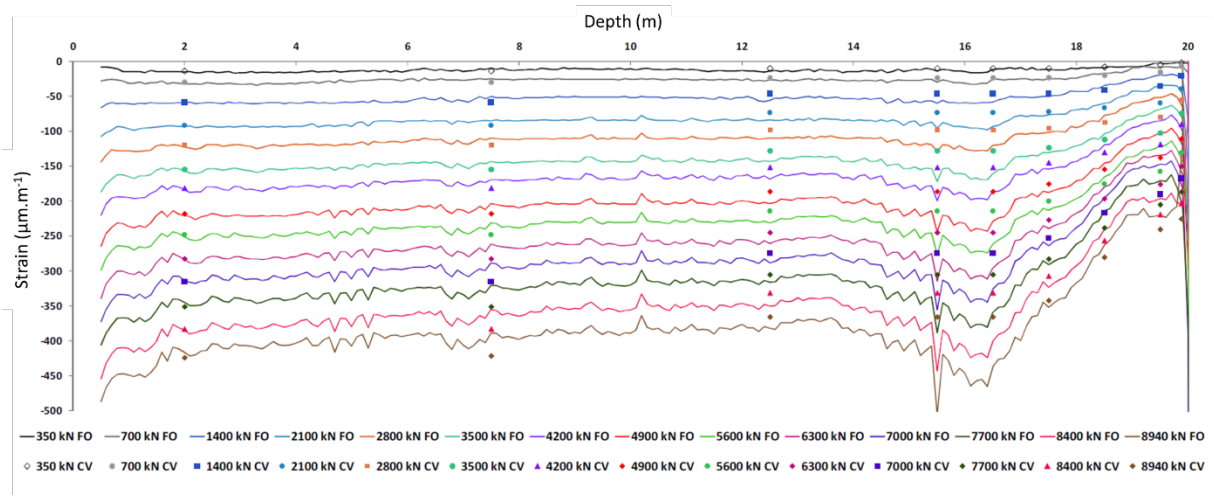

Figure 2-72 : Measured Strain profile with optical fibers sensors, and vibrating wire sensor.

2.8.3.2 Energy Pile instrumentation

Thermo-active geostructures have been used since the 1980s in Europe as pile foundations and then as diaphragm walls in Austria. This technology provides a clean energy source contributing to reduce the conventional energy sources consumption and reduce CO_2 emissions. The energy pile presented in the Figure 2-73, is the most used in our days. We have installed an optical fiber for strain and temperature measurements.

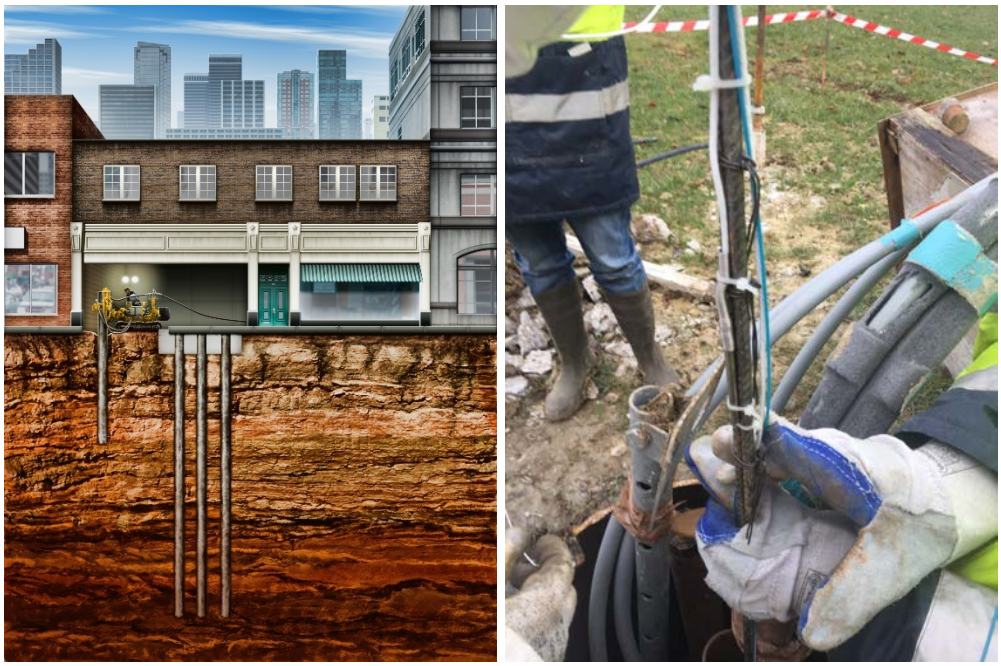

Figure 2-73 : example of energy pile, and the distributed optical fiber sensor installation.

Figure 2-74 presents the recorded data related to the pile profile, and the measured strain during mechanical tests, with increased charging 350kN to 900kN then discharging the pile and the strain profile at the end of the charging phase.

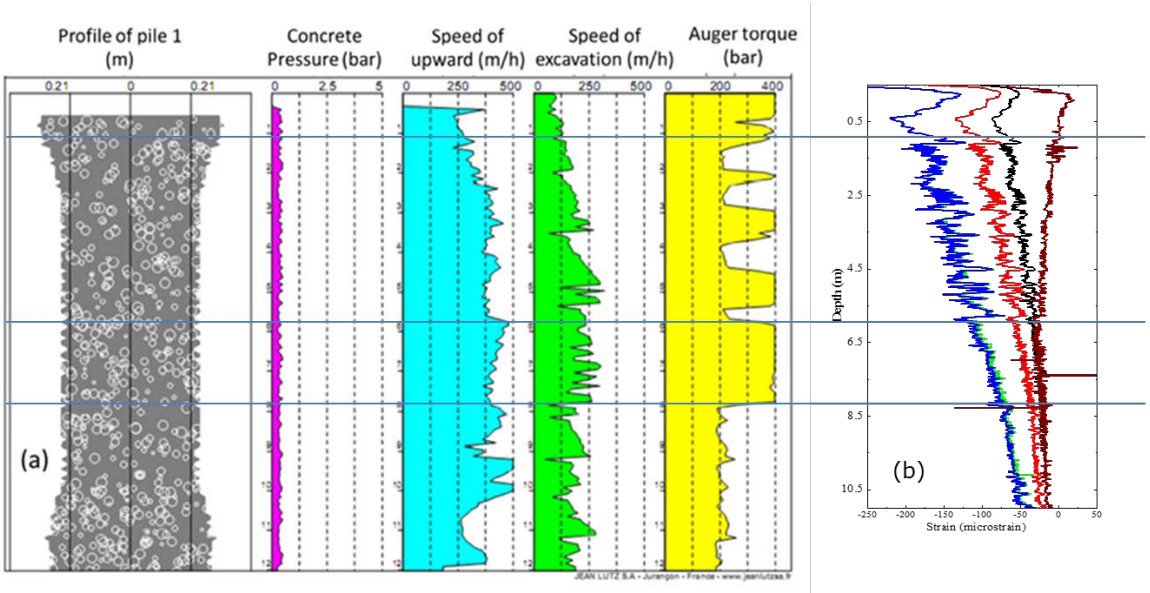

Figure 2-74 : (a) Data recorded during the piles' installation; (b) Measured strain profile during the mechanical charging tests (360kN, 540kN, 900kN, at the end and coming back to 0kN).

On the same pile we have applied a thermal charging during months, with alternatives cycles (heating/cooling). We present in Figure 2-75 the measured thermal profile based on Raman scattering.

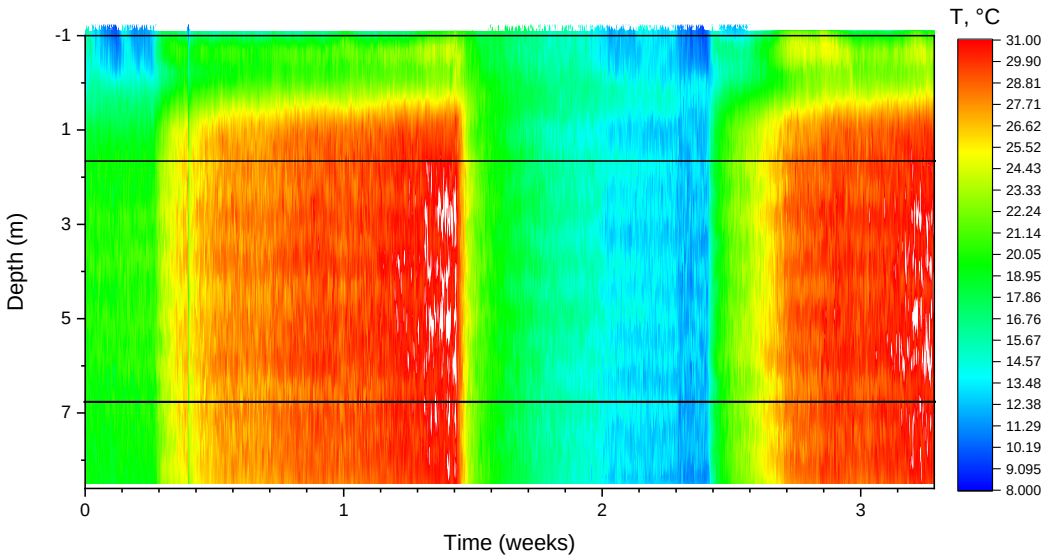

Figure 2-75 : Thermal profile measurement during 3cycles (3weeks), along the thermal pile.

The heating and cooling, combined with mechanical charging are programmed in July till September 2018. At the end of these tests we will have more analysis and we should submit an article relative to these works.

2.8.3.3 Geothermal soil management

The project SenseCity, is a very important case-study to validate the thermal measurement in soil. In this project we have installed more than 500m of optical fibers in the soil. The fibers were installed at 1.5m depth on one plane, as shown in the Figure 2-76. There are 3 heating centers with hot water pipes, the heating may be used to increase the temperature in the soil and study the propagation of heat with different conditions of humidity, pollutions in the soil etc.…

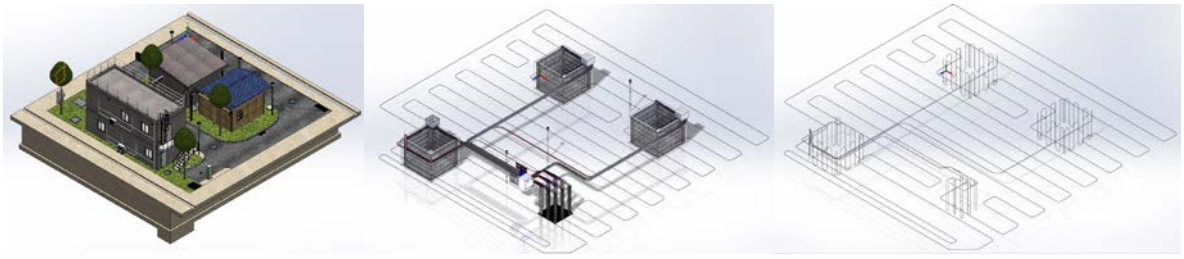

(a) (b) (c)

Figure 2-76 : (a). A global schema of the SenseCity climatized mini city; (b) the thermal controllers and pumping systems, and (c) the optical fiber sensing network.

The fibers were installed in January-February 2018. I have verified the good quality of the optical signal along all the sensing cables. The first tests will start in July 2018. The heating scenarios will be discussed before the starting date. Some results could be presented at the HdR defense date.

2.8.4 Photonic components characterization

Reflectometry techniques make it possible to study any waveguide structures, this solution provides an accurate estimation of the wavelength-dependent group refractive index and provides a spatial resolution (typically <5µm) for intra-chip reflections.

What we are working on, is to realize an active characterization of the internal structure of the semiconductor laser, and the analysis of the internal dispersion. The originality of this work is based on the high-resolution active characterization, that means analyzing the structure under electrical pumping, with lasing conditions.

The high repetition rate semiconductor lasers based on quantum well or quantum dash gain structures are presented in the Figure 2-77.

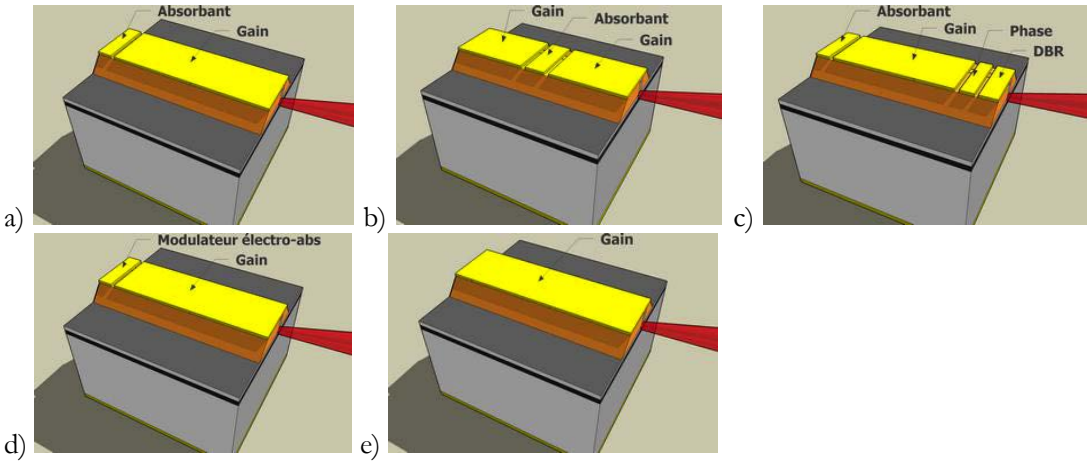

Figure 2-77 : simplified schema for mode locked semiconductor laser structures, for very high repletion rate generation: a) one gain section with saturable absorber[154], b) two sections laser with saturable absorber[155], c) DBR laser, formed by one gain section, saturable absorber, phase section and a DBR section[156], d) gain section with electro-modulated absorber section[157], e) Auto-pulsed laser formed by one gain section[158].

An experimental setup was realized Figure 2-78 to identify the different sections of the mode-locked semiconductor laser. Based on the different active and passive sections of the laser, we tried to study the evolution of optical spectrum, the optical gain, and the dispersion inside the cavity.

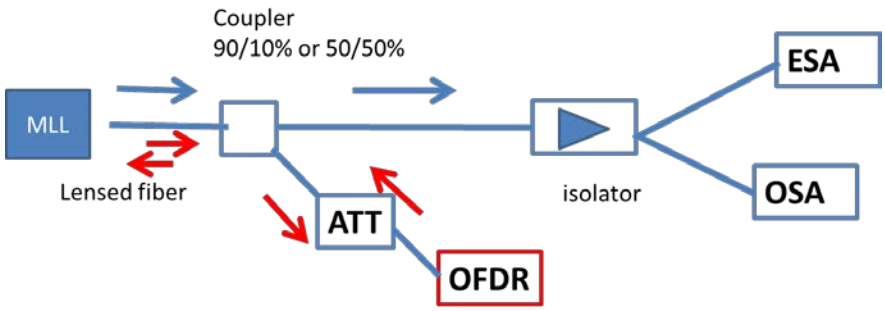

Figure 2-78 : C-OFDR analysis experimental setup for the mode locked laser (MLL), The optical attenuator is optional depending on power output of the laser, it's also possible to reduce fiber coupling ratio to remove attenuator, the coupled power of ~ -10dBm is sufficient for ESA and OSA assessment

The primary results from such test is shown on the Figure 2-79. In these results it's possible to see the different sections of the laser structure. The gain medium profile without the cavity effect can be seen too. Based on the chosen position on the cavity, we can analyze the local optical spectrum, and we should be limited by the sweep interval of the laser source in the C-OFDR system (1530nm-1615nm). We can see the effect of nonlinearity of the system response at the extremity of this spectral interval, compared to the optical spectrum measurements.

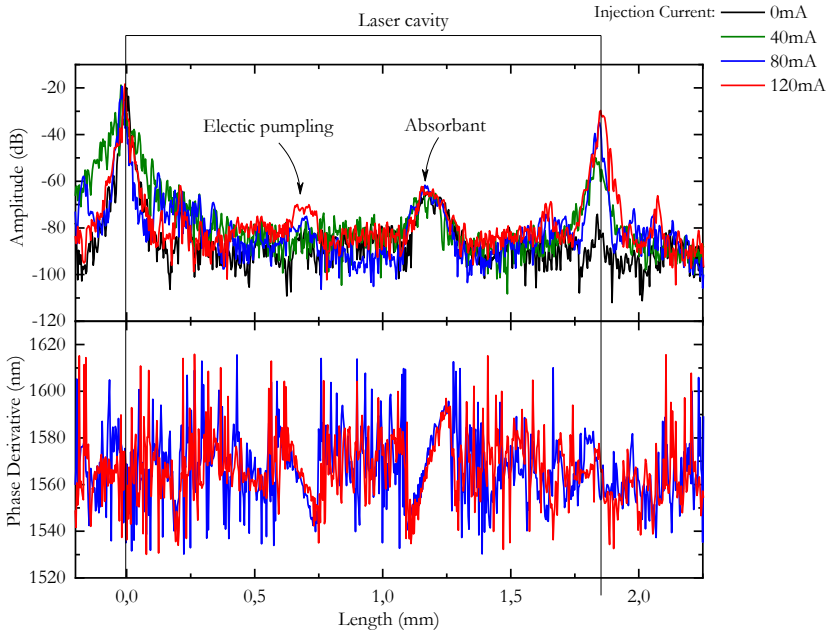

(a).

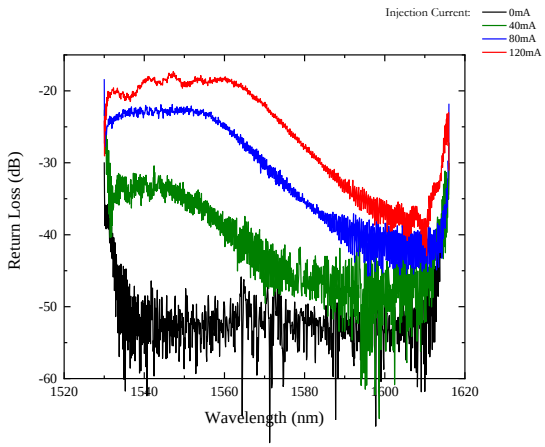

(b).

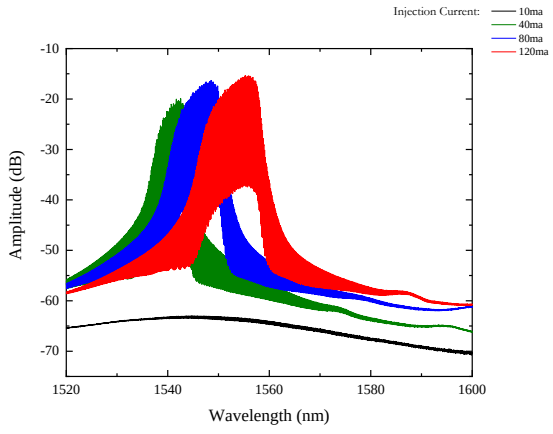

(c).

Figure 2-79 : C-OFDR analysis of laser cavity: a): laser cavity with all elements (mirrors, absorption zone and the electric contact zone for pumping, b) the measured intracavity gain using the C-OFDR schema, and (c) presents the optical output spectrum measured by an optical spectrum analyzer.

2.9 Summery and Roadmap Future Trends

I have described the main research activities realized since 2011. I have realized many Instrumentations of concrete structures, composite structures, and pile cases. Using the reflectometry solution to realize an active characterization of photonic component will present a very important axis in the future.

Beside the solution to realize a low-cost high-performance Brillouin scattering, based on dual frequency laser. I'll describe briefly the main ideas in my research project for the medium-term plan (2-4 years) and long-term plan (>5 years)

2.9.1 Distributed Optical Fiber Sensors Applications (medium-term)

The tests should continue to obtain more results in different configurations, like using the resonant/non-resonant feedback, verify that the attenuator is linear element and minimize its functionality, and at last to see the case of long delay feedback.

Based on these results, we think to make a project in cooperation with C2N, III-V Lab on this setup and try to create a simplified active setup for laser characterization.

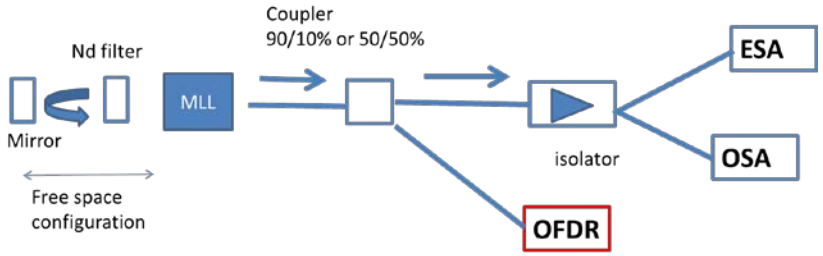

(a).

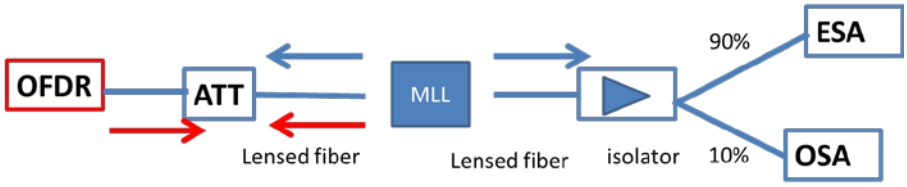

(b).

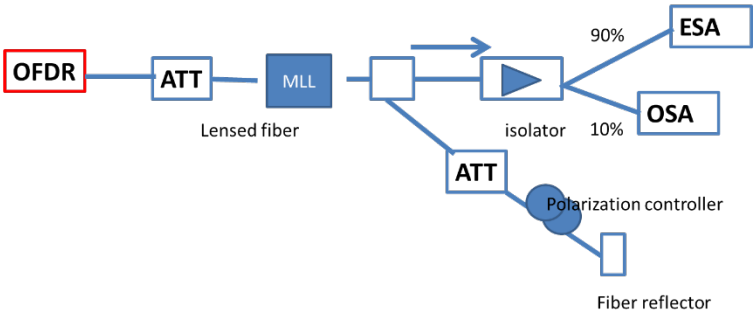

(c).

Figure 2-80 : a) with resonant/ non-resonant external optical feedback, b) Optical attenuator is optional depending on maximum acceptable power in OFDR, c) long delayed optical feedback.

2.9.2 Reliability of Optical Fiber Optic Sensors and interrogation systems (medium-term)

The basics of mechanical reliability of optical fibers was discussed many years ago, and the literature presents a considerable amount of information on that subject, for example optical fiber cables for the telecommunication industry are typically designed to have a lifetime exceeding 25 years [159]. In general, the mechanical reliability is qualified in a reasonable time. One therefore has to conduct accelerated tests at higher stress levels in the laboratory and extrapolate the results to the lower stress in-service conditions. Many previous works on how to deal with this has for example been published [160-162]. Browsing through some of these works, will can see that different models have been proposed to estimate the lifetime of a fiber. Where the fatigue during installation, and utilization inside the instrumented structure will decrease the lifetime of the cable.

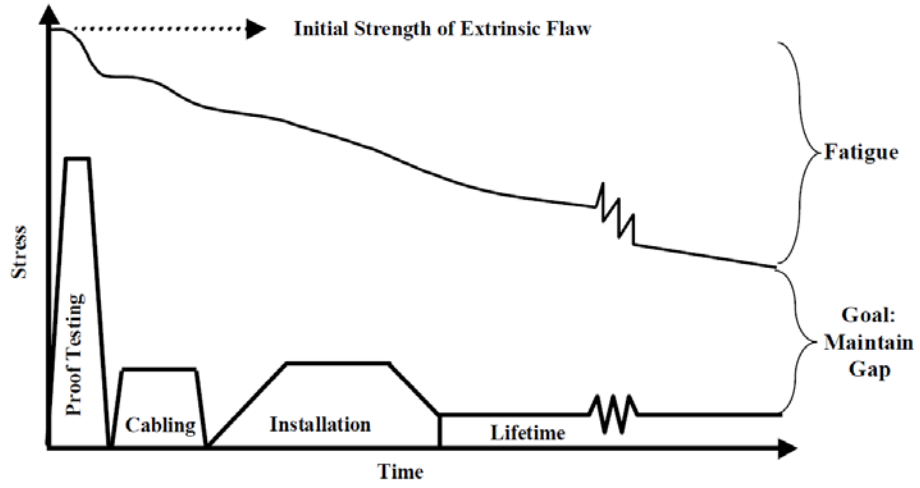

Figure 2-81 : Install stress and long-term stress of the glass is limited by standards to ensure the fiber lifetime in telecom applications[163].

We try to work with a PhD student to understand the impact of optical fiber cable mechanical structure degradation on the quality of the strain profile. Therefore, to predict the time to failure for a given applied service stress or the maximum allowed service stress that guarantees a specified service life one conventionally uses fracture mechanics fatigue equations relying on power law crack growth kinetics. The new parameter that we will study is related to the different environmental conditions (humidity, PH, …).

2.9.3 Distributed optical fiber sensors as perception neural networks for large scale infrastructures (medium-term)

This work is related to the GPE express at the Pont de Sevres metro station, presented in paragraph 2.8.1.4.2. The long fibers with multiple configurations will give a very rich and complex information about the structure evolution. The management of all the data with the different configurations of the optical fiber (linear: horizontal and vertical and circular), needs a software development with neural networks algorithms.

2.9.4 New design of optical fiber sensors (medium/long-term plan)

Mechanical deformations/thermal variations measurement along the optical fiber based on Rayleigh scattering, are carried out using optical heterodyning between two backscattered waves: one in the optical fiber and the other in a reference arm. This configuration is called C-OFDR (coherent optical frequency domain reflectometry), as presented in paragraph 2.4.2.2.1.

The current solution to obtain the strain/temperature variation, is done in five steps:

1-Obtain the print of the fiber (spectral scattering).

2-Apply a Fast Fourier transform (FFT) to calculate the distribution of the derivative of the reflectivity all along the fiber.

3–Choosing the spatial resolution and divide the sensing part of the fiber into multiple segments

4-Apply an Inverse Fast Fourier Transform (IFFT) for each segment individually.

5-Realize a 'cross correlation', between two states of each segment to obtain the deformation profile of the optical fiber.

New work concerns: designing, modeling the system operation, producing and characterizing its performance to measure deformations/thermal variations and crossing the actual OFDR-based system limits. These limits are mainly related to the performance of the laser source: stability, spectral linewidth and tunability range. The solution proposed in this thesis is to combine OTDR and OFDR techniques, using a frequency tunable laser around 1.55µm, with a temporal modulation. This solution maintains a high spatial resolution and a long sensing length. This proposition is a subject of a thesis to be supported by an industrial partner, and the thesis should start next year.

2.9.5 Distributed chemical sensors (long-term plan)

We have stated to make a bibliographic works to use the photonic characteristics of nanostructures (Semiconductor Carbone nanotubes and 2D structures), chemical sensing. The idea that we are working on is to realize a distributed spectroscopic analysis for some chemical

parameters, accompanied with thermal and mechanical measurement. The starting point will be with tilted fiber Bragg gratings, before going to distributed measurements.

2.10 Master and PhD Students projects involved in my scientific activities

To realize the objectives of my scientific project, I have supervised and co-supervised different Master and PhD students.

2.10.1 Master (M1 and M2)

Younes MOKRANI (2018), M2R at Université Paris Est	"Multi-Scale study of external sulphate attack in reinforced concrete structures evaluation using Distributed optical fiber sensors", Supervision rate 50%.
Melek-Merve Toktamis (2017), M2R at ESIEE-Paris	"Behavior of birefringent fibers in a polarimetric sensor", Supervision rate 100%.
Raphaël DÉMOLIS (2016), M2R at l'ENS-Cachan	"Composite reinforcement of concrete structures: experimental study", Supervision rate 35%.
ZAHRA Ali (2015), M2R at Université Paris-Sud.	"Simplified modeling of Brillouin gain spectra in optical fibers", Supervision rate 100%.
YAN Yan (2014), M2R LMMB at Université Paris VI.	"Modeling and measurement of Brillouin gain spectrum in optical fibers under strain conditions", Supervision rate 100%.
BILLON Astrid (2013), M2R at École Normale Supérieure de Paris	"Optical fiber strain measurements in concrete wall cladding", Supervision rate 35%.

2.10.2 PhD students

I'm involved in supervising different PhD students, I give in this part a complete list till 2018:

PhD student name	Martin CAHN (2017-2021)
PhD Title:	Dimensioning of underground structures intersection
Defense date	-
PhD supervisor	Denis BRANQUE
Supervision rate	25%
Doctoral school	ENTPE

Financement	Enterprise GEOS, INGEROP et SGP
Scientific production	
Actual professional situation	

PhD student name	Ismail ALJ (2017-2020)
PhD Title:	Durability of fiber -optic distributed measurement systems embedded into structures
Defense date	-
PhD supervisor	Karim BENZARTI
Supervision rate	30%
Doctoral school	L'école doctorale Sciences, Ingénierie et Environnement (SIE)
Financement	IFSTTAR (50%), IRSN (50%)
Scientific production	-
Actual professional situation	-

PhD. student name	Miyassa SALHI (2016-2019)
PhD. Title:	Study of low -cost fiber optic system monitoring structures, based on the Brillouin effect and analysis of influential parameters by statistical method
Defense date	Thesis in progress.
PhD. supervisor	Anne-Laure BILLABERT
Supervision rate	25%
Doctoral school	L'école doctorale Sciences, Ingénierie et Environnement (SIE)
Financement	Doctoral school
Scientific production	2 Nationale conferences
Actual professional situation	-

PhD student name	RAMAN Venkadesh (2014-2017)
PhD. Title:	A smart composite based on carbon fiber and epoxy matrix for new offshore wind-turbines. Numerical and analytical modeling.
Defense date	16 June 2017

PhD. supervisor	Monssef DRISSI-HABTI
Supervision rate	35%
Doctoral school	Centrale Nantes ED SPIGA
PhD Financement	EVEREST Project- IRT Jules Verne
Scientific production	3 articles, 3 International conferences.
Actual professional situation	Post-doctorat

PhD student name	CHACCOUR Léa (2013-2016),
PhD Title:	Development of dual-frequency VECSEL source for the measurement of Brillouin effect in optical fibers
Defense date	23 Septembre 2016
PhD supervisor	Patrice CHATELLIER
Supervision rate	50%
Doctoral school	Université Paris Est-L'école doctorale Sciences, Ingénierie et Environnement (SIE)
PhD Financement	IFSTTAR
Scientific production	1 article, 3 international conferences.
Actual professional situation	temporary teaching and research associate

2.11 Finished and actual projects

To simplify this step, I present all the projects I have worked on in a Timeline chart. I start from the date of my arrival at the ifsttar in 2011. The total budget of the projects is shown on the graph. In the case of specific long-term projects, only the budget related to distributed optical fiber sensing part is shown (GPE and ODOBA cases).

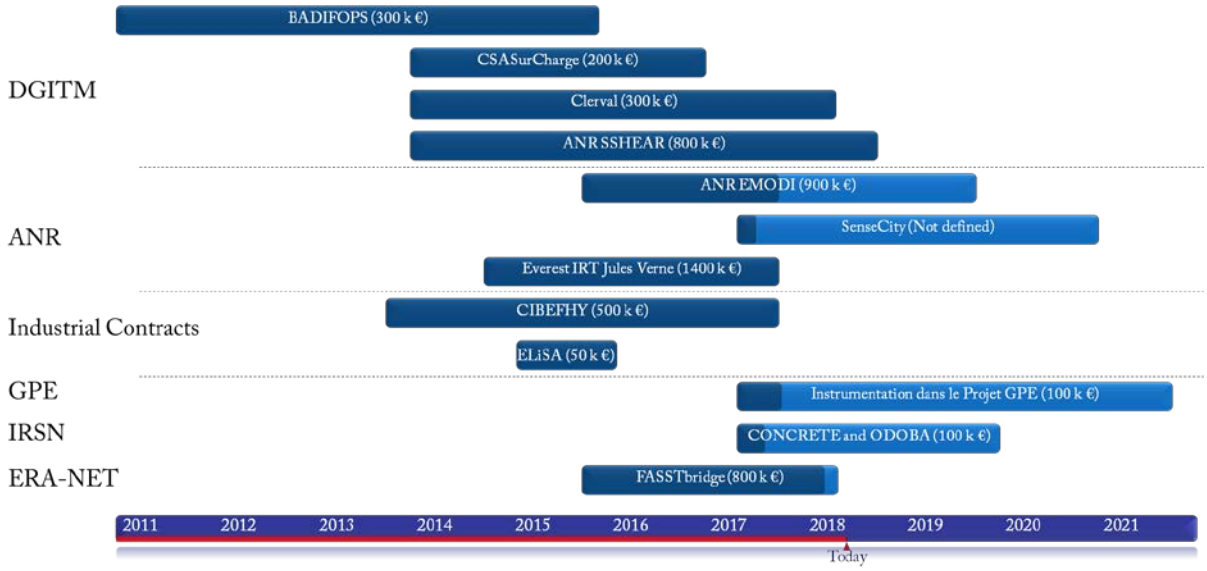

Figure 2-82 : Timeline chart of finished and actual projects. Expertise activities is not shown. Partners names in the different projects could be found the paragraph 1.5

2.12 Scientific and technical expertise activity

a) I have realized reviewing activity for different journals:

-IEEE Photonics Technology Letters.

-IEEE Photonics Journal.

-Applied Physics Letters.

-Springer Nature (Light: Science & Applications).

b) I have reviewed submitted projects related to fiber optics sensors for the ANR agency in 2014.

c) I am a member of the Technical Committee of:

-ALLSENSORS 2018: The Third International Conference on Advances in Sensors, Actuators, Metering and Sensing.

ALLSENSORS 2018 March 25, 2018 to March 29, 2018 - Rome, Italy

http://www.iaria.org/conferences2018/ALLSENSORS18.html

-3rd Global Summit & Expo on Materials, Photonics & Optical Instruments

Theme: Empowers the world with the knowledge of advancements in materials photonics and optical instruments.

November 12-14, 2018 at Toronto, Canada.

http://scientificfederation.com/materials-photonics-optical-instruments-2018/index.php

-ICSSIS 2018

2018 International Conference on Smart Sensing and Intelligent Systems (ICSSIS 2018)

http://www.icssis.org/commit.html

d) I have gained expertise to solve some technical problems related to fiber optic instrumentation. I report that since 2017, I have been referred by Luna-Technologies for the civil applications of distributed fiber optic sensors.

A confidentiality agreement was signed between IFSTTAR and the company Fibristerre in November 2015, to build a proposal for a project based on the know-how of Fibristerre in the B-OFDA solutions, and ifsttar in the solutions of instrumentation and dual-frequency laser sources.

3 Appendix

3.1 Curriculum vitæ

AGHIAD KHADOUR
Laboratoire instrumentation, simulation et informatique scientifique (LISIS)
Cité Descartes
14-20 Bd Newton – 77447 Marne-la-Vallée Cedex 2 – France
Phone number: (+33) 01.81.66.83.88 Born on 23/07/1975
E-mail: aghiad.khadour@ifsttar.fr

EDUCATION :

2005-2009	PhD in Physics from École Polytechnique, Palaiseau
2004-2005	Master of research in Optoelectronics at the École Polytechnique, Palaiseau
1995-1997	Engineer degree in Optoelectronics at Higher Institute for Applied Sciences and Technology (HIAST) Damascus, Syria.

POSITIONS HELD

January 2015-…	Senior Researcher, IFSTTAR-Paris Optical fiber sensors for civil engineering structures, geotechnical applications, composite structures. Design of Brillouin based distributed optical fiber sensors
October 2010 – December 2014	Associate Researcher, IFSTTAR-Paris Optical fiber sensors for civil engineering structures, geotechnical applications, composite structures.
September 2009 – September 2010	Postdoctoral Researcher, CORIA - Rouen University Carbone nanotubes sorting using photoluminescence characteristics.
December 2005 – September 2009	Research engineer, LPN-CNRS/Ecole Polytechnique – Palaiseau - France VECSEL Lasers

March 1998 – October 2004	Research engineer, HIAST Optoelectronics Department – Damascus Solid state lasers, semiconductor diode lasers, optical systems design

TEACHING ACTIVITY

- Optical Waveguides and optical fibers:

International Master of Electronics - ESIEE-Paris, 17h/Year, (2011-2018)

- Electromagnetic wave propagation:

Engineering Grande Ecole ESIEE Paris, 8h/Year, (2014-2018)

- Hyper-frequency and optical transmission:

University Institutes of Technology (Créteil-Vitry) – Telecom and networks department, 12h/Year, (2011-2018)

-Fibres Optiques :

University Institutes of Technology (Créteil-Vitry) – Telecom and networks department, 16h/Year, (2014-2016)

- Ondes électromagnétiques et Fibres Optiques :

University Institutes of Technology (Créteil-Vitry) – Telecom and networks department, 14h/Year, (2011-2017)

- Phase Locked loops:

University Institutes of Technology (Créteil-Vitry) – Telecom and networks department, 21h/Year, (2012-2014)

3.2 Publications

3.2.1 Articles

[Patent]: "Dual frequency laser for Brillouin optical fiber sensor': FR15 58913, (International extension has been accepted).

[Book chapter] Aghiad Khadour, Julien Waeytens, "Monitoring with optical fiber sensors, " in Eco-efficient Repair and Rehabilitation of Concrete Infrastructures, ELSEVIER SCIENCE & TECHNOLOGY, éditeurs F. Pacheco-Torgal, R. E. Melchers, A. Sáez, N. De Belie, K. V. Tittelboom and X. Shi, 24 November 2017 (p 97-123)

[1] 'Response of UHPFRC columns submitted to combined axial and alternate flexural loads' P. Marchand, F. Baby, A. Khadour, Ph. Rivillon, J-C. Renaud; L. Baron; G. Généreux, J-P. Deveaud, A. Simon, F. Toutlemonde : accepted and to appear in Journal of Structural Engineering

[2] 'Experimental investigations of the FRP rebars to concrete bond behavior using continuous optical fiber sensors' Arnaud Rolland, Marc Quiertant, Aghiad Khadour, Sylvain Chataigner, Karim Benzarti, Pierre Argoul, accepted after revision 13-12-2017, to appear in: Construction and Building Materials.

[3] "Fiber Optic Sensor Embedment Study for Multi-Parameter Strain Sensing" Drissi-Habti M, Raman V, Khadour A, Timorian S. Sensors (Basel). 2017 Mar 23;17(4).

[4] "Cross-Polarized Dual-Frequency VECSEL at 1.5μm for Fiber-based Sensing Applications", L. Chaccour, G. Aubin, K. Meghem, J-L. Oudar, A. Khadour, P. Chatelier, S. Bouchoule, in IEEE Photonics Journal PP(99):1-1 October 2016.

[5] "Numerical simulation analysis as a tool to identify areas of weakness in a turbine wind-blade and solutions for their reinforcement", V. Raman, M. Drissi-Habti, L. Guillaumat, A. Khadour. Composites Part B: Engineering, Volume 103, 15 October 2016, Pages 23–39.

[6] "Qualification of a distributed optical fiber sensor bonded to the surface of a concrete structure: a methodology to obtain quantitative strain measurements", A. Billon, J-M Henault, M. Quiertant, F. Taillade, A. Khadour, R-P Martin and K. Benzarti, Smart Materials and Structures, vol. 24, p. 115001, (2015).

[7] "Bond behaviour of reinforcing bars in UHPFRC", P. Marchand, F. Baby, A. Khadour, T. Battesti, P. Rivillon, M. Quiertant, H-H Nguyen, G. Généreux, J-P Deveaud, A. Simon, F. Toutlemonde, Materials and Structures, 1-17 (2015).

[8] "Recent experimental investigations on reinforced UHPFRC for applications in earthquake engineering and retrofitting", F. Toutlemonde, A. Simon, P. Rivillon, P. Marchand, F. Baby, M. Quiertant, A. Khadour, J. Cordier, T. Battesti, RILEM-fib-AFGC International Symposium on Ultra-High Performance Fibre-Reinforced Concrete 597–606, (2014).

[9] "Experimental investigation on strain distribution in reinforcing bars by means of fiber-optic sensors", A. Khadour, M. Quiertant, F. Baby, P. Marchand, P. Rivillon, A. Simon, F. Toutlemonde, Studies and Researches–V.33 Graduate School in Concrete Structures – Fratelli Pesenti Politecnico di Milano, Italy, pp 85-99 (2014).

[10] "Instrumentation par fibres optiques des ouvrages en BA pour la mesure répartie des déformations de traction des armatures", M. Quiertant, F. Baby, A. Khadour, P. Marchand, P. Rivillon, F. Toutlemonde. Revue Instrumentation Mesure Métrologie. Numéro spécial Capteurs à fibre optique - Développements et applications. Janvier-juin 2013, vol. 13, n° 1-2/2013. p. 131-147.

[11] "Picosecond to sub-picosecond pulse generation from mode-locked VECSELs at 1.55 μm", S. Bouchoule, Z. Zhao, A. Khadour, E. Galopin, J.-C. Harmand, J. Song, G. Aubin, J. Decobert, J.-L. Oudar, Proc. SPIE 8242, 824203 (2012).

[12] "130 mW average power, 4.6 nJ pulse energy, 10.2 ps pulse duration from an Er3+ fiber oscillator passively mode locked by a resonant saturable absorber mirror", A. Cabasse, D. Gaponov, K. Ndao, A. Khadour, J.-L. Oudar, G. Martel, Opt. Lett. 36, 2620 (2011).

[13] "Ultrashort pulse generation from 1.56 μm mode-locked VECSEL at room temperature", A. Khadour, S. Bouchoule, G. Aubin, J.-C. Harmand, J. Decobert, J.-L. Oudar, Optics Express 18, 19902 (2010)

[14] "Timing Jitter Reduction of a Mode-locked VECSEL Using an Optically Triggered SESAM", G. Baili, M. Alouini, L. Morvan, D. Dolfi, A. Khadour, S. Bouchoule, J.-L. Oudar, IEEE Phot. Techn. Lett. 22, 1434 (2010).

[15] "Thermal optimization of 1.55 um OP-VECSEL with hybrid metal-metamorphic mirror for single-mode high power operation". J.-P. Tourrenc, S. Bouchoule, A. Khadour, J.-C. Harmand, A. Miard, J. Decobert, N. Lagay, X. Lafosse, I. Sagnes, L. Leroy, J.-L. Oudar, Opt. Quant. Electron. 40, 155 (2008).

[16] "High power single-longitudinal-mode OP-VECSEL at 1.55 μm with hybrid metal-metamorphic Bragg mirror", J.P. Tourrenc, S. Bouchoule, A. Khadour, J. Decobert, A. Miard, J.C. Harmand, and J.L. Oudar, Electron. Lett., vol. 43(14), pp. 754-755, 2007.

3.2.2 International conferences

[1] "Steel Bridge Strengthening with CFRP Strips: Mechanical Behaviour Analysis Using High Resolution Distributed Optical-Fibre Sensors" Aghiad Khadour, Gilles Foret, Marc Quiertant, Sylvain Chataigner, IABSE Symposium Nantes 2018.

[2] “Distributed optical fibre sensors to monitor prestressed concrete bridge beam strengthened with bonded FRP” Aghiad Khadour, Marc Quiertant, Gonzague Six, Corentin Le Roy, Christophe Aubagnac, 9th International Conference on Fibre-Reinforced Polymer (FRP) Composites in Civil "Engineering (CICE 2018), PARIS 17-19 JULY 2018.

[3] “Experimental investigations on the local bond behavior between concrete and FRP rebars using distributed optical fiber sensors” A. Rolland, K. Benzarti, M. Quiertant, P. Argoul, S. Chataigner and A. Khadour, 9th International Conference on Fibre-Reinforced Polymer (FRP) Composites in Civil Engineering (CICE 2018), PARIS 17-19 JULY 2018.

[4] “Fiber Optic Sensor Embedment Study for Multi-Parameter Strain Sensing in smart composites” Monssef Drissi-habti, Venkadesh Raman, Aghiad Khadour, American Society for Composites (ASC) 32nd Annual Technical Conference in October 23-25, 2017

[5] “Numerical simulation analysis for identification of areas of high stress-concentration in turbine wind-blade-reinforcements scenarios” Venkadesh Raman, Monssef Drissi-Habti and Aghiad Khadour, 6th Asia-Pacific Conference on FRP in Structures (APFIS 2017)

[6] “Investigation of a low-cost weigh-in-motion system based on fiber-optic sensor”, A. Khadour, L-M. COTTINEAU, 7th International Conference on Weigh-In-Motion - ICWIM7 Foz do Iguaçu, 7-10/11/2016

[7] “Dual-Frequency VECSEL at Telecom Wavelength for Sensing Applications”, Léa Chaccour, Guy Aubin, Kamel Merghem, Jean-Louis Oudar, Aghiad Khadour, Patrice Chatellier and Sophie Bouchoule, OPTICS 2016, International Conference on Optical Communication Systems, (2016).

[8] “10 GHz orthogonal polarized dual frequency VECSEL at 1550nm”, L. Chaccour, A. Khadour, S. Bouchoule, J-L. Oudar, P. Chatellier, 3rd International Conference and Exhibition on Lasers, Optics & Photonics September 01-03, 2015, Valencia, Spain.

[9] “Instrumentation of large scale direct shear test to study the progressive failure of concrete/rock interface”, H. Mouzannar, M. Bost, P. Joffrin, C. Pruvost, F. Rojat, J. Blache, A. Houel, M. Valade, A. Khadour, S. Chataigner, J-F.David, Y. Falaise and M. Quiertant, accepted in 8th RILEM, International Conference on Mechanisms of Cracking and debonding In Pavements, Rilem (2016).

[10] "Experimental investigation of a pre-stressed concrete bridge girder reinforced with bonded FRP", C. Aubagnac, D. Germain, A. Houel, R. Sadone, J-P. Maherault, J-J Brioist, Claire Marcotte, Sylvain Chataignier, A. Khadour, M. Quiertant, J-P Sellin, accepted in 8th RILEM, International Conference on Mechanisms of Cracking and debonding In Pavements, Rilem (2016).

[11] "Bond Of UHPFRC To Reinforcing Bars: Experimental Determination And Code Provisions Calibration", F. Toutlemonde, P. Marchand, F. Baby, A. Khadour, T. Battesti, P. Rivillon, G. Généreux, accepted in HiPerMat 2016.

[12] "Quantitative Strain Measurement with Distributed Fiber Optic Systems: Qualification of a Sensing Cable Bonded to the Surface of a Concrete Structure", A. Billon, J-M Henault, M. Quiertant, F. Taillade, A. Khadour, et al, EWSHM - 7th European Workshop on Structural Health Monitoring, Jul 2014, Nantes, France. 2014.

[13] "Prestressed concrete structures: cracking analysis and strand behavior", A. Michou, F. Benboudjema, A. Khadour, G. Nahas, P. Wyniecki, Y. Berthaud, ICEM16 - 16th International Conference on Experimental Mechanics. 2014. Parallel keynote lecture.

[14] "Analyse du comportement de poutres en béton précontraint : instrumentation des torons de précontrainte par fibres optiques", A. Michou, F. Benboudjema, A. Khadour, G. Nahas, P. Wyniecki, Y. Berthaud, Regroupement Francophone pour la Recherche et la Formation sur le Béton (RF)2B. 2014. keynote lecture.

[15] "Numerical Modeling to Analyse Optical Fiber Measurements along a Steel-Concrete Interface", A. Tixier, C. Rospars, F. Dufour, A. Khadour, M. Quiertant, B. Masson, , Computational Modeling of Fracture and Failure of Materials and Structures, Czech Technical University in Prague, pp: 40, Prague, République Tchèque, 5-7 juin 2013.

[16] "Distributed Deformation Monitoring of Reinforcement Bars Using Optical fibers for SHM" A. Khadour, M. Quiertant, F. Baby, P. Marchand, P. Rivillon, and F. Toutlemonde. Seventh International conference Concrete Under severe conditions environment and loading (CONSEC13), Nanjing-China - September 23-25 (2013).

[17] "UHPFRC applications for earthquake engineering and retrofitting" F. Toutlemonde, P. Rivillon, A. Simon, P. Marchand, G. Généreux, F. Baby, A. Khadour, M. Chenaf, J.-P. Deveaud, Z. Hajar. UHPFRC 2013 – Designing and Building with UHPFRC: from innovation to large-scale realizations, Marseille (France) - September 30-October 2, 2013.

[18] "Deformation Monitoring of Reinforcement Bars with a Distributed Fiber Optic Sensor for the SHM of Reinforced Concrete Structures", M. Quiertant, F. Baby, A. Khadour, P. Marchand, P. Rivillon, 9th International Conference on NDE in Relation to Structural

Integrity for Nuclear and Pressurized Components, Seattle, Washington, USA - May 22-24, (2012).

[19] "VECSEL technology for modelocking at 1.55 μm", S. Bouchoule, A. Khadour, Z. Zhao, J. Decobert, J.-C. Harmand, J.-L. Oudar, Invited talk - SPIE, Photonics West / LASE Conference, San Francisco, CA, USA, 22 - 27 January (2011).

[20] "Room-temperature picosecond mode-locked pulse genreration from a 1.55 μm VECSEL with an InGaAsN/GaAsN fast saturable absorber mirror", A. Khadour, S. Bouchoule , J. Decobert, J.-C. Harmand, and J.-L. Oudar, Oral, 22nd Int. Conf. on Indium Phosphide and Related Materials IPRM'10, Takamatsu, Japan, May 31-June 4 (2010).

[21] "Generation 1.7-ps mode-locked pulse with low RF linewidth from A 1.55 μm vecsel operating at 25 °C" A. Khadour, Z. Zhao, S. Bouchoule, J. Decobert, J.-C. Harmand, J.-L. Oudar. Oral, 23rd Annual Meeting of the IEEE Photonics Society, IEEE-LEOS 2010, Denver, Colorado, November 9-13 (2010).

[22] "Which carbon nanotube-based saturable absorber for high power mode-locked fiber laser?", A. Cabasse, A. Khadour, and G. Martel, ONERA Scientific days - A nanoworld tubes, Chatillon, France, 8 - 9 Avril (2010).

[23] A. Cabasse, A. Khadour, G. Maulion, G. Martel, T. Nguyen, J.-L. Oudar, S. Maine, R. Fleurier,Y. Battie, B. Tr´etout, O. Jost, " Which saturable absorber for high power mode-locked fiber laser ? Multiple quantum wells versus carbon nanotubes ", 4th EPS-QEOD EUROPHOTON CONFERENCE, Hambourg, Allemagne, August 31st - September 3th (2010).

[24] "Influence of growth technique and sorting of CNT for efficient mode-locking of fiber lasers", A. Cabasse, A. Khadour, G. Martel, B. Tr´etout, S. Maine, A. Loiseau, R. Fleurier, J.-S. Lauret A. Ambrosio, P. Maddalena, V. Grossi, M. Passacantando, S. Santucci, O. Jost, M. Mertig, and J. Posseckardt, ChemOnTubes, Arcachon, France11 - 15 Avril, (2010).

[25] "Which Saturable Absorber Mirror for High-Power fs Fiber Laser? Multiple Quantum Wells vs. Carbon Nanotubes ", A. Cabasse, A. Khadour, G. Maulion, H.-T. Nguyen, J.-L. Oudar, G. Martel, V. Grossi, M. Passacantando, S. Santucci, A. Ambrosio, C. Romano, P. Maddalena, J. Posseckardt, M. Mertig, O. Jostf, R. Fleurier, S. Maine, Y. Battie, B. Tretout, A. Loiseau, J.-S. Lauret, Journées Nationales en Nanosciences et Nanotechnologies, J3N – Lille (2010).

[26] "Mode Locked 1550 nm VECSEL Using a Two Quantum Wells GaInNAs Saturable Absorber", A. Khadour, S. Bouchoule, G. Aubin, J. P. Tourrenc, A. Miard, J. C. Harmand, J.

Decobert, J. L. Oudar, Oral, International Conference on Lasers and Electro-optics, CLEO'08, San Jose, CA, USA, May 4-9, (2008).

[27] "Mode-locked OP-VECSEL at 1550nm with line width <10 kHz", A. Khadour, S. Bouchoule, G. Aubin, J.P. Tourrenc, A. Miard, J.C. Harmand, J. Decobert, J.L.Oudar, 3rd EPS-QEOD EUROPHOTON CONFERENCE, Paris - France, August 31st - September 5th, (2008).

[28] "Mode Locking of Optically Pumped Long Wavelength InP-Based Semiconductor Disk Lasers with GaInNAs Saturable Absorber", A. Khadour, S. Bouchoule, G. Aubin, J.P. Tourrenc, A. Miard, J.C. Harmand, J. Decobert, J.L. Oudar, 20th Int. Conf. on Indium Phosphide and Related Materials IPRM'08, Versailles, France, 25-29 May, (2008).

[29] "High-Power 1.55μm VECSEL for mode-locked pulse generation with an InGaAsN/GaAsN fast saturable absorber mirror", A. Khadour, S. Bouchoule, J.P. Tourrenc, J. Decobert, J.G. Provost, A. Miard, J.C. Harmand, and J.L. Oudar, Oral, 21st IEEE Lasers and Electro Optics Society Annual Meeting, IEEE-LEOS 2008, Newport Beach, CA, USA, November 9-13 (2008).

[30] "High-power single-longitudinal-mode VECSEL at 1.55 μm with an hybrid metal-metamorphic Bragg mirror" J.P. Tourrenc, S. Bouchoule, A. Khadour, J.G. Provost,.J. Decobert, A. Miard, J.C. Harmand, J.L. Oudar, Oral, 20th Annual Meeting of the IEEE, Lasers and Electro-Optics Society,.IEEE- LEOS 2007. Lake Buena Vista, FL, USA, The 21-25 October (2007).

[31] "High-Power RT CW Operation of OP-VECSELs at 1550nm with Hybrid Metallic-Metamorphic Mirrors", S. Bouchoule, J.-P. Tourrenc, A. Khadour, J.-C. Harmand, J. Decobert , and J.-L. Oudar, European Semiconductor Laser Workshop 2007, ESLW 2007, September 14 - 15, Berlin, Germany (2007).

[32] "High-Power RT CW Operation of an OP-VECSEL at 1.56μm with Hybrid Metallic-Dielectric Mirrors", J. P. Tourrenc, S. Bouchoule, A. Khadour, J. Decobert, A. Miard, J. C. Harmand, J. L. Oudar, Oral Comm., Session Vertical external cavity surface emitting lasers, Paper CB1-3-MON, Conference on Lasers and Electro-Optics and International Quantum Electronics Conference CLEO/Europe-IQEC 2007, Munich, Germany, June 17-22, 2007.

[33] "Single transverse mode RT CW operation of an OP-VECSEL at 1.56 um with hybrid metallic-metamorphic mirrors", J. P. Tourrenc, S. Bouchoule, A. Khadour, J. Decobert, A. Miard, J. C. Harmand, J. L. Oudar, International Workshop on PHysics & Applications of SEmiconductor LASERs (PHASE), Supélec, Campus de Metz, March 28-30 (2007)

[34] “Thermal optimization of 1,55 um OP-VECSELs”, J. P. Tourrenc, A. Khadour, S. Bouchoule, J. Decobert, X. Lafosse, L. Leroy, I. Sagnes, J. L. Oudar. Poster, International Workshop on PHysics & Applications of SEmiconductor LASERs (PHASE), Supélec, Campus de Metz, March 28-30 (2007)

3.2.3 National conferences

[1] “ Etude paramétrique de la résistance à l’arrachement d’un ancrage passif scellé au rocher ” M. Bost, D.-A. Ho, C. Pruvost, A. Khadour, P. Joffrin, M. Huteau, P. Robit, Journées Nationales de Géotechnique et de Géologie de l'Ingénieur (jngg2018)

[2] “ Investigation de la simulation système par circuits équivalents des capteurs à fibre optique ”, M.Salhi, S.Faci, A-L.Billabert, A.Khadour, S.Mostarshedi, C.Algani, Journées Nationales Microondes 16-19mai 2017.

[3] “ Analyse du comportement de poutres en béton précontraint : instrumentation des torons de precontrainte par fibres optiques ”, A. Michou, F. Benboudjema, A. Khadour, G. Nahas, P. Wyniecki, Y. Berthaud, Quinzième édition des Journées Scientifiques du Regroupement Francophone pour la Recherche et la Formation sur le Béton $(RF)^2B$.

[4] “ Analyse par fibres optiques et par corrélation d’images d’essais d’adhérence acier-béton ”, Alexandre Michou, Farid Benboudjema, Yves Berthaud, Georges Nahas, Pierre Wyniecki and Aghiad Khadour.

[5] “Etude expérimentale de la liaison acier - béton sous compression par mesures de fibres optiques”, A. Tixier, C.Rospars, F. Dufour, A. Khadour, M. Quiertant, B. Masson. 21ème Congrès Français de Mécanique. Bordeaux, 26 au 30 août 2013.

[6] “ Etude expérimentale de la liaison acier - béton sous compression par mesures de fibres optiques”, A. Tixier, C. Rospars, F. Dufour, A. Khadour, M. Quiertant, B. Masson, AUGC Cachan, France, 29-31 mai 2013.

[7] “Instrumentation des barres d’acier par fibres optiques”, A. Khadour, M. Quiertant, F. Baby, Journées, Capteurs à fibre optique ou guide planaire, GO2S, Saint-Etienne, 6 et 7 Février (2012).

[8] “Quel Absorbant Saturable pour les Lasers à fibres verrouillés en phase : Nanotubes de Carbone ou Puits Quantiques ?”, A. Cabasse, A. Khadour, G. Maulion, G. Martel, H.-T. Nguyen, J.-L. Oudar, O. Jost, R. Fleurier, S. Maine, Y. Battie et B. Trétout, pp. 156-158. 29émes Journées Nationales d'Optique Guidée JNOG, Besançon, 20-22 Octobre (2010).

[9] “VECSEL monomode-longitudinal à 1,55µm de haute puissance à température ambiante avec un miroir de Bragg hybride métal-métamorphique” Poster, J.P. Tourrenc, S. Bouchoule,

A. Khadour, J.G. Provost, J. Decobert, A. Miard, J.C. Harmand and J.L. Oudar, 26èmes Journées Nationales d'Optique Guidée JNOG, Grenoble 2 au 5 juillet (2007).

3.2.4 National seminars

[1] " Projet Clerval : Retour d'expérience sur l'utilisation de capteurs distribués à fibre optique " G. Six, A. Khadour, M. Quiertant, A. Flety, O. Pisseloup, A. Gagnon, J. Roth, C. Le Roy, C. Aubagnac, Journées Techniques Ouvrages d'Art 2017.

[2] " Essais expérimentaux du programme BADIFOPS " MARCHAND P., BABY F., KHADOUR A. et al. Journées Ouvrages d'Art 2016, Bordeaux

[3] " Auscultation dynamique par extensomètre à fibre optique longue base ", CUMUNEL G., ARGOUL P., QUIERTANT M., KHADOUR A. Journées Ouvrages d'Art 2016, Bordeaux

[4] "Poutre de Clerval : Instrumentation et suivi en cours de chargement, J-J. Brioist, S. Chataigner, M. Quiertant, A.Khadour, Journées Ouvrages d'Art 2015, Nantes.

[5] "Présentation des premiers résultats de l'expérimentation de la poutre du VIPP de Clerval", C. Aubagnac, D. Germain,A. Houel, R. Sadone, J-P Maherault, J-J Brioist, C. Marcotte, S. Chataigner, A. Khadour, M. Quiertant, GC'2015 Paris,18 et 19 mars 2015.

[6] "Caractérisation d'armatures en matériaux composites pour le renforcement de structures, et comportement mécanique de l'interface armature/béton". A. Rolland, K. Benzarti, M. Quiertant, P. Argoul, S. Chataigner, A. Khadour, Journées Techniques Ouvrages d'Art 2014, Champs-sur-Marne.

[7] "Les expérimentations dans le projet BADIFOPS", P. Marchand, F. Baby, M. Quiertant, A. Khadour, Journées Ouvrages d'Art 2014, Champs-sur-Marne.

[8] "Détection précoce des défaillances d'étanchéité d'ouvrages d'art- Intérêt de la fibre optique -Étude de faisabilité sur modèle réduit de tablier", G. Le Briand, A. Khadour, F. Taillade, B. Thauvin, Journées techniques Ouvrages d'Art Dijon, 5 - 6 juin 2013.

[9] "Instrumentation des armatures par les fibres optiques", A. Khadour, M. Quiertant, F. Baby, Premier congrès francophone des applications des fibres optiques, Paris 23-25 Octobre (2012).

[10] "Instrumentation des barres d'acier par fibres optiques", A. Khadour, M. Quiertant, F. Baby, Journées, Capteurs à fibre optique ou guide planaire, GO2S, Saint-Etienne, 6 et 7 Février (2012).

3.2.5 Invited talks

[1] "Active Intra-Chip photonic components characterization using High resolution optical frequency domain reflectometry", 3rd Global Summit & Expo on Materials,Photonics & Optical Instruments (GSEMPOI 2018(November 12-14, 2018 at Toronto, Canada).

[2] “Steel bridge strengthening with CFRP strips: mechanical characterization using distributed optical-fiber sensors” Aghiad Khadour, Gilles Foret, Marc Quiertant, Sylvain Chataigner, 9th International Conference on Fibre-Reinforced Polymer (FRP) Composites in Civil Engineering (CICE 2018), PARIS 17-19 JULY 2018.
[3] ‘Les applications des capteurs distribués à fibres optiques en géotechnique et en génie civil’, Congres Optique, Optique Toulouse-2018, 3-6 Juillet 2018.
[4] ‘Applications des Capteurs à Fibres Optiques dans le génie civil : étude des cas à l’IFSTTAR’, 2ème Journée Thématique du Club Fibres Optiques et Réseaux, Université de Cergy-Pontoise, ENSEA.
[5] ‘Développement d’un capteur à fibre optique polarimétrique peu sensible à la température’, A. Khadour, 4ème Congrès des Applications des Fibres Optiques, Paris, 22-24 Septembre 2015.
[6] ‘Capteurs optiques et dispositifs de vision pour les systèmes de transports intelligents’, Journée thématique Photonique et Véhicules Intelligents, Grenoble, le 09 avril 2015.
[7] Présentation au conseil scientifique (CS) de l’IFSTTAR des travaux du projet BADIFOPS, la présentation est faite le 5 juin 2014.
[8] Présentation au Conseil des Structures de Recherche (CSR) de l’IFSTTAR des travaux du projet BADIFOPS, la présentation est faite le 19 juin 2014.
[9] ‘L'utilisation de la fibre optique en Génie Civil’, École normale supérieure Paris-Saclay 28 janvier 2014.
[10] ”Optical fiber-based sensors and VeCSEL’s”, Seminar at ESYCOM laboratory, 16 January 2014.

3.2.6 Research reports

[1] A. Khadour, A. Herrera, F. Baby, P. Marchand, M. Quiertant. Plans d’instrumentations par fibres optiques. Livrable du projet BADIFOPS du programme C2D2 du RgC&u - lot n° 1- tâche n° E. 33 pages. Sept 2012.
[2] A. Khadour, exploitation méthodologique de l’instrumentation FO. Livrable du projet BADIFOPS du programme C2D2 du RgC&u - lot n° 2- tâche n° F. 25 pages. Sept 2013.
[3] A. Khadour, Livrable CSASurcharges : “ état de l’art et la Technique d’instrumentation ”, - phase 1, tâches 1, 15 pages, Avril 2015.
[4] E. Saint-Jacques, A. Khadour, S. Buttigieg, E. Dumont, N. Hautière, “Elisa-Investigation on the night-time visibility of pavement marking in wet conditions”, 15 Feb. 2015 (confidential).
[5] N. Hautier, E. Dumont, R. Brémond, A. Khadour, “Elisa – Driver visibility reduction in rainy weather”, 1st Sep. 2015 (confidential).

[6] A. Khadour, M. Quiertant, “ Rapport d’instrumentation de poutre de Clerval-Bilan des mesures par fibres optiques : essai de flexion 3 points “, 23.11.2015.

[7] A. Khadour, “ Rapport : résultats d’instrumentation du pieu par fibre optique (la Défense tour Alto) ”, 13 juin 2016 (confidential).

[8] A. Khadour, Livrable CSASurcharges : “ Validation d’un capteur polarimétrie pour le pesage en marche ”, - phase 2, tâches 1, 10 pages, mai 2017.

[9] A. Khadour, Ph. Reiffsteck , “ Rapport de validation d’instrumentation par fibres optiques de chantier FIVC-Bilan de mesures par fibres optiques Juillet-Novembre 2017 ”, Nov. 2017.

[10] A. Khadour, M. Quiertant, “ Rapport d’instrumentation de poutre de Clerval-Bilan des mesures par fibres optiques : Essais de flexion ‘effort tranchant’”, 02.03.2018.

3.2.7 PhD dissertation

[1] A. Khadour, "1.55 μm mode-locked vertical external cavity semiconductor laser for all-optical linear sampling applications," Ecole Polytechnique X, 2009.

4 Bibliography

[1] A. Caragliu, C. Del Bo, and P. Nijkamp, "Smart Cities in Europe," *Journal of Urban Technology,* vol. 18, no. 2, pp. 65-82, 2011/04/01 2011.

[2] M. S. Obaidat and P. Nicopolitidis, *Smart Cities and Homes: Key Enabling Technologies*. Elsevier Science, 2016.

[3] B. Jank, *Instrumentation, Control and Automation of Water and Wastewater Treatment and Transport Systems 1993*. Elsevier Science, 2016.

[4] H. N. Cho, D. M. Frangopol, and A. H. S. Ang, *Life-Cycle Cost and Performance of Civil Infrastructure Systems*. Taylor & Francis, 2007.

[5] M. K. Barnoski and S. M. Jensen, "Fiber waveguides: a novel technique for investigating attenuation characteristics," *Applied Optics,* vol. 15, no. 9, pp. 2112-2115, 1976/09/01 1976.

[6] W. Eickhoff and R. Ulrich, "Optical frequency domain reflectometry in single-mode fiber," *Applied Physics Letters,* vol. 39, no. 9, pp. 693-695, 1981.

[7] *Distributed Fiber Optic Sensor Market*. Available: https://www.psmarketresearch.com/market-analysis/distributed-fiber-optic-sensor-market

[8] A. H. Hartog, *An Introduction to Distributed Optical Fibre Sensors*. CRC Press, 2017.

[9] G. Rajan and B. G. Prusty, *Structural Health Monitoring of Composite Structures Using Fiber Optic Methods*. CRC Press, 2016.

[10] F. Ansari, *Sensing Issues in Civil Structural Health Monitoring*. Springer Netherlands, 2005.

[11] K. C. Kao and G. A. Hockham, "Dielectric-fibre surface waveguides for optical frequencies," *Proceedings of the Institution of Electrical Engineers,* vol. 113, no. 7, pp. 1151-1158, 1966.

[12] K. C. Kao and G. A. Hockham, "Dielectric-fibre surface waveguides for optical frequencies," *IEE Proceedings J Optoelectronics,* vol. 133, no. 3, pp. 191-198, 1986.

[13] J. Hecht, *City of Light: The Story of Fiber Optics*. Oxford University Press, USA, 1999.

[14] F. P. Kapron, D. B. Keck, and R. D. Maurer, "Radiation Losses in Glass Optical Waveguides," *Applied Physics Letters,* vol. 17, no. 10, pp. 423-425, 1970.

[15] H. Kanamori *et al.*, "Transmission characteristics and reliability of pure-silica-core single-mode fibers," *Journal of Lightwave Technology,* vol. 4, no. 8, pp. 1144-1150, 1986.

[16] S. Makovejs *et al.*, "Record-Low (0.1460 dB/km) Attenuation Ultra-Large Aeff Optical Fiber for Submarine Applications," in *Optical Fiber Communication Conference Post Deadline Papers*, Los Angeles, California, 2015, p. Th5A.2: Optical Society of America.

[17] Y. Tamura *et al.*, "Lowest-ever 0.1419-dB/km loss optical fiber," in *2017 Optical Fiber Communications Conference and Exhibition (OFC)*, 2017, pp. 1-3.

[18] J. M. López-Higuera, *Handbook of optical fibre sensing technology*. Wiley, 2002.

[19] J. A. Buck, *Fundamentals of Optical Fibers, 2nd Edition*. 2004.

[20] P. Dragic and J. Ballato, "Materials Development for Advanced Optical Fiber Sensors and Lasers," in *Handbook of Optical Fibers*, G.-D. Peng, Ed. Singapore: Springer Singapore, 2018, pp. 1-33.

[21] J. B. MacChesney, R. Bise, and A. Méndez, "Overview of Materials and Fabrication Technologies," in *Specialty Optical Fibers Handbook*Burlington: Academic Press, 2007, pp. 69-94.

[22] J. M and M. Y. Jamro, *Optical Fiber Communications: Principles and Practice*. Financial Times/Prentice Hall, 2009.

[23] D. J. Richardson, "New optical fibres for high-capacity optical communications," *Philos Trans A Math Phys Eng Sci,* vol. 374, no. 2062, Mar 6 2016.

[24] K. Imamura, K. Mukasa, R. Sugizaki, Y. Mimura, and T. Yagi, "Multi-core holey fibers for ultra large capacity wide-band transmission," in *2008 34th European Conference on Optical Communication*, 2008, pp. 1-2.

[25] A. Kumar, R. K. Varshney, and K. Thyagarajan, "Birefringence calculations in elliptical-core optical fibres," *Electronics Letters,* vol. 20, no. 3, pp. 112-113, 1984.

[26] J. D. Love, R. A. Sammut, and A. W. Snyder, "Birefringence in Elliptically Deformed Optical Fibers," (in English), *Electronics Letters,* vol. 15, no. 20, pp. 615-616, 1979.

[27] T. Schreiber *et al.*, "Stress-induced single-polarization single-transverse mode photonic crystal fiber with low nonlinearity," *Opt Express,* vol. 13, no. 19, pp. 7621-30, Sep 19 2005.

[28] J. Noda, K. Okamoto, and Y. Sasaki, "Polarization-Maintaining Fibers and Their Applications," (in English), *Journal of Lightwave Technology,* vol. 4, no. 8, pp. 1071-1089, Aug 1986.

[29] Q. Yu, X. Bao, and L. Chen, "Strain dependence of Brillouin frequency, intensity, and bandwidthin polarization-maintaining fibers," *Opt. Lett.,* vol. 29, no. 14, pp. 1605-1607, 2004.

[30] Y. H. Kim and K. Y. Song, "OTDR based on Brillouin dynamic grating in an e-core two-mode fiber for simultaneous measurement of strain and temperature distribution," in *2017 25th Optical Fiber Sensors Conference (OFS)*, 2017, pp. 1-4.

[31] Y. Mizuno, N. Hayashi, H. Tanaka, Y. Wada, and K. Nakamura, "Brillouin scattering in multi-core optical fibers for sensing applications," *Scientific Reports,* Article vol. 5, p. 11388, Jun 13 2015.

[32] Z. Zhao, M. Tang, S. Fu, W. Tong, and D. Liu, "Distributed and discriminative Brillouin optical fiber sensing based on heterogeneous multicore fiber," in *2017 Optical Fiber Communications Conference and Exhibition (OFC)*, 2017, pp. 1-3.

[33] Z. Zhao, M. Tang, L. Wang, S. Fu, W. Tong, and C. Lu, "Enabling simultaneous DAS and DTS measurement through multicore fiber based space-division multiplexing," in *Optical Fiber Communication Conference*, San Diego, California, 2018, p. W2A.7: Optical Society of America.

[34] R. W. Boyd and D. Prato, *Nonlinear Optics*. Elsevier Science, 2008.

[35] D. Marcuse, *Principles of optical fiber measurements*. Academic Press, 1981.

[36] J. Stone and C. A. Burrus, "Reduction of the 1.38- μ m Water Peak in Optical Fibers by Deuterium-Hydrogen Exchange," *Bell System Technical Journal,* vol. 59, no. 8, pp. 1541-1548, 1980.

[37] M. Ohashi, M. Tateda, K. Shiraki, K. Tajima, and K. Tsujikawa, "Optical fiber loss reduction," *Electronics and Communications in Japan (Part I: Communications),* vol. 79, no. 12, pp. 1-15, 1996.

[38] K. Tsujikawa, K. Tajima, and J. Zhou, "Intrinsic loss of optical fibers," *Optical Fiber Technology,* vol. 11, no. 4, pp. 319-331, 2005/10/01/ 2005.

[39] "Raman-Brillouin-Rayleigh Diffusion," in *Introduction to Optics*New York, NY: Springer New York, 2005, pp. 479-515.

[40] A. J. Rogers, "Distributed optical-fibre sensors," *Journal of Physics D: Applied Physics,* vol. 19, no. 12, p. 2237, 1986.

[41] R. Alan, "Distributed optical-fibre sensing," *Measurement Science and Technology,* vol. 10, no. 8, p. R75, 1999.

[42] M. Ohashi, K. Shiraki, and K. Tajima, "Optical loss property of silica-based single-mode fibers," *Journal of Lightwave Technology,* vol. 10, no. 5, pp. 539-543, 1992.

[43] D. J. Lockwood, "Rayleigh and Mie Scattering," in *Encyclopedia of Color Science and Technology*, M. R. Luo, Ed. New York, NY: Springer New York, 2016, pp. 1097-1107.

[44] R. Menzel, *Photonics: Linear and Nonlinear Interactions of Laser Light and Matter*. Springer Berlin Heidelberg, 2013.

[45] A. Smekal, "Zur Quantentheorie der Dispersion," *Die Naturwissenschaften,* vol. 11, no. 43, pp. 873-875, 1923/10/01 1923.

[46] C. V. Raman, "A new radiation," *Indian J. Phys.,* vol. 2, pp. 387-398, 1928.

[47] G. Landsberg and L. Mandelstam, "Eine neue Erscheinung bei der Lichtzerstreuung in Krystallen," *Die Naturwissenschaften,* journal article vol. 16, no. 28, pp. 557-558, July 01 1928.

[48] B. R. Masters, "CV Raman and the Raman effect," *Optics and Photonics News,* vol. 20, no. 3, pp. 40-45, 2009.

[49] M. A. Farahani and T. Gogolla, "Spontaneous Raman scattering in optical fibers with modulated probe light for distributed temperature Raman remote sensing," *Journal of Lightwave Technology,* vol. 17, no. 8, pp. 1379-1391, 1999.

[50] E. Karamehmedovic, *Incoherent Optical Frequency Domain Reflectometry for Distributed Thermal Sensing*. 2006.

[51] H. S. Pradhan and P. K. Sahu, "Characterisation of Raman distributed temperature sensor using deconvolution algorithms," *IET Optoelectronics,* vol. 9, no. 2, pp. 101-107, 2015.

[52] M. Dammig, G. Zinner, F. Mitschke, and H. Welling, "Stimulated Brillouin-Scattering in Fibers with and without External Feedback," (in English), *Physical Review A,* vol. 48, no. 4, pp. 3301-3309, Oct 1993.

[53] R. De Micheli and L. Giulotto, "Brillouin Scattering by Acoustic Field of Limited Coherence," *Journal of the Optical Society of America,* vol. 61, no. 8, pp. 1007-1011, 1971/08/01 1971.

[54] R. M. Shelby, M. D. Levenson, and P. W. Bayer, "Guided acoustic-wave Brillouin scattering," (in Eng), *Phys Rev B Condens Matter,* vol. 31, no. 8, pp. 5244-5252, Apr 15 1985.

[55] A. J. Poustie, "Guided acoustic-wave Brillouin scattering with optical pulses," *Opt Lett,* vol. 17, no. 8, pp. 574-6, Apr 15 1992.

[56] D. Heiman, D. S. Hamilton, and R. W. Hellwarth, "Brillouin scattering measurements on optical glasses," (in English), *Physical Review B,* vol. 19, no. 12, pp. 6583-6592, 1979.

[57] E. P. Ippen and R. H. Stolen, "Stimulated Brillouin scattering in optical fibers," *Applied Physics Letters,* vol. 21, no. 11, pp. 539-541, 1972.

[58] A. Zadok, A. Eyal, and M. Tur, "Stimulated Brillouin scattering slow light in optical fibers [Invited]," (in English), *Applied Optics,* vol. 50, no. 25, pp. E38-E49, Sep 1 2011.

[59] T. Horiguchi, T. Kurashima, and M. Tateda, "Tensile strain dependence of Brillouin frequency shift in silica optical fibers," *IEEE Photonics Technology Letters,* vol. 1, no. 5, pp. 107-108, 1989.

[60] T. Horiguchi, K. Shimizu, T. Kurashima, M. Tateda, and Y. Koyamada, "Development of a Distributed Sensing Technique Using Brillouin-Scattering," (in English), *Journal of Lightwave Technology,* vol. 13, no. 7, pp. 1296-1302, Jul 1995.

[61] W. Zou, X. Long, and J. Chen, "Brillouin Scattering in Optical Fibers and Its Application to Distributed Sensors," in *Advances in Optical Fiber Technology: Fundamental Optical Phenomena and Applications*, M. Yasin, H. Arof, and S. W. Harun, Eds. Rijeka: InTech, 2015, p. Ch. 01.

[62] K. Petermann, "Microbending loss in monomode fibres," *Electronics Letters,* vol. 12, no. 4, pp. 107-109, 1976.

[63] J. A. Jay, "An overview of macrobending and microbending of optical fibers," *White paper of Corning,* pp. 1-21, 2010.

[64] S. E. Miller and I. P. Kaminow, *Optical fiber telecommunications II*. Boston: Academic Press, 1988.

[65] B. Ward and J. Spring, "Finite element analysis of Brillouin gain in SBS-suppressing optical fibers with non-uniform acoustic velocity profiles," *Opt Express,* vol. 17, no. 18, pp. 15685-99, Aug 31 2009.

[66] F. Wu *et al.*, "A New G. 652D, Zero Water Peak Fiber: Optimized for Low Bend Sensitivity in Access Networks," *WIRE AND CABLE TECHNOLOGY INTERNATIONAL,* vol. 35, no. 6, p. 66, 2007.

[67] H. Murayama, D. Wada, and H. Igawa, "Structural health monitoring by using fiber-optic distributed strain sensors with high spatial resolution," *Photonic Sensors,* vol. 3, no. 4, pp. 355-376, 2013.

[68] M. K. Barnoski and S. M. Jensen, "Fiber waveguides: a novel technique for investigating attenuation characteristics," *Appl Opt,* vol. 15, no. 9, pp. 2112-5, Sep 1 1976.

[69] M. K. Barnoski, M. D. Rourke, S. M. Jensen, and R. T. Melville, "Optical time domain reflectometer," *Appl Opt,* vol. 16, no. 9, pp. 2375-9, Sep 1 1977.

[70] E. G. Neumann, "Optical time domain reflectometer: comment," (in eng), *Appl Opt,* vol. 17, no. 11, p. 1675, Jun 1 1978.

[71] P. Healey, "Instrumentation principles for optical time domain reflectometry," *Journal of Physics E: Scientific Instruments,* vol. 19, no. 5, p. 334, 1986.

[72] M. Tateda and T. Horiguchi, "Advances in optical time domain reflectometry," *Journal of Lightwave Technology,* vol. 7, no. 8, pp. 1217-1224, 1989.

[73] B. L. Danielson, "Optical time-domain reflectometer specifications and performance testing," (in eng), *Appl Opt,* vol. 24, no. 15, pp. 2313-22, Aug 1 1985.

[74] M. Zoboli and P. Bassi, "High spatial resolution OTDR attenuation measurements by a correlation technique," *Appl Opt,* vol. 22, no. 23, pp. 3680-1, Dec 1 1983.

[75] B. F. Levine, C. G. Bethea, and J. C. Campbell, "1.52 μ m room-temperature photon-counting optical time domain reflectometer," *Electronics Letters,* vol. 21, no. 5, pp. 194-196, 1985.

[76] P. Healey and P. Hensel, "Optical time domain reflectometry by photon counting," *Electronics Letters,* vol. 16, no. 16, pp. 631-633, 1980.

[77] M. Nazarathy *et al.*, "Real-time long range complementary correlation optical time domain reflectometer," *Journal of Lightwave Technology,* vol. 7, no. 1, pp. 24-38, 1989.

[78] H. H. Gilgen, R. P. Novak, R. P. Salathe, W. Hodel, and P. Beaud, "Submillimeter optical reflectometry," *Journal of Lightwave Technology,* vol. 7, no. 8, pp. 1225-1233, 1989.

[79] W. V. Sorin and D. F. Gray, "Simultaneous thickness and group index measurement using optical low-coherence reflectometry," *IEEE Photonics Technology Letters,* vol. 4, no. 1, pp. 105-107, 1992.

[80] S. Mechels, K. Takada, and K. Okamoto, "Optical low-coherence reflectometer for measuring WDM components," *IEEE Photonics Technology Letters,* vol. 11, no. 7, pp. 857-859, 1999.

[81] A. J. Rogers, "Polarisation optical time domain reflectometry," *Electronics Letters,* vol. 16, no. 13, pp. 489-490, 1980.

[82] D. Uttam and B. Culshaw, "Precision time domain reflectometry in optical fiber systems using a frequency modulated continuous wave ranging technique," *Journal of Lightwave Technology,* vol. 3, no. 5, pp. 971-977, 1985.

[83] J. P. v. d. Weid, R. Passy, G. Mussi, and N. Gisin, "On the characterization of optical fiber network components with optical frequency domain reflectometry," *Journal of Lightwave Technology,* vol. 15, no. 7, pp. 1131-1141, 1997.

[84] K. Yuksel, M. Wuilpart, V. Moeyaert, and P. Megret, "Optical frequency domain reflectometry: A review," in *2009 11th International Conference on Transparent Optical Networks*, 2009, pp. 1-5.

[85] A. G. Stove, "Linear FMCW radar techniques," *IEE Proceedings F Radar and Signal Processing,* vol. 139, no. 5, pp. 343-350, 1992.

[86] G. Jihong, C. Spiegelberg, and J. Shibin, "Narrow linewidth fiber laser for 100-km optical frequency domain reflectometry," *IEEE Photonics Technology Letters,* vol. 17, no. 9, pp. 1827-1829, 2005.

[87] R. Passy, N. Gisin, and J. V. d. Weid, "High-Sensitivity-Coherent Optical FrequencyDomain Reflectometry for Characterization of Fiber-optic Network Components," *Photonics Technology Letters, IEEE,* vol. 7, no. 6, pp. 667-669, 1995.

[88] B. J. Soller, S. T. Kreger, D. K. Gifford, M. S. Wolfe, and M. E. Froggatt, "Optical Frequency Domain Reflectometry for Single- and Multi-Mode Avionics Fiber-Optics Applications," in *IEEE Conference Avionics Fiber-Optics and Photonics, 2006.*, 2006, pp. 38-39.

[89] M. Froggatt, B. Soller, D. Gifford, and M. Wolfe, "Correlation and keying of Rayleigh scatter for loss and temperature sensing in parallel optical networks," in *Optical Fiber Communication Conference, 2004. OFC 2004*, 2004, vol. 2, p. 3 pp. vol.2.

[90] M. Froggatt and J. Moore, "High-spatial-resolution distributed strain measurement in optical fiber with rayleigh scatter," *Appl Opt,* vol. 37, no. 10, pp. 1735-40, Apr 1 1998.

[91] D. K. Gifford, M. E. Froggatt, M. S. Wolfe, S. T. Kreger, A. K. Sang, and B. J. Soller, "Millimeter Resolution Otpical Reflectometry Over Up to Two Kilometers of Fiber Length," in *2007 IEEE Avionics, Fiber-Optics and Photonics Technology Conference*, 2007, pp. 52-53.

[92] J. Nakayama, K. Iizuka, and J. Nielsen, "Optical fiber fault locator by the step frequency method," *Applied Optics,* vol. 26, no. 3, pp. 440-443, 1987/02/01 1987.

[93] D. W. Dolfi, M. Nazarathy, and S. A. Newton, "5-mm-resolution optical-frequency-domain reflectometry using a coded phase-reversal modulator," *Opt Lett,* vol. 13, no. 8, pp. 678-680, 1988/08/01 1988.

[94] M. E. Froggatt and D. K. Gifford, "Rayleigh backscattering signatures of optical fibers-Their properties and applications," in *Optical Fiber Communication Conference and Exposition and the National Fiber Optic Engineers Conference (OFC/NFOEC), 2013*, 2013, pp. 1-3.

[95] Y. Koyamada, M. Imahama, K. Kubota, and K. Hogari, "Fiber-optic distributed strain and temperature sensing with very high measurand resolution over long range using coherent OTDR," (in English), *Journal of Lightwave Technology,* vol. 27, no. 9, pp. 1142-1146, May 1 2009.

[96] Z. Yang, P. Shi, and Y. Li, "Research on COTDR for measuring distributed temperature and strain," in *2011 Second International Conference on Mechanic Automation and Control Engineering*, 2011, pp. 590-593.

[97] R. Posey, G. A. Johnson, and S. T. Vohra, "Strain sensing based on coherent Rayleigh scattering in an optical fibre," *Electronics Letters,* vol. 36, no. 20, pp. 1688-1689, 2000.

[98] Y. Wang, B. Jin, Y. Wang, D. Wang, X. Liu, and Q. Bai, "Real-Time Distributed Vibration Monitoring System Using Φ-OTDR," *IEEE Sensors Journal,* vol. 17, no. 5, pp. 1333-1341, 2017.

[99] G. Tu, B. Yu, S. Zhen, K. Qian, and X. Zhang, "Enhancement of Signal Identification and Extraction in a Φ-OTDR Vibration Sensor," *IEEE Photonics Journal,* vol. 9, no. 1, pp. 1-10, 2017.

[100] Q. Yan, M. Tian, X. Li, Q. Yang, and Y. Xu, "Coherent Φ-OTDR based on polarization-diversity integrated coherent receiver and heterodyne detection," in *2017 25th Optical Fiber Sensors Conference (OFS)*, 2017, pp. 1-4.

[101] X. Bao, D.-P. Zhou, C. Baker, and L. Chen, "Recent Development in the Distributed Fiber Optic Acoustic and Ultrasonic Detection," *Journal of Lightwave Technology,* vol. 35, no. 16, pp. 3256-3267, 2017.

[102] S. Ying, W. Chen, L. Xiao-hui, W. Chang, and P. Gang-ding, "Phase-OTDR based on space difference of Rayleigh backscattering," in *2016 15th International Conference on Optical Communications and Networks (ICOCN)*, 2016, pp. 1-3.

[103] G. Tu, X. Zhang, Y. Zhang, F. Zhu, L. Xia, and B. Nakarmi, "The Development of an Φ-OTDR System for Quantitative Vibration Measurement," *IEEE Photonics Technology Letters,* vol. 27, no. 12, pp. 1349-1352, 2015.

[104] H. Cai *et al.*, "Coherent detection based Φ-OTDR and its application," in *2015 Opto-Electronics and Communications Conference (OECC)*, 2015, pp. 1-3.

[105] A. Khadour and J. Waeytens, "5 - Monitoring of concrete structures with optical fiber sensors," in *Eco-Efficient Repair and Rehabilitation of Concrete Infrastructures*: Woodhead Publishing, 2018, pp. 97-121.

[106] B. Soller, D. Gifford, M. Wolfe, and M. Froggatt, "High resolution optical frequency domain reflectometry for characterization of components and assemblies," *Opt Express,* vol. 13, no. 2, pp. 666-74, Jan 24 2005.

[107] B. J. Soller, M. Wolfe, and M. E. Froggatt, "Polarization resolved measurement of Rayleigh backscatter in fiber-optic components," 2005.

[108] D. K. Gifford *et al.*, "Swept-wavelength interferometric interrogation of fiber Rayleigh scatter for distributed sensing applications," 2007, vol. 6770, pp. 67700F-67700F-9.

[109] G. Elsa, "Perspectives on stimulated Brillouin scattering," *New Journal of Physics,* vol. 19, no. 1, p. 011003, 2017.

[110] A. Zarifi, B. Stiller, M. Merklein, K. Vu, S. J. Madden, and B. J. Eggleton, "Distributed Brillouin Scattering Measurement with Sub-mm Spatial Resolution," in *Frontiers in Optics 2017*, Washington, D.C., 2017, p. FTu4A.5: Optical Society of America.

[111] X. Bao and L. Chen, "Recent progress in Brillouin scattering based fiber sensors," *Sensors (Basel),* vol. 11, no. 4, pp. 4152-87, 2011.

[112] M. A. Soto, "Distributed Brillouin Sensing: Time-Domain Techniques," in *Handbook of Optical Fibers*, G.-D. Peng, Ed. Singapore: Springer Singapore, 2018, pp. 1-91.

[113] A. Wosniok, "Distributed Brillouin Sensing: Frequency-Domain Techniques," in *Handbook of Optical Fibers*, G.-D. Peng, Ed. Singapore: Springer Singapore, 2018, pp. 1-25.

[114] W. Zou, X. Long, and J. Chen, "Distributed Brillouin Sensing: Correlation-Domain Techniques," in *Handbook of Optical Fibers*, G.-D. Peng, Ed. Singapore: Springer Singapore, 2018, pp. 1-31.

[115] S. L. Floch and F. Sauser, "New improvements for Brillouin optical time-domain reflectometry," in *2017 25th Optical Fiber Sensors Conference (OFS)*, 2017, pp. 1-4.

[116] T. Kurashima, T. Horiguchi, and M. Tateda, "Distributed-Temperature Sensing Using Stimulated Brillouin-Scattering in Optical Silica Fibers," (in English), *Opt Lett,* vol. 15, no. 18, pp. 1038-1040, Sep 15 1990.

[117] T. Horiguchi, T. Kurashima, and M. Tateda, "A Technique to Measure Distributed Strain in Optical Fibers," (in English), *Ieee Photonics Technology Letters,* vol. 2, no. 5, pp. 352-354, May 1990.

[118] T. Kurashima, T. Horiguchi, H. Izumita, S.-i. Furukawa, and Y. Koyamada, "Brillouin optical-fiber time domain reflectometry," *IEICE transactions on communications,* vol. 76, no. 4, pp. 382-390, 1993.

[119] K. Shimizu, T. Horiguchi, Y. Koyamada, and T. Kurashima, "Coherent self-heterodyne detection of spontaneously Brillouin-scattered light waves in a single-mode fiber," (in eng), *Opt Lett,* vol. 18, no. 3, p. 185, Feb 1 1993.

[120] D. Garus, K. Krebber, F. Schliep, and T. Gogolla, "Distributed sensing technique based on Brillouin optical-fiber frequency-domain analysis," (in eng), *Opt Lett,* vol. 21, no. 17, pp. 1402-4, Sep 1 1996.

[121] D. Garus, T. Gogolla, K. Krebber, and F. Schliep, "Brillouin optical-fiber frequency-domain analysis for distributed temperature and strain measurements," (in English), *Journal of Lightwave Technology,* vol. 15, no. 4, pp. 654-662, Apr 1997.

[122] R. Bernini, A. Minardo, and L. Zeni, "Stimulated Brillouin scattering frequency-domain analysis in a single-mode optical fiber for distributed sensing," *Opt Lett,* vol. 29, no. 17, pp. 1977-9, Sep 1 2004.

[123] K. Hotate and T. Hasegawa, "Measurement of Brillouin gain spectrum distribution along an optical fiber using a correlation-based technique - Proposal, experiment and simulation," (in English), *Ieice Transactions on Electronics,* vol. E83c, no. 3, pp. 405-412, Mar 2000.

[124] K. Hotate and M. Tanaka, "Distributed fiber Brillouin strain sensing with 1-cm spatial resolution by correlation-based continuous-wave technique," (in English), *Ieee Photonics Technology Letters,* vol. 14, no. 2, pp. 179-181, Feb 2002.

[125] K.-Y. Song, Z. He, and K. Hotate, "Effects of Intensity Modulation of Light Source on Brillouin Optical Correlation Domain Analysis," *Journal of Lightwave Technology,* vol. 25, no. 5, pp. 1238-1246, 2007.

[126] K. Y. Song, Z. He, and K. Hotate, "Distributed strain measurement with millimeter-order spatial resolution based on Brillouin optical correlation domain analysis," *Opt Lett,* vol. 31, no. 17, pp. 2526-8, Sep 1 2006.

[127] K. Hotate and H. Zuyuan, "Synthesis of optical-coherence function and its applications in distributed and multiplexed optical sensing," *Journal of Lightwave Technology,* vol. 24, no. 7, pp. 2541-2557, 2006.

[128] Z. He and K. Hotate, "Synthesized optical coherence tomography for imaging of scattering objects by use of a stepwise frequency-modulated tunable laser diode," *Optics Letters,* vol. 24, no. 21, pp. 1502-1504, 1999/11/01 1999.

[129] G. Bolognini and A. Hartog, "Raman-based fibre sensors: Trends and applications," *Optical Fiber Technology,* vol. 19, no. 6, pp. 678-688, 2013/12/01/ 2013.

[130] J. Geng, S. Staines, M. Blake, and S. Jiang, "Distributed fiber temperature and strain sensor using coherent radio-frequency detection of spontaneous Brillouin scattering," *Applied Optics,* vol. 46, no. 23, p. 5928, 2007/08/10 2007.

[131] G. Jihong, S. Staines, W. Zuolan, Z. Jie, M. Blake, and J. Shibin, "Highly stable low-noise Brillouin fiber laser with ultranarrow spectral linewidth," *IEEE Photonics Technology Letters,* vol. 18, no. 17, pp. 1813-1815, 2006.

[132] E. C. Cook, P. J. Martin, T. L. Brown-Heft, J. C. Garman, and D. A. Steck, "High passive-stability diode-laser design for use in atomic-physics experiments," *Review of Scientific Instruments,* vol. 83, no. 4, p. 043101, Apr 2012.

[133] S. C. Her and C. Y. Huang, "Effect of coating on the strain transfer of optical fiber sensors," *Sensors (Basel),* vol. 11, no. 7, pp. 6926-41, 2011.

[134] F. Ansari and Y. Libo, "Mechanics of Bond and Interface Shear Transfer in Optical Fiber Sensors," (in English), *Journal of Engineering Mechanics,* vol. 124, no. 4, pp. 385-394, Apr 1998.

[135] Y. E. Pak, "Longitudinal shear transfer in fiber optic sensors," *Smart Materials and Structures,* vol. 1, no. 1, p. 57, 1992.

[136] H. Wang and Z. Zhou, "A Review on Strain Transfer Mechanism of Optical Fiber Sensors," *Pacific Science Review,* vol. 14, no. 3, p. 248~252, 2012.

[137] R. Bernini *et al.*, "Identification of defects and strain error estimation for bending steel beams using time domain Brillouin distributed optical fiber sensors," *Smart Materials and Structures,* vol. 15, no. 2, p. 612, 2006.

[138] A. Nanni, C. C. Yang, K. Pan, J. S. Wang, R. Robert, and J. Michael, "Fiber-Optic Sensors for Concrete Strain-Stress Measurement," *ACI Materials Journal,* vol. 88, no. 3, 5/1/1991 1991.

[139] I. Iskhakov, Y. Ribakov, K. Holschemacher, and T. Mueller, "High performance repairing of reinforced concrete structures," *Materials & Design,* vol. 44, pp. 216-222, 2013/02/01/ 2013.

[140] B. A. Tayeh, B. H. A. Bakar, M. A. M. Johari, and Y. L. Voo, "Utilization of Ultra-high Performance Fibre Concrete (UHPFC) for Rehabilitation – A Review," *Procedia Engineering,* vol. 54, pp. 525-538, 2013/01/01/ 2013.

[141] J. S. Leng *et al.*, "Structural NDE of concrete structures using protected EFPI and FBG sensors," *Sensors and Actuators A: Physical,* vol. 126, no. 2, pp. 340-347, 2006/02/14/ 2006.

[142] M. Iten, *Novel Applications of Distributed Fiber-optic Sensing in Geotechnical Engineering*. Vdf-Hochschulverl. an der ETH, 2012.

[143] T. Guo, A. Li, Y. Song, B. Zhang, Y. Liu, and N. Yu, "Experimental study on strain and deformation monitoring of reinforced concrete structures using PPP-BOTDA," (in English), *Science in China Series E: Technological Sciences,* vol. 52, no. 10, pp. 2859-2868, Oct 2009.

[144] A. B. Huanga, J. T. Lee, C. C. Wang, Y. T. Ho, and T. S. Chuang, "Field Monitoring Of Shield Tunnel Lining Using Optical Fiber Bragg Grating Based Sensors," presented at the Proceedings of the 18th Southeast Asian Geotechnical Conference (18SEAGC) & Inaugural AGSSEA Conference (1AGSSEA), 2013.

[145] F. Dutalloir, T. Thibaux, G. Cadoret, and G. Birelli, "Un nouveau béton très hautes performances : le BSI. – Première application industrielle / B.S.I. : A new, very high performance concrete. Initial industrial application," presented at the La technique française du Béton, AFPC-AFREM, XIII° congrès de la FIP, 1998.

[146] F. Pigeon, S. Pelissier, A. Mure-Ravaud, H. Gagnaire, and C. Veillas, "Optical fibre young modulus measurement using an optical method," *Electronics Letters,* vol. 28, no. 11, pp. 1034-1035, 1992.

[147] A. Mita and I. Yokoi, "Fiber Bragg grating accelerometer for structural health monitoring," in *Fifth International Conference on Motion and Vibration Control (MOVIC 2000), Sydney, Australia*, 2000: Citeseer.

[148] P. Antunes *et al.*, "Optical Sensors Based on Fiber Bragg Gratings for Structural Health Monitoring," in *New Developments in Sensing Technology for Structural Health Monitoring*, S. C. Mukhopadhyay, Ed. Berlin, Heidelberg: Springer Berlin Heidelberg, 2011, pp. 253-295.

[149] P. Antunes, F. Domingues, M. Granada, and P. André, "Mechanical properties of optical fibers," in *Selected Topics on Optical Fiber Technology*: InTech, 2012.

[150] Available: https://www.hbm.com/en/2489/strain-gauges-adhesives-x120-two-component-adhesive/

[151] M. M. Shokrieh and R. Rafiee, "Simulation of fatigue failure in a full composite wind turbine blade," *Composite Structures,* vol. 74, no. 3, pp. 332-342, 2006/08/01/ 2006.

[152] E. N. Barton, S. L. Ogin, A. M. Thorne, G. T. Reed, and B. H. Le Page, "Interaction between optical fibre sensors and matrix cracks in cross-ply GRP laminates—part 1: passive optical fibres," *Composites Science and Technology,* vol. 61, no. 13, pp. 1863-1869, 2001/10/01/ 2001.

[153] N. C. Eaton, R. C. Drew, and H. Geiger, "Finite element stress and strain analysis in composites with embedded optical fiber sensors," *Smart Materials and Structures,* vol. 4, no. 2, p. 113, 1995.

[154] K. Y. Lau, I. Ury, and A. Yariv, "Passive and active mode locking of a semiconductor laser without an external cavity," *Applied Physics Letters,* vol. 46, no. 12, pp. 1117-1119, 1985.

[155] R. L. Fork, B. I. Greene, and C. V. Shank, "Generation of optical pulses shorter than 0.1 psec by colliding pulse mode locking," *Applied Physics Letters,* vol. 38, no. 9, pp. 671-672, 1981.

[156] S. Arahira, Y. Matsui, and Y. Ogawa, "Mode-locking at very high repetition rates more than terahertz in passively mode-locked distributed-Bragg-reflector laser diodes," *IEEE Journal of Quantum Electronics,* vol. 32, no. 7, pp. 1211-1224, 1996.

[157] T. Ohno, F. Nakajima, T. Furuta, and H. Ito, "240 GHz active modelocked laser diode," *Electronics Letters,* vol. 41, no. 19, pp. 1057-1059, 2005.

[158] C. Gosset *et al.*, "Subpicosecond pulse generation at 134GHz using a quantum-dash-based Fabry-Perot laser emitting at 1.56 μ m," *Applied Physics Letters,* vol. 88, no. 24, p. 241105, 2006.

[159] W. Griffioen *et al.*, *Reliability of Optical Fibres and Components: Final Report of COST 246*. Springer London, 1999.

[160] F. Berghmans, S. Eve, and M. Held, "An Introduction to Reliability of Optical Components and Fiber Optic Sensors," in *Optical Waveguide Sensing and Imaging*, W. J. Bock, I. Gannot, and S. Tanev, Eds. Dordrecht: Springer Netherlands, 2008, pp. 73-100.

[161] M. J. Matthewson, S. o. P.-o. I. Engineers, and C. R. Kurkjian, *Optical Fiber and Fiber Component Mechanical Reliability and Testing* (no. vol. 4639). SPIE, 2002.

[162] M. J. Matthewson and S. o. p.-o. i. engineers, *Optical fiber reliability and testing: 19-20 September 1999, Boston, Massachusetts* (no. vol. 3848). Society of Photo Optical, 1999.

[163] R. J. Castilone, G. Glaesemann, and T. A. Hanson, *Extrinsic strength measurements and associated mechanical reliability modeling of optical fiber*. 2000.